UNIVERSITY OF TRENTO - Italy

International Doctoral School in Biomolecular Sciences
XXV Cycle

Genetically encoded division machinery for cell free synthetic biology

Tutor

Sheref Samir Mansy

Armenise Harvard Laboratory of synthetic and reconstructive biology

CIBIO (Centre for Integrative Biology)

Ph.D. Thesis of

Paola Torre

Armenise- Harvard Laboratory of synthetic and reconstructive biology

CIBIO (Centre for Integrative Biology)

Academic Year 2012-2013

List of abbreviations

ATPS aqueous two-phase systems

A3PS aqueous three phase systems

CFP cyan fluorescent protein

DOPG 1,2-dioleoyl-sn-glycero-3-[phospho-rac-(1-glycerol)]

FITC fluorescein isothiocyanate

GVs giant vesicles

His x histidine tag

kDa kilo Dalton

MW Molecular weight

MWCO Molecular weight cut off

PC phosphatidylcoline

PCR polymerase chain reaction

PEG polyethylene glycol

sfGFP super folder GFP

T/T transcription/translation

w/ o water in oil

YFP yellow fluorescent protein

Abstract

The *de novo* construction of cellular life requires, in part, the assembly of components that confer the ability to replicate. Herein we describe efforts to reconstitute parts of the *Escherichia coli* cell division machinery inside of water-in-oil emulsion compartments and synthetic phospholipid vesicles. The system was built with DNA and purified transcription and translation machinery housed in a compartment. A particular emphasis was placed on FtsZ, a protein that oligomerizes into a ring at the midcell and splits the cell into two. FtsZ does not contain a membrane interaction domain. *In vivo*, FtsZ interactions with the membrane are mediated by FtsA and ZipA. Therefore, the influence of FtsA on the behavior of FtsZ also was investigated. Fluorescently tagged constructs were used to facilitate evaluation by microscopy. The data showed that FtsZ readily assembles into rings in the presence of FtsA, thereby suggesting that the Fts system can be exploited for building a genetically encoded, self-replicating, cell-like system. We also explored additional methods of dividing compartments, such as the use of aqueous two and three phase systems.

Chapter 1

Chapter 1

1.Introduction

Projects that fall within the "Synthetic Biology Space" either construct in *vivo or* in *vitro* living or life-like systems[1,2,3]. In other words, synthetic biology deals with life or tries to mimic it. Those that are engaged with in *vivo* studies, engineer biomolecules and genomes and implement them in extant cells or organisms follow a "top down strategy"[4]. On the other hand, synthetic biologists that decide to face in *vitro* studies, design biomolecules and genomes for the generation of synthetic cells from scratch embrace a "bottom up strategy".[5]

Two frequent terms encountered in synthetic biology are "minimal" and "artificial". A minimal cell is a cell that has the minimal requirements and parts to be considered alive. An artificial cell is made from artificial components[6-8]. Whatever could be the design of the *de novo* cell, the synthetic biologist, as the word synthesis from the ancient Greek σύνθεσις (putting together) suggests, will put together well characterized biological parts and assemble them in different ways in order to obtain desired function. The biological parts are like a defined set of Lego bricks that could be assembled in different ways in order to get different functions (Fig 1).

The most attractive and desired functionality to be reproduced in a synthetic cell are functions that mimic key properties of life. In this experimental work we embraced a "bottom up strategy" aimed at mimicking a key feature of life, that of cellular replication. We assembled components of the division machinery system of *E. coli* reconstituting in a first step, with purified proteins and then with DNA and purified transcription translation machinery housed in phospholipid vesicles and water-oil (w/o) emulsions. Further, we developed new compartments for the potential localization and topography of our genetically encoded system.

In chapter one an overview of our "synthetic minimal cell" (Fig.1.2) synthesized from the bottom up is presented. Herein we will describe a model of

cell replication, the genetically encoded system for the proteins FtsZ and FtsA (*E. coli* cell division proteins), the compartments used (phospholipid vesicles and water-oil emulsions), and finally a cytoplasm-like model (ATPS in water-oil emulsions).

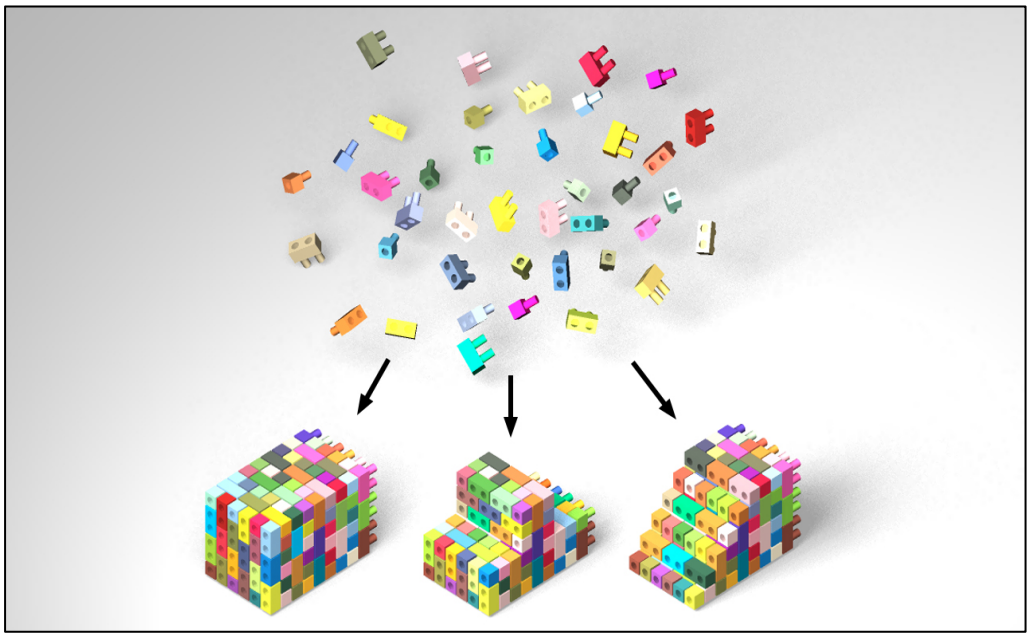

Fig.1: The desire of the synthetic biologist. Defined parts assembled in different ways, for different desired functionality. *Retrieved from Wikimedia.*

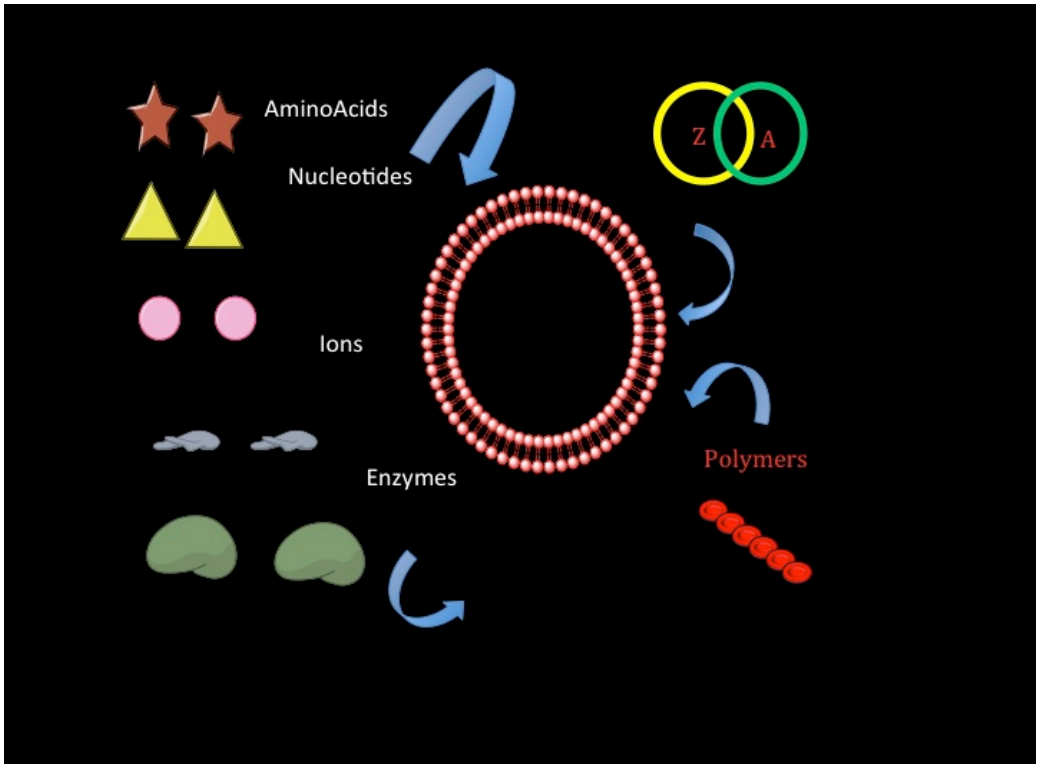

Fig. 1.2 : An overview of the synthetic minimal cell assembled from the bottom-up. The aim is to reconstitute in cell-like compartments a transcription and translation system for the production of a minimal division machinery , made of FtsZ and FtsA. The system is assembled from the scratch, starting from simple chemical molecules such as nucleotides, amino acids and simple biomolecules as ribosomes, tRNAs and enzymes. The surplus value is represented by the fact that has also an internal compartmentalization, obtained by the addition of polymers.

1.1 *E. coli* cell division is an excellent model of cell replication.

There is no life without replication and without replication there is no evolution. Our aim is to mimic replication, both DNA replication and cell body division for a better comprehension of life and its diversity. We use *E. coli* as our cell model system.

Cell division in *E. coli*, as in other bacterial cells, is driven by the divisome[8-9] a multi protein machinery system (Fig.1.3). The machinery is composed of a dozen proteins and among these, a protein called FtsZ (filamentous thermo sensitive protein) plays a pivotal role. FtsZ is a structural homologue of the eukaryotic protein tubulin[10,11] and undergoes a GTP-dependent self-assembly into polymers which form the Z ring. The Z ring has a dynamic structure that generates a constriction force necessary for the cell to divide and serves as a scaffold for the recruitment of the downstream components of the divisome.

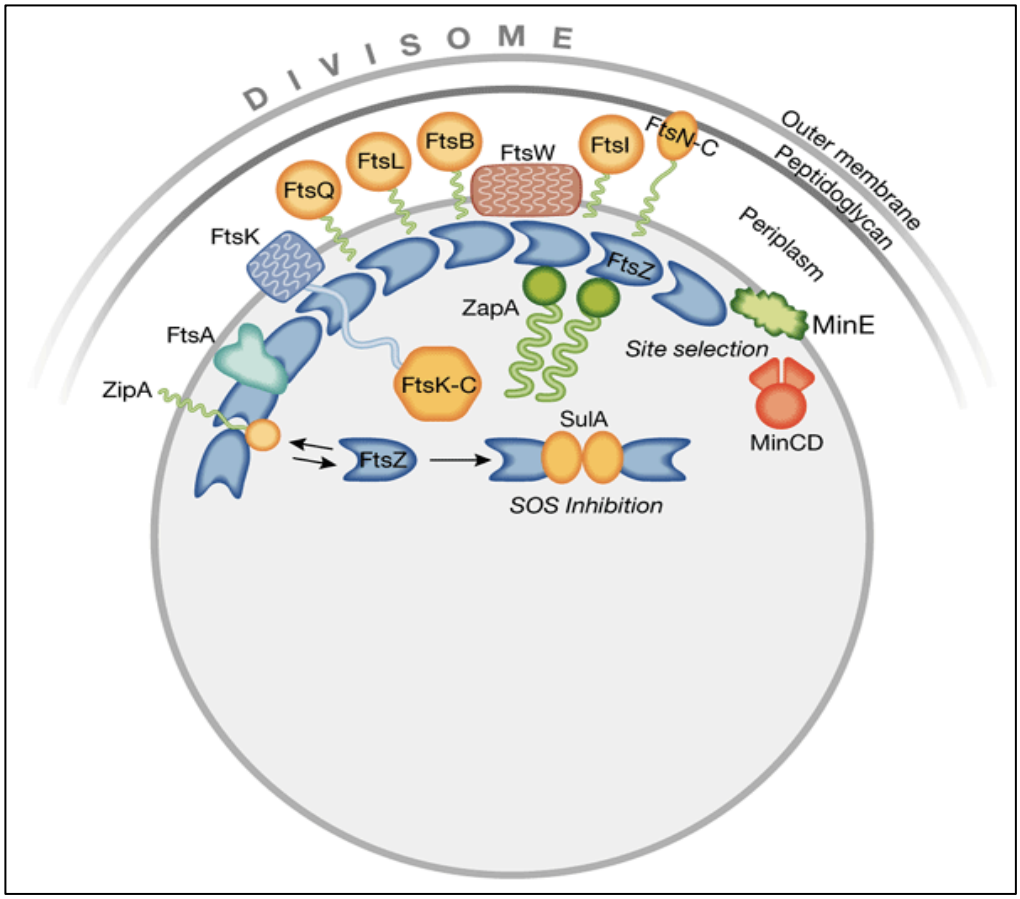

Fig1.3: The Divisome of *E. coli* is a multi protein machinery system, composed by a dozen of proteins participating to the process of cell division. Between these proteins FtsZ and FtsA are playing a pivotal role. Vicente et *al*., *EMBO reports* **4**, 655–60 (2003).

The process of cytokinesis in *E. coli* requires some proteins and some events to occur. Cytokinesis occurs after chromosome replication and segregation. The Z ring is localized at the midpoint of the rod, perpendicular to the long axis of the cell. This specific positioning of the ring permits the division of the cell in two daughter cells (Fig 1.4). A precision so strict is guaranteed by the synergistic action of two protein systems able to spatially regulate the cell division: the Noc system and the Min system. The Noc system[13], inhibits division in the vicinity of the chromosome (the nucleoid), ensuring that chromosomes are not bisected by the septum. The Min system prevents the formation of the Z ring at the cell poles and avoids the potential formation of DNA minicells[14].

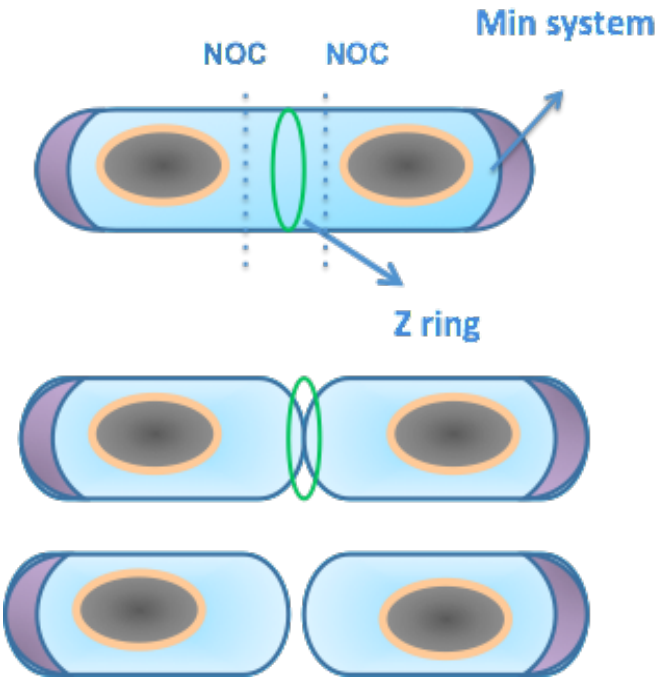

Fig. 1.4: *E. coli* cell division. After replication of the chromosome, the Z ring, formed by FtsZ polymerization, divides the cell in two exactly identical daughter cells. The strict positioning of the ring is guaranteed by the Noc system and the Min system. The Noc system avoids cell division in proximity of the chromosome, the Min system in the proximity of the cell poles.

The Min system is composed of MinC, MinD and MinE. MinC is the direct inhibitor of FtsZ polymerization and binds MinE that interacts with MinD, an ATPase membrane protein. MinE moves MinD from the cell poles to the middle of the rod, hydrolyzing the ATP bound to MinD. Min E is the protein responsible of the oscillation that regulates the positioning of the Z ring in the middle of the cell.

1.2 The keystones of the divisome: FtsZ, ZipA and FtsA

The spatial disposition of the Z ring is controlled by the Min and the Noc system, but the ring needs to be tethered to the membrane in order to generate the constriction force for cell division. FtsA and ZipA tether the Z ring to the membrane and in combination with FtsZ are considered the proto-ring elements.

ZipA is a trans-membrane protein, which tethers the Z ring to the membrane through interactions between its C terminus and the conserved C-terminal tail of FtsZ, made of 10 amino acids (DYLDIPAFLR) [15]. Given the role of ZipA in Z ring tethering, it has been shown that a gain of function point mutation in FtsA (R286WFtsA) [16] can render *E. coli* independent of ZipA. Therefore, it appears that FtsA is the primary tether of the Z ring to the membrane.

FtsA is a homologue of the eukaryotic actin[17-18] and interacts with the membrane through an amphipathic helix of 15 amino acids (GSWIKRLVSWLRKEF) present at the C -terminus of the protein sequence. The ratio of FtsA versus FtsZ, plays a crucial role in cell division. This ratio is roughly 1:5, with approximately 700 molecules of FtsA and 3200 molecules of FtsZ per cell[19].

1.3 Reconstitution of minimal cell division machinery in *vitro*.

To date it is possible to model simpler division systems in *vitro* despite the redundancy of the divisome and complexity of division in *vivo*. The imitation in *vitro* of cell replication focuses on two main aspects, the reconstitution of a minimal divisome and the development of cell-like compartments able to mimic the physicochemical but also mechanical process of division.

There are marvelous examples of bottom-up reconstitution of minimal cell division machinery in *vitro*. Erickson and colleagues engineered FtsZ-YFP-MinD, a modified version of FtsZ , able to insert directly into the membrane of multilamellar liposomes[20-21]. This version of FtZ is able to polymerize and to form Z-rings in tubular liposomes, causing indentations within the membranes. The Min protein system was reconstituted on supported lipid bilayers, generating protein waves, correspondent to the oscillation produced in *vivo*[22] and proto ring elements (FtsZ, FtsA and ZipA) of the Divisome were assembled in Giant Vesicles (GVs) [23](Fig 1.5).

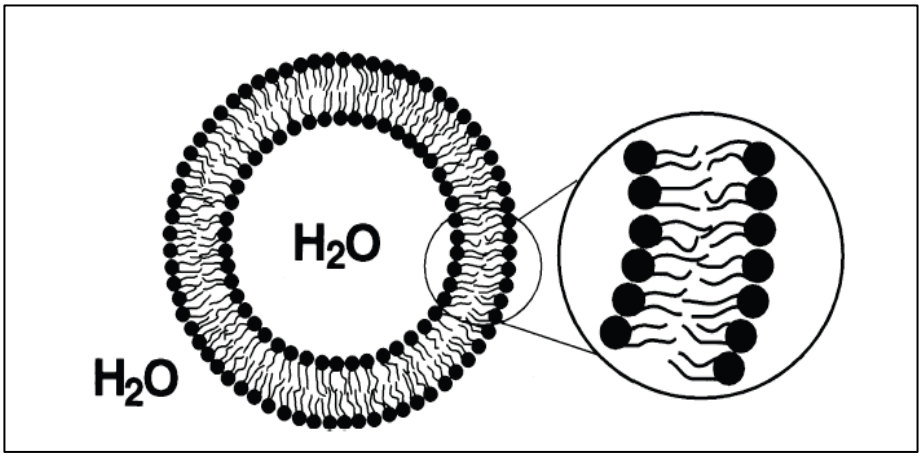

Fig. 1-5: Structure of a Giant Vesicle having one lipid bilayer (unilamellar). Reprinted with permission from Menger and Angelova, Acc. Chem. Res. 1998, 31, 789-797. Copyright 1998American Chemical Society.

The design of minimal models does not take in account that replication is also a physicochemical process. There are several examples of vesicle division mechanisms that do not rely on protein activity and were built in *vitro*. Membranes composed of three different lipids that phase separate into liquid ordered and disordered domains result in membrane curvature, budding and division by osmotic pressures[24]. While GVs with an encapsulated aqueous two phase system have budding morphology that undergo division in hypertonic solution. In both cases there is a single cycle of division, because the asymmetries are not retained in the daughter vesicles [25-26]. The combination of liquid ordered and disordered domains and the encapsulation of ATPS in GVs allow a second cycle[27]. In the Sugawara laboratory an alternative pathway was developed that uses DNA replication to drive vesicle division[28]. A cationic composition of the lipid membranes is combined with the replication of the DNA by PCR and then ionic interactions between the lipids and the DNA result in vesicle division. This system combines two processes crucial for the construction of cellular life, genomic replication and compartment division. In our system we privilege the feature of compartment division.

Our plan was to synthesize a genetically encoded minimal divisome with a cell-free system in multi-compartmentalized, cell-like compartments containing aqueous two-phase systems.

1.4 Cell free-systems for protein synthesis.

Cell-free systems are our toolbox for the synthesis of a minimal synthetic cell. We worked with transcription translation systems from cellular extracts and purified T/T as the PURESYSTEM.

We have availability of several sources for cell-free transcription-translation systems consisting of cell extracts from *Escherichia coli* (ECE), rabbit reticulocytes (RRL), wheat germ (WGE), and insect cells (ICE) [29]. Since these cells behave very differently, the extracts derived from them do as well. In general the choice of which kind of cellular extract is used is dictated by the kind of

biologically active protein that has to be produced. The factors to be considered are, of course, the yield of the protein needed, the origin and the complexity of the protein, the cost, and the downstream processing necessary[30]. Proteins for our minimal cell division machinery system were produced by *E. coli* cell extract (Promega S30) supplied with a T7 RNA polymerase or by fully purified transcription/translation (T/T) components from *E. coli* (PURExpress® from NEB).

The advantages of using a cellular lysate from *E. coli* is that it gives high yield of proteins, from hundreds of micrograms per milliliter to milligrams per milliliter in a batch reaction, depending on the protein of interest. Furthermore, in *E. coli* lysate are present factors that can help the folding of the proteins. The disadvantage is the presence of nucleases, meaning that higher amounts of DNA and circular DNA are needed. An example of *E. coli* cell lysate for the expression of a minimal protein system in vesicles is the synthesis of the bacterial actin-like proteins, MreB and MreC[31]. This example is significant because the synthesis of MreB and MreC within vesicles shows the possibility to co-express different proteins at the same time in just one compartment using a cell-free system as source of transcription and translation machinery.

In contrast, using the PURESYSTEM (PURExpress® from NEB) we can count upon a system made of fully defined, purified components, of which we know exactly the composition. The PURESYSTEM[32] contains recombinant histidine-tagged amino acyl tRNA synthetases, initiation factors, elongation factors, release factors, ribosome recycling factors, methionyl-tRNA transformylase, 70S ribosomes, amino acids, rNTPs, and tRNAs. The mixture additionally includes T7 RNA polymerase, creatine kinase, myokinase, nucleoside-di-phosphate kinase, and pyrophosphatase. The PURESYSTEM is free of inhibitory substances such as nucleases, proteases, and enzymes that hydrolyze nucleotide triphosphate, so you can work with low quantity of DNA for a high level of expression. The PURESYSTEM has been successful for other groups, i.e. Yomo and colleagues used the PURESYSTEM for in *vitro* compartmentalization (IVC) in liposomes. [33,34.]

1.5 Cell-like compartments: water-in-oil emulsion droplets and phospholipid vesicles.

The cell-like compartments used in the following experiments for the synthesis or reconstitution of a minimal divisome are water in oil emulsions (w/o emulsions) and phospholipid vesicles. W/o emulsions are heterogeneous systems, made of a disperdent phase (oil) and a dispersed phase (water). Water in oil emulsions have features of great stability, due to the presence of surfactants in their composition, and great efficiency of encapsulation. Emulsions droplets can be as small as bacteria, with diameters of 1 μm and volumes of less than a femtolitre, or can have droplets of diameters up to 100 μm and volumes of nearly 1 nanolitre. Their high capacity (**>**10^{10} droplets in 1 mL of emulsion), the ease of preparation, and their high stability over a broad range of temperatures, pH and salt concentrations render w/o emulsion ideal for compartmentalizing biochemical and genetic reactions[35]. W/o emulsions have been used for a long time for direct in *vitro* evolution and recently as container for biochemical reactions. [34,35,36]

Lipid vesicles are formed by self-assembly and are composed of bilayer membranes surrounding an aqueous core. The membrane is composed of double chain amphiphiles, most notably glycerophospholipids, but can also contain cholesterol, integral membrane proteins, and ion channels. Vesicles spontaneously assembly in aqueous solution to form micron-scale compartments. A myriad of molecules such as proteins, enzymes, and nucleic acids, as well as polymers, hydrogels, and small vesicles have been encapsulated during vesicle formation[37-39]. Additionally, several types of biochemical reactions have been reconstituted inside of vesicles, including transcription and translation[40].

1.6 Water- oil emulsion Aqueous Two Phase System (ATPS).

ATPS is a good imitation of the cytoplasm. In living cells the presence of the cytoplasm provides compartmentalization, macromolecular crowding and small volume to the cell[42,43] , features that play an important role, facilitating and regulating intracellular reactions and moreover providing a heterogeneous distribution of molecules. This is the reason for which we think that just a boundary with an aqueous phase is not representative of a cell, and we considered logic the incorporation of a synthetic cytoplasm in cell-like compartment.

When two or more incompatible polymers are mixed at appropriate concentrations in aqueous solution, phase separation occurs resulting in two aqueous phases or microcompartments[44-45]. Immiscibility arises due to the high molecular weight of the polymers combined with interactions (van der Waals, hydrogen bonding, and ionic forces) between the polymer segments and can be influenced by temperature, inorganic salts, and pH .

We encapsulated in emulsion aqueous two phase systems made of polymers such as dextran, polyethylen glycol (PEG) and aqueous three phase systems made of dextran, PEG and ficoll dispersed in water, developing multicompartment systems useful for protein localization.

Chapter 2

Development of multi compartmentalized water-in-oil emulsion for the topography of genetically encoded system.

2.1 Introduction

The synthesis of our minimal artificial cell requires a logical choice of proteins from the divisome and the development of compartments with physicochemical properties able to make division. Keating and colleagues, as mentioned before, developed GVs ATPS as models of non living cell-like compartments. GVs ATPS are models of cell apolarity, have a budding morphology after osmotic deflation, and are able to divide asymmetrically. Although the presence of the ATPS inside the GVs is able to mimic the cytoplasm[46,47] , there are no biological features in these multi-compartmentalized systems. The bottleneck is represented by the encapsulation of ATPS inside GVs. ATPS can be captured by GVs only through a phase transition, a process not compatible with *in vitro* transcription/translation machinery and consequentially not compatible with building cellular mimics from the bottom-up. Phase diagrams help to determine the conditions necessary and the polymer concentrations needed to achieve immiscibility at different temperatures.

We demonstrated that w/o emulsion, due to their high stability and high efficiency of encapsulation of water phases, are good cell-like compartments for the development of genetically encoded systems. W/o emulsions are able not only to encapsulate directly ATPS in two phases, but also ATPS containing all the components necessary for in *vitro* transcription/translation reaction. Furthermore, the process of encapsulation is independent of phase diagrams and temperature transitions, permitting the development of complex compartments made of three polymers, called Aqueous Three Phase System (A3PS). A3PS, composed of dextran 10 kDa, ficoll 400 kDa and PEG 8 kDa are new

compartments and permit to have a more compartmentalized environment for the spatial localization of biological components.

2.2 Materials and Methods

2.2.1 Chemical and Materials

Polymers PEG 8,000 Da, PEG 5,000 Da, dextran 10,000 Da, ficoll 400,000 Da and PEG 5,000 Da (o-(2-aminoethyl)-o-methylpolyethylene) were purchased from Sigma-Aldrich. PEG 20,000 Da was purchased from Nektar. Mineral Oil (#M-5904) , Span 80 (Fluka) and Tween 80 (#P-8074) for the emulsion composition were purchased from Sigma-Aldrich. Sodium Dodecyl Sulphate (SDS) powder was purchased by Sigma-Aldrich. Alexa 647-conjugated dextran 10,000 Da and Alexa 488 for PEG labeling were purchased from Molecular Probes, Life Technologies. Tethramethylrhodamine isothiocyanate conjugated ficoll 40,000 Da was purchased from Sigma-Aldrich. Distilled water was purified to a resistivity of ≥ 18.2 MΩ with a Barnstead NANOPure Diamond system. Silicone spacers were from Molecular Probes (Life Technologies) and were used to enclose ATPS/emulsions on microscope slides for imaging.

2.2.2 ATPS and A3PS composition.

Three different ATPS compositions were encapsulated in mineral oil emulsions: 19.8% dextran 10 kDa and 2.8% PEG 8 kDa, 10 % dextran 10 kDa and 7% PEG 8kDa and18.5 % dextran 10 kDa and 5.5% PEG 8 kDa. The polymers were dissolved in distilled water purified to a resistivity of ≥ 18.2 MΩ and stirred on a magnetic stir plate until the solution became turbid.

The A3PS composition inserted in emulsion was 19.8% dextran 10 kDa, 2.8% PEG 8 kDa, 6% Ficoll 400 kDa. A3PS were produced by simply pipetting with a positive displacement pipettman1 mL of Ficoll 400 kDa, 30% w/w stock

solution into a bulk ATPS of 19.8% w/w dextran 10kDa, 2.8% w/w PEG 8 kDa . The final composition of A3PS is 19.8% w/w dextran 10kDa, 6% Ficoll 400 kDa and 2.8% PEG 8 kDa.

2.2.3 Treatment of the w/o emulsion with SDS.

A stock solution of 2 M SDS was prepared in 70% methanol. To 50 μL of ATPS (19.8% dextran 10 kDa, 2.8% PEG 8 kDa) in an Eppendorf tube, the SDS was added to a final concentration of 0.1 μM, 1 μM, 10 μM, 25 mM, 100 mM.

2.2.4 Encapsulation of Aqueous Two phase System in w/o emulsion.

The oil phase was freshly prepared by mixing 4.5% (vol/vol) Span 80 and 0.5 % (vol/vol) Tween 80 in 0.95 mL of mineral Oil. This mixture was vortex until the Span 80 was completely dissolved in the mineral oil. 0.05 mL of bulk ATPS or bulk A3PS were added to the oil phase and vigorously vortex until the dispersion became cloudy.

2.2.5 Encapsulation of in vitro transcription/translation system in ATPS/emulsion and expression of m YPET

The mixture for protein production was prepared in a test tube by adding 250 ng of plasmid DNA encoding mYPet to 20 μL of the in vitro transcription/translation system. For the in ***vitr***o transcription/translation system we used the PURESYSTEM (NEB, New England Biolabs). The reaction was performed on ice in order to prevent unnecessary reaction and then the reaction was encapsulated in ATPS, gently mixing in an Eppendorf tube 25 μL of ATPS (19.8 % dextran 10 kDa, 2.8 % PEG 8 kDa) and 25 μL of reaction. The reaction was encapsulated inside the ATPS was further encapsulated into to the oil phase, as described previously[48]. The expression of mYPET was obtained by incubating the emulsion at 37 °C for at least 2 hours.

2.2.6 Preparation of A2PS and A3PS/emulsion samples and PURE SYSTEM ATPS/Emulsion samples for confocal microscopy.

The dextran phase in A2PS/emulsion samples was labeled with Alexa 647 conjugated dextran 10 kDa or with Alexa 647 conjugated dextran 40kDa with a final concentration of 4 mg/mL. The PEG phase in A2PS/emulsion samples was labeled with Alexa 488 conjugated PEG 20 kDa with a final concentration of 7.2 mg/mL. The dextran phase in A3PS/emulsion samples was labeled with Alexa 647 conjugates dextran 10 kDa or with Alexa 647 conjugated dextran 40 kDa with a final concentration of 0.8 mg/mL. The PEG phase was labeled with Alexa 488 conjugated PEG 20 kDa or PEG 5 KDa with a final concentration of 3.6 mg/mL. Finally the Ficoll phase, in A3PS emulsion, was labeled with tethramethylrhodamine isothiocyanate at a final concentration of 12 mg/mL. The expression of mYPet, that has an excitation wavelength at 517nm and an emission at 530 nm, inside ATPS/emulsion was evaluated by confocal microscopy exploiting the fluorescent properties of the protein.

A2PS, A3PS and PURE SYSTEM /ATPS emulsion samples were observed in sample chambers, constructed by placing a 20 x 5-mm silicon spacer (Molecular Probes) onto a microscope slide.

2.2.7 Instrumentation.

Confocal images were obtained with a Leica TCS SP5 laser scanning confocal inverted microscope using a 63x oil objective equipped with galvanometric stage and a 63.3x /1.4 NA HCX PL APO oil - immersion objective. Z step size was 0.3 μm or where mentioned 0.1 μm. Ar, He and Ne laser lines were used for mYPet (λ = 517 nm), Alexa-647 (λ = 633 nm), Alexa 488 (λ = 488 nm) excitation, Rhodamine thio-isocyanate (λ = 543 nm). Fluorescence emission was collected in the ranges 527–600, 670–750 (Alexa 647), 498-550 nm, 553-600 for mYPet, Alexa 647, and Alexa 488, Rhodamine Thioisocianate, respectively. For the two- and three-color analysis, a sequential image acquisition was used to

reduce crosstalk between different signals below 5%. Multichannel images were analyzed in ImageJ (NIH.gov).

2.3 Results and Discussion

2.3.1 Encapsulation of ATPS in w/o emulsions.

In general the construction of a phase diagram is of crucial importance for the encapsulation of ATPS in GVs and for the understanding of polymer compositions to use. In order to define the conditions for the encapsulation of ATPS inside of water-in-oil emulsions we tried to build phase diagrams at different temperatures using the method of cloud point titration. In this method, one aqueous polymer solution (PEG 8 kDa) is added drop wise to the other aqueous polymer solution (dextran 10 kDa) until the solution turns opaque, an indication that the polymer solution is entering in the two-phase region. Water is then added to the point at which the solution turns clear. The weights of the polymer solutions are recorded at each step, and the procedure is repeated. A graph of the polymer weight percent compositions is constructed, and the compositions at which the solution is one or two-phases is determined by a binodial curve. At polymer weight percentage below the binodial, the solution exists as a single phase while above the line, phase separation will occur. In Fig. 2.1 is reported a phase diagram at 4 °C for our system made of PEG 8 kDa and dextran 10 kDa. The phase diagram reported does not show the typical profile of a binodial curve, but was useful to verify some points above the curve, if arise in two phase, and a couple below the curve, if arise in one phase.

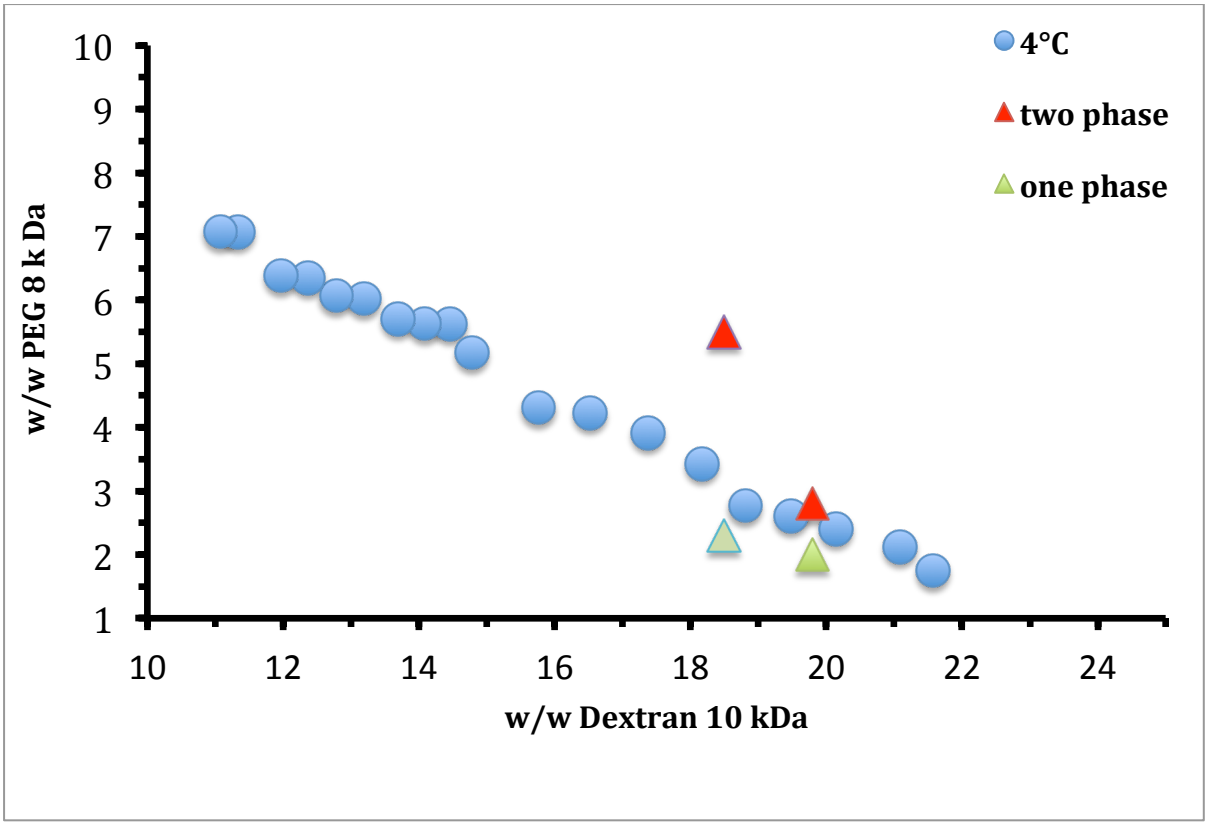

Fig 2.1: Phase diagram at 4°C for dextran 10 kDa and PEG 8 kDa. The profile of the curve does not correspond to the profile of a binodial curve. In general, a solution of 20% w/vol dextran 10 kDa was titrated with a solution 30% dextran w/vol and added drop wise to the other aqueous polymer solution (dextran 10 kDa) until the solution turns opaque, an indication that the polymer solution is entering in the two-phase region. Water is then added to the point at which the solution turns clear. The weights of the polymer solutions are recorded at each step, and the procedure is repeated, until to obtain 19 points. The phase of some points above the curve (red triangles) and the phase of some points below the curve (green triangles) was verified.

We encapsulated in w/o emulsion by vigorous vortexing an ATPS composition of 19.8% dextran 10 kDa and 2.8% w/w PEG 8 kDa, which in bulk solution appeared in two phase. The emulsion was able to encapsulate the ATPS directly in two phase and the droplets appear surrounded by mineral oil (Fig.2.2). In addition the droplets show a budding morphology.

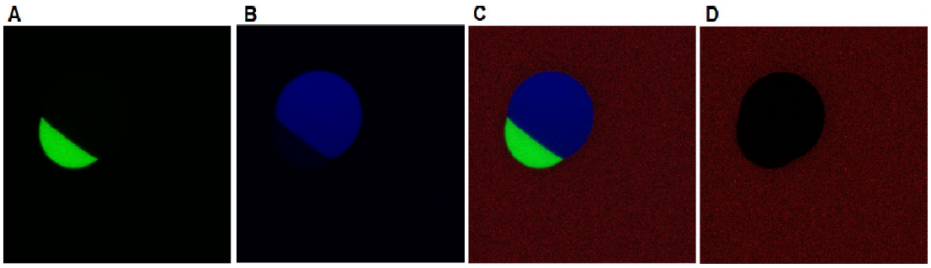

` **2.2**: A composition 19.8% dextran 10 kDa and 2.8 % PEG 8 kDa is encapsulated in w/ o emulsion. The dextran occupy the major part of the volume of the droplets .The droplets show a budding morphology. The rhodamine is spread in the oil. W/o emulsions ATPS are false colored, in green for PEG 8 kDa labeled with PEG 20kDa-Alexa 488(A), in blu for Dextran 10 kDa labeled with Dextran 20kDa-Alexa 647(B), in red for the mineral oil labeled with Rhodamine-HCl(D). Panel C is a merge of all the three channels.

We observed that the composition of the emulsion used, 4.5% (vol/vol) Span 80 and 0.5 % (vol/vol) Tween 80 in 0.95 mL of mineral oil provided a good efficiency of encapsulation. In fact, with a modification of the percentage in volume of the surfactants to 3% (vol/vol) Tween 80 and 2% (vol/vol) Span 80, the emulsion lost the ability of retaining the two phases (Fig 2.3). We observed many droplets containing just the dextran phase or the PEG phase

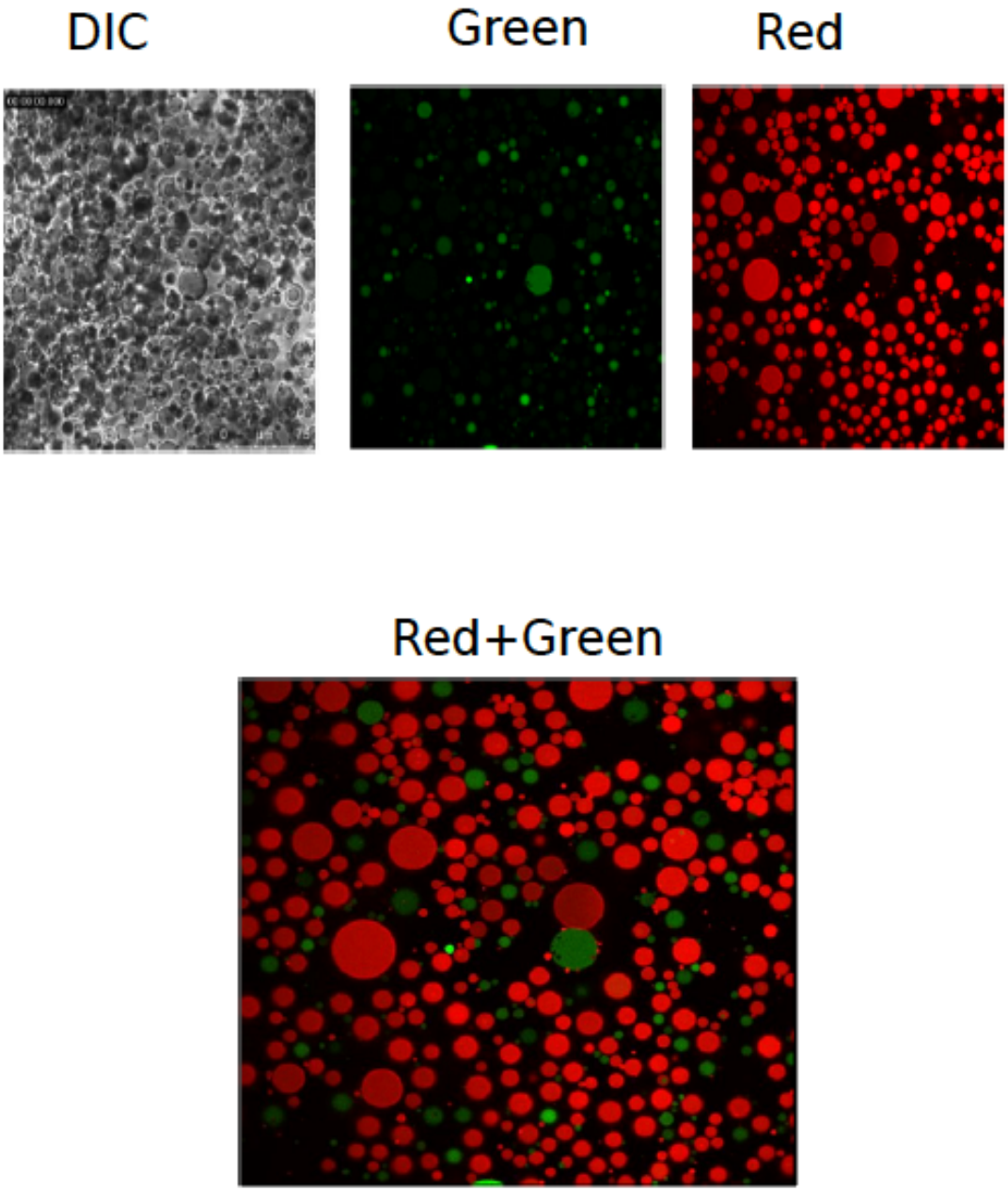

Fig 2.3: w/o emulsion ATPS with a modified surfactant composition. The efficiency of encapsulation of the emulsion of the two phases is reduced The droplets are not compartmentalized anymore, but retain in their inner volume, the PEG or the dextran. False color in red for Dextran labeled with Dextran 20kDa-Alexa 647, and green for PEG labeled with PEG 20kDa-Alexa 488.

The droplets had an interesting budding morphology (Fig.2.4) without the presence of any osmotic deflation and we observed that the polymers composition influenced the morphology of the droplets.

In contrast, another composition encapsulated (5.5% w/w PEG 8kDa and 18.5% w/w Dextran 10 kDa), existing in two phases according to the phase diagram, showed a non budding morphology (Fig. 2-4, B), but clearly the droplets had two compartments. In both the cases the PEG occupy less volume compared to the dextran.

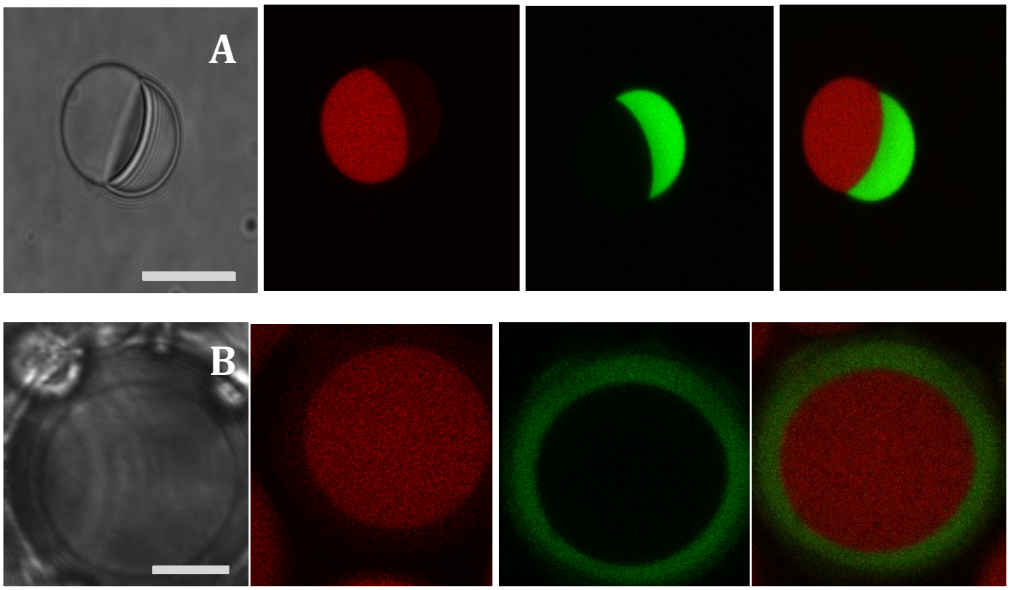

Fig 2.4: ATPS encapsulated in water-oil emulsions. Not all the composition give rise to the same morphology. Two different ATPS composition were realized in bulk solution: 19.8% dextran 10 kDa and 2.8% PEG 8 kDa, 5.5% w/w PEG 8kDa, 18.5% w/w Dextran 10 kDa. In panel A, correspondent to a composition 19.8% w/w dextran 10 kDa and 2.8%w/w PEG 8 kDa water-oil emulsion show a budding morphology. Scale bar is 10 μm. In panel B water-oil emulsion show a non budding morphology. Scale bar is 10 μm. On the left DIC images. Fluorescence images have been false colored: PEG is labeled with PEG 20kDa-Alexa 488 and is green. Dextran is labeled with dextran 20kDa-Alexa 647 and is red.

The same polymer composition, dextran 10 kDa, 10% w/w and PEG 8 KDa 7% w/w, previously encapsulated in GVs is easily encapsulated in w/o emulsion directly in two phase without any phase transition and similarly assumed a budding morphology (Fig 2-5). The advantage of our system is that we were able to encapsulate the polymers directly in two phase without undergo to phase transition, that in the case of the ATPS composition in GVs, was occurring at 43°C.

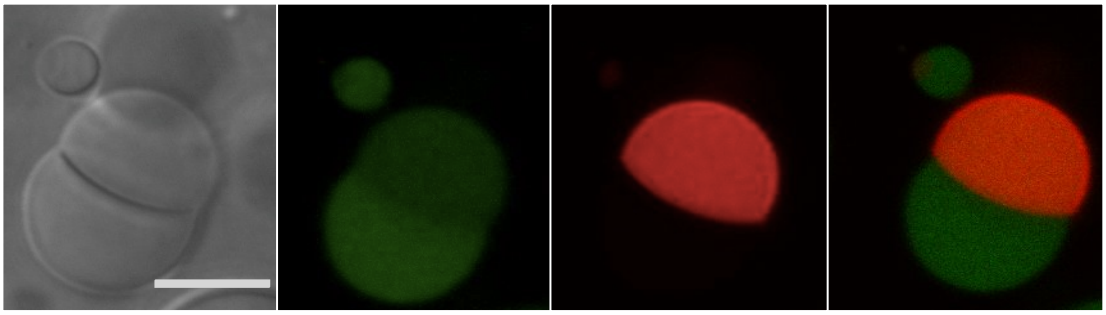

Fig 2.5: ATPS encapsulated in water-oil emulsions. The ATPS composition encapsulated is dextran 10 kDa, 10% w/w and PEG 8 KDa 7% w/w. This composition was previously encapsulated in giant vesicles. W/o/ATPS show a budding morphology. Scale bar is 25 μm. On the left DIC images are shown. Fluorescence images have been false colored: PEG is labeled with PEG 20kDa-Alexa 488 and is green. Dextran is labeled with Dextran 20kDa-Alexa 647 and is red.

2. 3.2 Treatment of w/o emulsions with SDS micelles.

The budding morphology showed by certain ATPS composition lead us to test the efficiency of the droplets to retain two phases. We treated a w/o ATPS (19.8% dextran 10 kDa, 2.8% PEG 8 kDa) with SDS micelles in order to see changing of morphology. We noticed that in absence of SDS or in the presence of a low amount of SDS, such as 0.1 mM and 1 mM, the w/o emulsions keep the compartmentalization in two phase and the budding morphology (Fig.2.6-Fig 2.7). Increasing the concentration of the SDS in the sample, we observed droplets containing just one of the two phases in their inner volume, suggesting that the droplets were dividing. In some samples treated with 25 mM SDS, we noticed droplets directed to a process of fission (Fig.2.8)

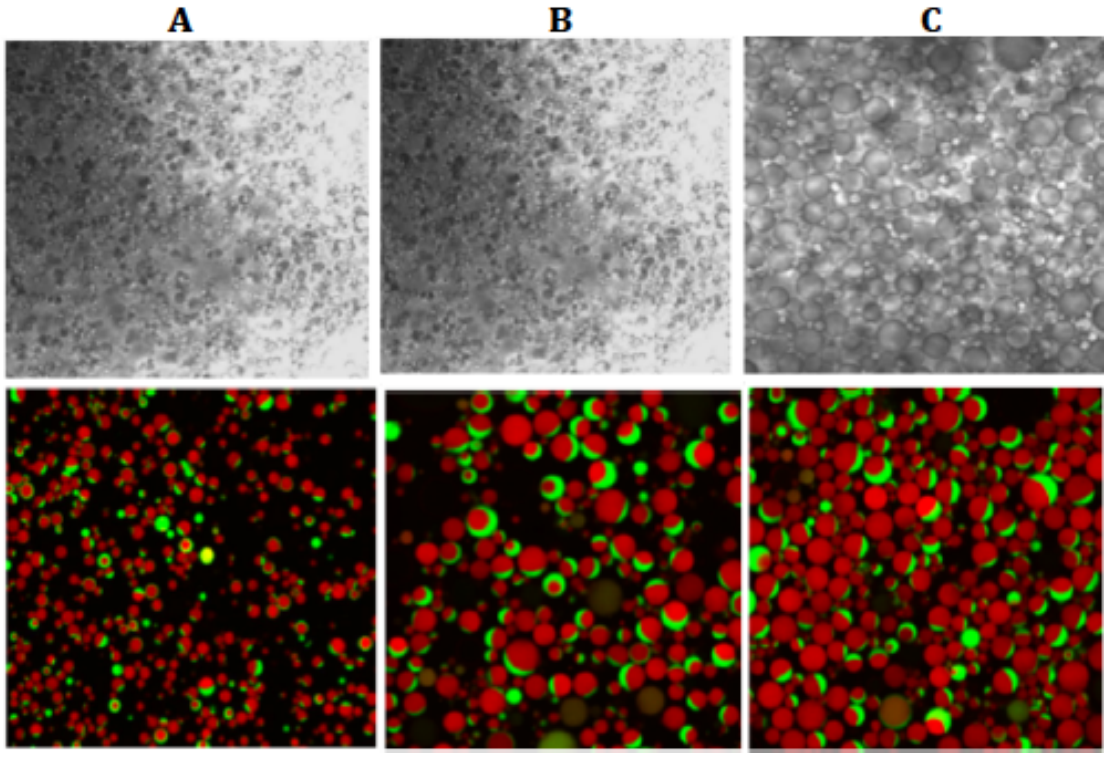

Fig. 2.6: SDS causes changing in the morphology of the w/o ATPS droplets. In absence of the SDS (panel A) the droplets have the ability of retain two phases in their inner volume. The major amount of droplets of dextran, false colored in red and labeled with dextran 20 kDa-Alexa 647, is due to the fact that the ATPS composition used forecasts an higher amount of dextran versus PEG (19.8 % dextran 10 kDa and 2.8 % PEG 8 kDa). In presence of 0.1 μM (panel B) and 1 μM (panel C) the droplets are still retaining their internal compartmentalization. The images on the top are acquired in bright-field, the images on the bottom are merge of red (dextran) and green (PEG), labeled as mentioned other times.

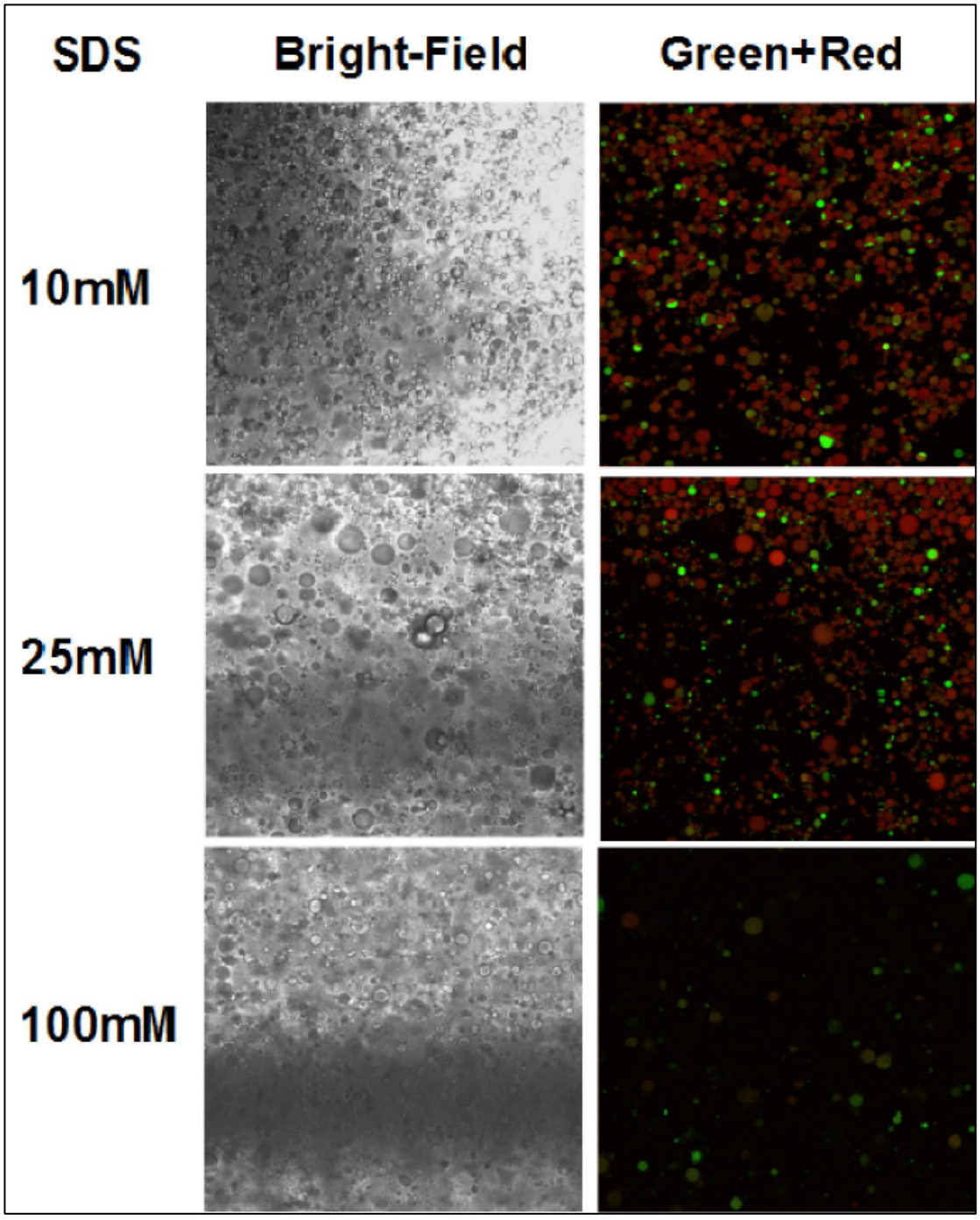

Fig.2.7: SDS causes changing in the morphology of the w/o ATPS droplets. The behavior observed suggests the possibility that the droplets, in presence of micelles of SDS can divide. Increasing concentration of SDS progressively, it is possible to see that the droplets loose their ability to retain the two phases. Bright field and merged images (dextran false colored in red, PEG false colored in green).

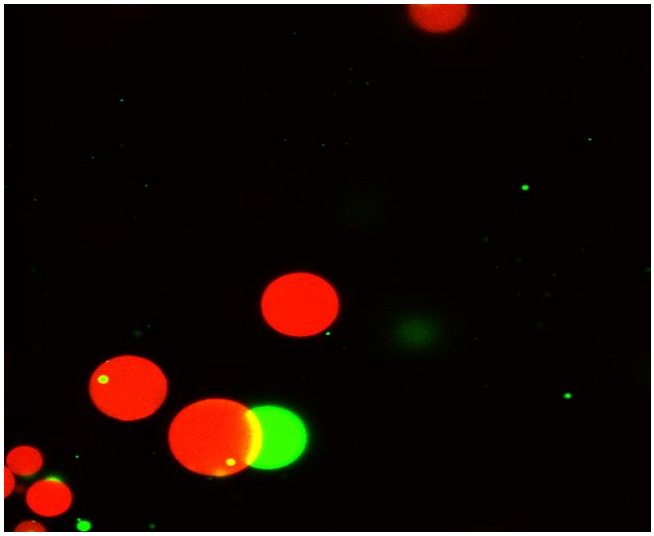

Fig 2.8: Fission of w/o emulsion ATPS in presence of 25 mM of SDS. Together with the loosing of ability of retaining two phases, we noticed that some droplets were engaged in a process of fission. This fact strongly motivated us to consider that division was occurring.

2.3.3 Expression of fluorescent proteins in w/o ATPS.

Multi compartmentalized water-in-oil emulsion with their features of easy preparation, have the big advantage of direct encapsulation of ATPS, showing ideal characteristics to guest in *vitro* T/T. Ideally an in *vitro* T/T, housed in compartments like these, should be able to produce proteins and the proteins once produced could distribute in one of two compartments. We successfully expressed mYPET in w/o emulsions, using the PURESYSTEM. The protein once produced preferred mostly the dextran phase (Fig 2.9). mYPet has an excitation wavelength at 517 nm and an emission at 530 nm, and its expression was evaluated by confocal microscopy.

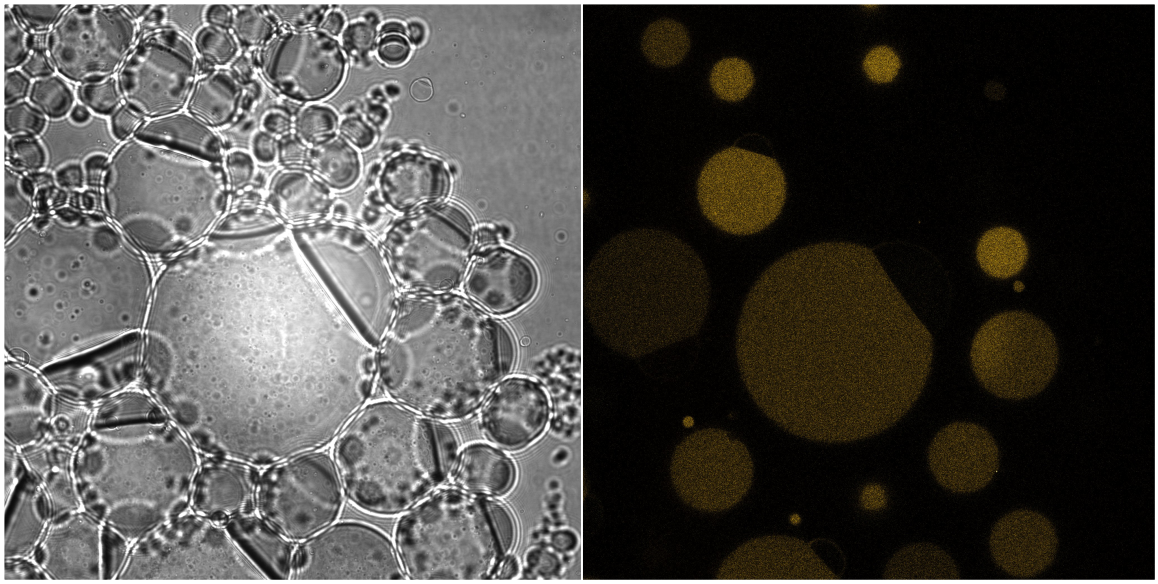

Fig 2.9: Expression by PURE SYSTEM of A206KYPet in w/o/ATPS. A PURE SYSTEM reaction expressing mYPet, was mixed with 25 μL of ATPS, then encapsulated in w/o emulsion and incubated for 2 h at 37°C.The protein prefers the Dextran phase. On the left BF image on the right fluorescence image false colored in gold. Scale bar is 10 μm. The expression of mYPet (Ex=517nm, Em=530nm) inside ATPS/emulsion was evaluated by confocal microscopy exploiting the fluorescent properties of the protein.

We aim to build genetically encoded systems in multi compartmentalized w/o emulsions for spatially localized biological components. In particular we want to build a genetically encoded system expressing FtsZ and FtsA and localize them in these compartments. In Fig.2.10 we show expression of YFP-FtsZ-FtsA inside w/o ATPS emulsions. We can notice expression of YFP-FtsZ-FtsA with a distribution in the dextran phase with some polymers distributing at the interface.

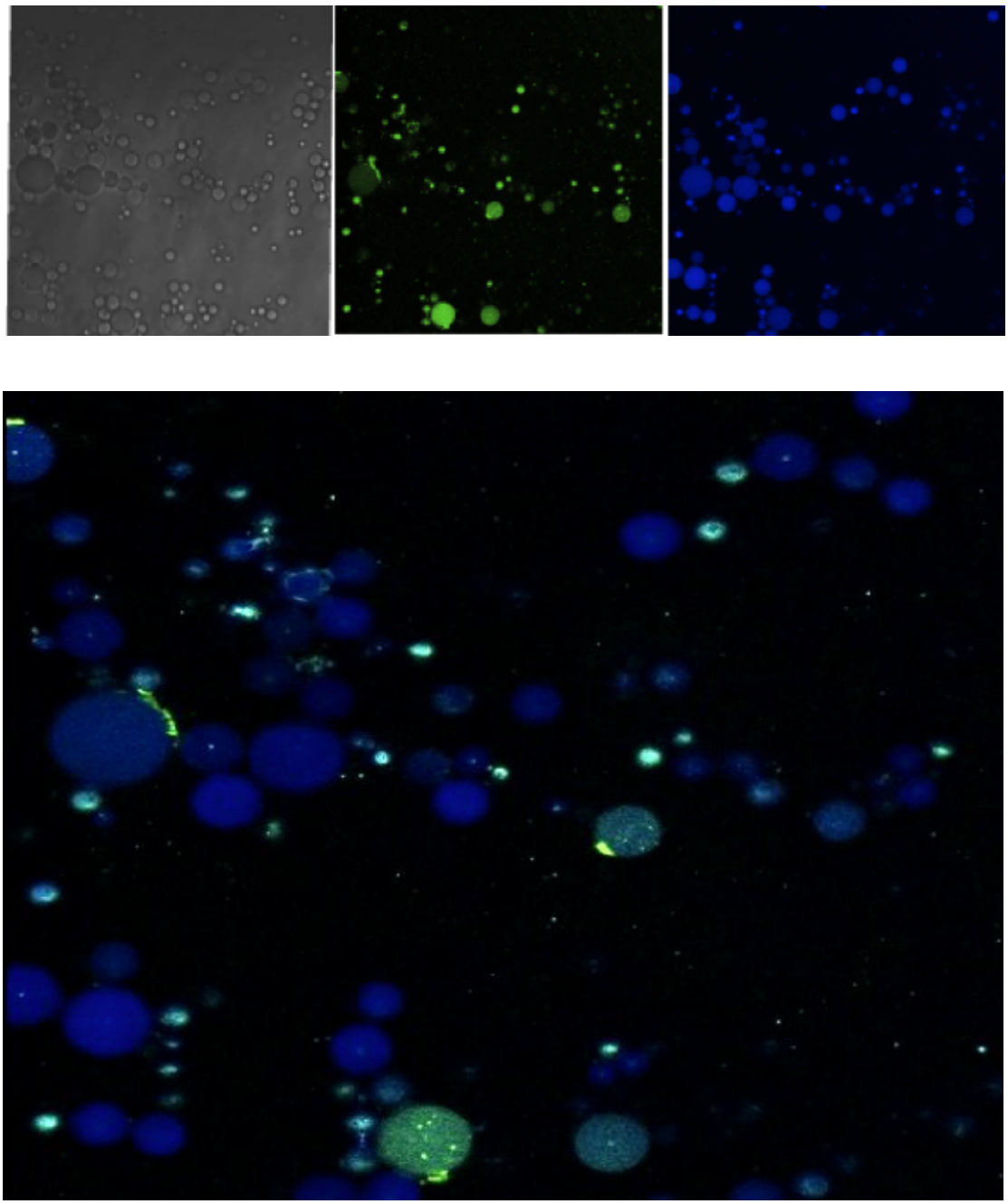

Fig 2.10:YFP-FtsZ-FtsA is expressed by PURESYSTEM in w/o emulsions ATPS after 2 h. Is possible to notice some aggregation of FtsZ proto filaments in the dextran phase.
Top, from the right, DIC image of a w/o emulsion ATPS expressing a YFP-FtsZ-FtsA by PURESYSTEM. False coloration green is for the expression of YFP-FtsZ-FtsA (YFP=YPet, Ex=517 nm, Em=530 nm), false coloration is blu for Dextran 10 kDa labeled with Dextran 20 kDa -Alexa 647.

2.3.4 Encapsulation of A3PS in w/o emulsions.

The exciting possibility of spatially localizing proteins once produced, lead us to develop water-in-oil emulsions containing Aqueous Three Phase Systems (A3PS). Aqueous Three Phase Systems are made of three polymers: dextran 10 kDa, PEG 8 kDa and Ficoll 400 kDa. The third phase is generated simply by adding a solution of 30% w/w of Ficoll 400 kDa to an ATPS with a composition of 19.8% w/w Dextran and 2.8% w/w PEG 8 kDa. Water-in-oil emulsions, also in this case, showed to be ideal for the direct encapsulation of A3PS in three phases (Figure 2.11). The third phase is represented by the Ficoll 400 and is the dark phase between the dextran phase (Dextran 40 kDa-Alexa647) and the PEG phase (PEG 20 kDa- Alexa 488), (Fig 2.11).

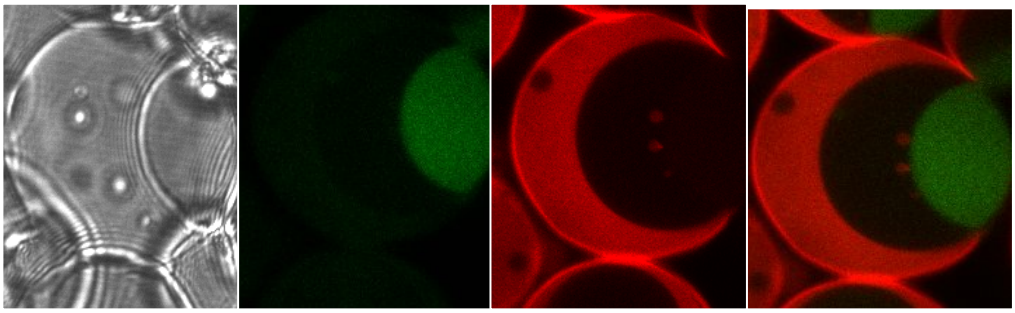

Fig 2.11: A3PS are directly encapsulated inside water-oil emulsion. A3PS are produced by adding ficoll 400 kDa, to a bulk ATPS made of 19.8% dextran 10 kDa and 2.8% PEG 8 kDa. On the left DIC image. Fluorescent images are false colored in red for Dextran 40kDa-Alexa 647, in green PEG 20kDa-Alexa 488 . In the middle of this two phase there is the ficoll 400 kDa, labeled with ficoll 40 kDa tethramethylrhodamine isothiocyanate . Scale bar is10 μm.

In order to confirm the presence of the third phase between the Dextran and the PEG, we labeled the Ficoll 400 kDa using ficoll 40 kDa tethramethylrhodamine isothiocyanate. The emulsion is able to retain effectively in the aqueous compartment three polymers that separate according to their physicochemical properties and their molecular weight (Fig.2.10).

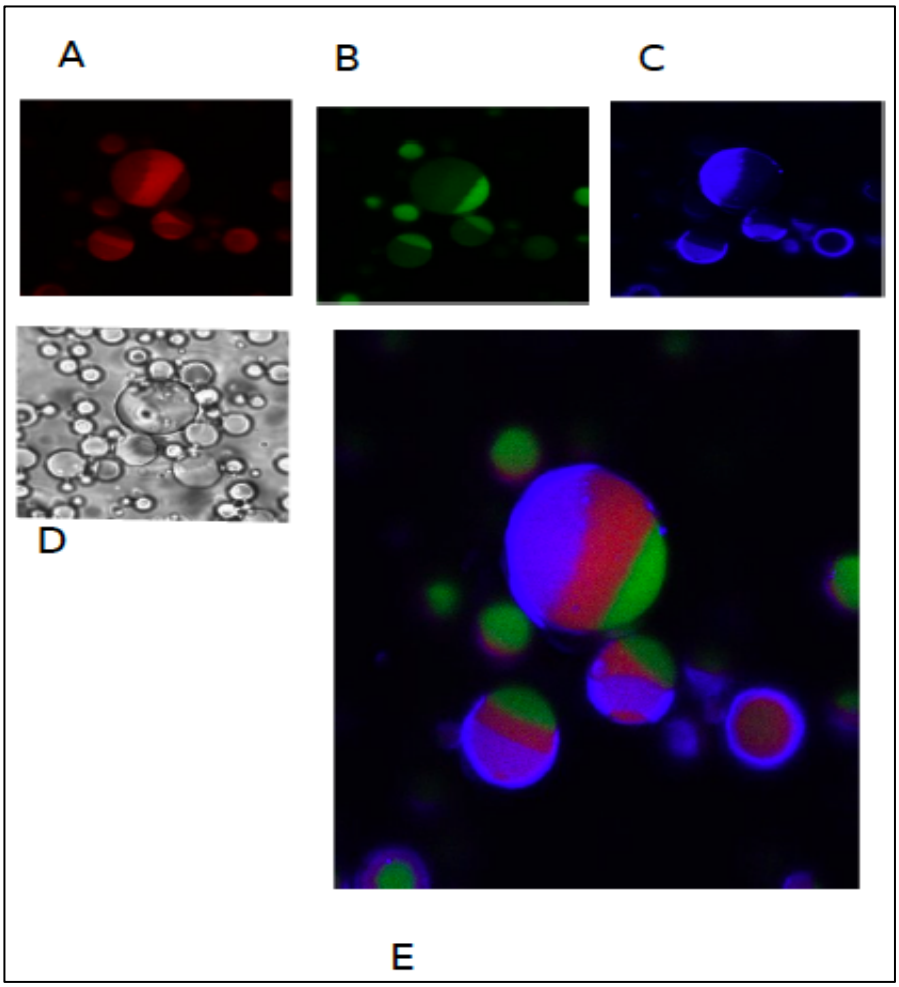

Fig 2.10: Is possible to label the third phase constituted by the ficoll 400 kDa in w/o A3PS. The A3PS composition is of 19.8% dextran 10 kDa, 2.8% PEG 8 kDa, 6 % ficoll 400 kDa. DIC images(panel D). Fluorescent images are false colored, in red for the Ficoll 400 kDa labeled with Ficoll 40 kDa tethramethylrhodamine isothiocyanate (panel A), in green for PEG labeled with PEG 20 kDa- Alexa 488 (panel B), in blu for Dextran labeled with Dextran 40kDa-Alexa 647. Scale bar is 25 μm.

Chapter 3

Reconstitution of a synthetic minimal divisome in w/o emulsions and in phospholipids vesicles

3.1 Introduction

Cell body division is a feature of life still difficult to be reproduced in a laboratory. There are advancements, as discussed before, that demonstrate the possibility to reconstitute the main features of cell body division in cell-like compartments and the difficulty in mediating compartments division. Herein we describe our efforts to reconstitute a genetically encoded system of minimal division machinery both in phospholipids vesicles and in w/o emulsions. We developed a genetically encoded system made of FtsZ and FtsA. FtsZ and FtsA , in w/o emulsions and in phospholipids vesicles, assemble together and form ring-like structures.

The assembly of our genetically encoded system required the engineering of some fluorescent constructs to monitor the expression of FtsZ and FtsA in the compartments and the choice of a T/T system for their optimal expression. Ericksson and colleagues, as discussed in the first chapter, demonstrated that a FtsZ-YFP-MinD, purified and encapsulated in multilamellar tubular liposomes[21] , is able to reproduce the typical phenomena of cell division. FtsZ, in this construct, comprise amino acids from 1-366 of *E.* coli sequence and at the C-terminus has a yellow fluorescent protein (YFP-Venus) followed by an amphiphatic helix made of 15 aminoacids (FIEEEKKGFLKRLFGG). It is important to notice that the amphiphatic helix is the membrane targeting sequence (MTS) of MinD and is similar to the amphiphatic helix of FtsA sequence.[49] Although FtsZ-YFP-MinD forms polymers in liposomes that generate membrane indentations, the Z-ring does not divide the liposome into daughter compartments.

FtsZ-YFP-MinD is an engineered version of FtsZ with remarkable activity that, nevertheless, is incapable of mediating divison. We envisioned exploiting similar and more natural divisome machinery in cell-like compartments. However, our systems would be genetically encoded rather than relying on purified proteins. Towards this end, we engineered a pool of genetic constructs that were tested in *vitro* and then were combined in compartments in order to have a system potentially able to divide. Our pool of genetic constructs for FtsZ is represented by FtsZ-YFP-MinD and YFP-FtsZ, for FtsA by Cyan fluorescent protein FtsA and superfolder-GFP-FtsA. Unfortunately, we were not able to produce in *vitro* a fluorescent version of FtsA and this lead us to design a system with just FtsZ labeled with a YFP. FtsZ and FtsA, although successfully produced in compartments, are not able to generate division and constriction of the compartments but are able to assemble in ring-like structures.

3.2 Results and Discussion

3.2.1Engineering of fluorescent genetic constructs for the synthesis of a minimal divisome made of FtsZ and FtsA.

The detection of our genetically encoded system in *vitro* or in compartments needs the engineering of fluorescent genetic constructs. The engineering of fluorescents constructs permit evaluation by fluorescence spectroscopy and fluorescence microscopy of the synthesis of our minimal division machinery system in *vitro* and in compartments. In order to reach this goal, we engineered fluorescent genetic constructs for FtsZ and FtsA.

FtsZ-YFP-MinD is our model construct for FtsZ. The sequence of FtsZ-YFP-MinD was synthesized in a pUC57 vector by Genscript and then was subcloned in a pET21b vector. The design of the construct made by Ericksson, comprised 1-366 amino acids of the FtsZ sequence from *E.* coli. In contrast, our version of FtsZ-YFP-MinD comprised 1-368 amino acids of the sequence of FtsZ from *E. coli*, optimized by Genscript, followed by a YFP-Venus and a C-terminal helix from *E.*

coli MinD. FtsZ-YFP-MinD at the N-terminus has a tag of 6 Histidines (6HisX), useful for the later purification of the protein. Competent *E. coli* cells were transformed with the construct synthesized in a pUC57 vector, encoding 6HisX-FtsZ-YFP-MinD. The plasmid DNA was extracted and purified and then amplified by polymerase chain reaction (PCR). Two different polymerases were tested, HotStart *Taq* DNA polymerase (NEB) and *Taq* DNA polymerase (RBC). The main difference between these two DNA polymerases is represented by the fact that the HotStart *Taq* DNA polymerase does not have activity at room temperature. HotStart *Taq* DNA polymerase is a mixture of *Taq* DNA polymerase and an aptamer-based inhibitor. The inhibitor binds reversibly to the enzyme, inhibiting polymerase activity at temperatures below 45°C, but releases the enzyme during normal cycling conditions, allowing reactions to be set up at room temperature. The presence of the inhibitor helps the specificity of the reaction of DNA amplification. However, both the two polymerases were able to amplify the gene encoding for FtsZ-YFP-MinD (Fig.3.1). The insert amplified by *Taq* polymerase was digested with NdeI and XhoI and ligated into a pET21b vector.

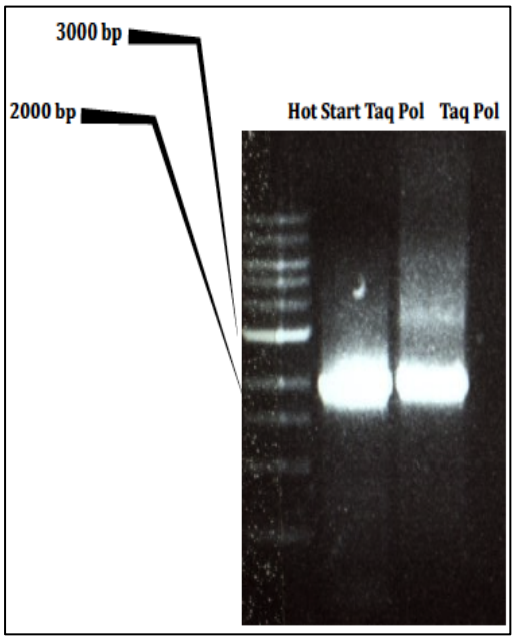

Fig.3.1: 1% agarose gel electrophoresis in Tris-Acetate-EDTA (TAE) buffer 1X. *ftsZ-yfp-minD* (pUC57) is properly amplified by Hot Start DNA polymerase (NEB) and *Taq* DNA Polymerase (RBC). The length of the gene is 1962bp. The ladder used is a 1kb ladder (NEB).

FtsZ-YFP-MinD served as model for the later engineering of our own construct YFP-FtsZ. This construct is designed in order to have the YFP (YPet) at the N-terminus of FtsZ and the C-terminus free for the interaction with FtsA. YFP-FtsZ was synthesized by Genscript in a pUC57 vector and comprised the whole sequence of FtsZ from *E. coli*. YFP-FtsZ was amplified by Hot Start *Taq* DNA polymerase (NEB) and *Taq* DNA polymerase (RBC) (Fig.3.2) and then isolated from pUC57 by BamHI and NdeI digestion followed by ligation into pET21b. We were able to subclone easily two fluorescent versions for FtsZ, ready to be used in our genetically encoded system.

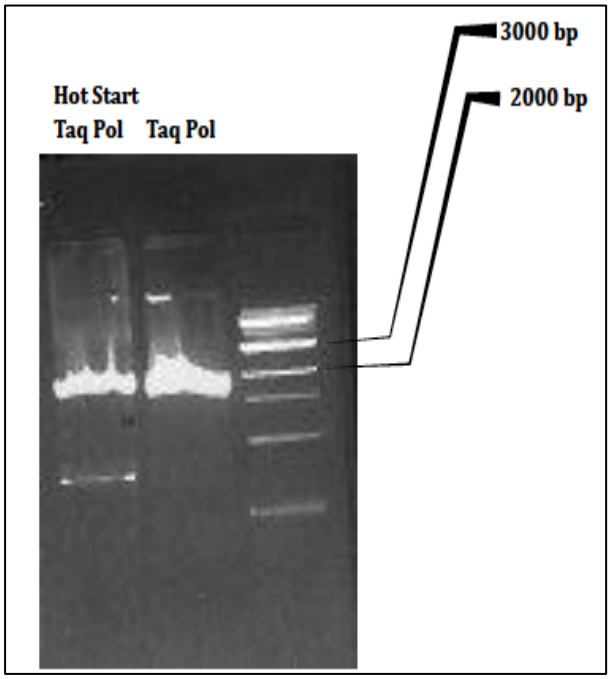

Fig.3.2: 1% agarose gel electrophoresis in Tris-Acetate-EDTA (TAE) buffer 1X. *yfp-ftsZ* (pUC57) is properly amplified by Hot Start DNA *Taq* polymerase (NEB) and *Taq* DNA polymerase (RBC).The length of the gene is 2015 bp. The ladder used is a 1 kb ladder (NEB).

We attempted to make fluorescent constructs also for FtsA, and in turn designed FtsA with the N-terminus fused with a fluorescent protein and the C-terminus free for the interaction with the membrane. The fluorescent proteins were designed with a 6 HisX tag at the N terminus. The constructs that we made for FtsA were labeled with a Cyan fluorescent protein (CFP-FtsA, CFP-R286W FtsA) or with super folder GFP (sfGFP-FtsA).

CFP-FtsA was synthesized by Genscript in a pUC57 vector and then subcloned in a pET21b vector. The CFP in this construct is a CyPet. CFP-FtsA in pUC57 was amplified by a HotStart Taq polymerase (NEB) and Taq polymerase (RBC) (Fig.3.3) and then digested by NdeI and BamHI and ligated into pET21b. For the construction of our genetically encoded system, on one hand we aimed to be minimal, respecting the logic of the cell division machinery system of *E. coli* and selecting the two key proteins that drive cell division, FtsZ and FtsA. On the other hand, we built a pool of genetic constructs to be combined in order to get compartments division. For this reason we enriched our pool of proteins with a mutated version of FtsA, R286W FtsA. R286W FtsA in *vivo* can substitute FtsA and divide *E. coli* cells, replacing the need of ZipA for cell division, and furthermore acts on FtsZ filaments .[50] This mutated version synthesized by Genscript in a pUC57 vector, was amplified by PCR (Fig. 3.4) and sub cloned exactly in the same way of CFP-FtsA.

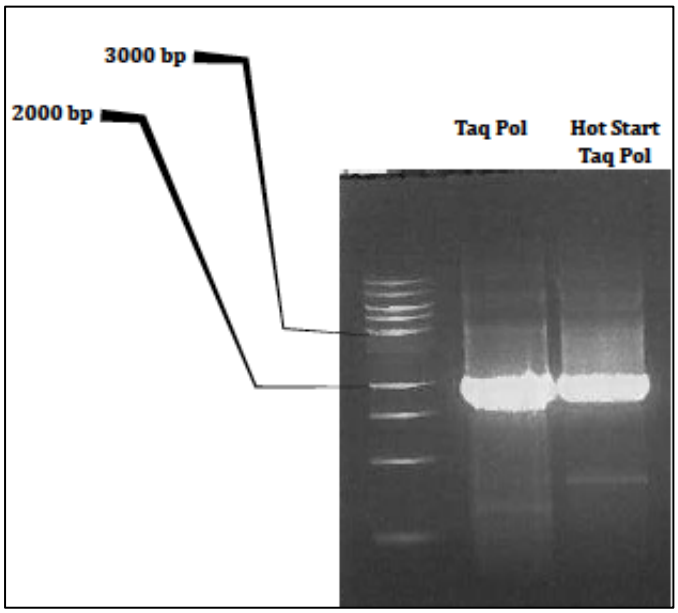

Fig.3.3: 1% agarose gel electrophoresis in Tris-Acetate-EDTA (TAE) 1X. *cfp-ftsA* (pUC57) is properly amplified by Hot Start DNA *Taq* Polymerase (NEB)and *Taq* DNA Polymerase (RBC). The length of the gene is 2070bp. The ladder used is a 1kb ladder (NEB).

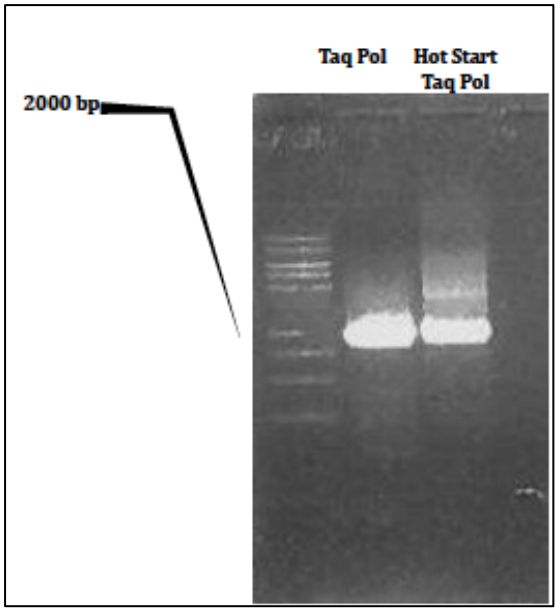

Fig.3.4: 1% agarose gel electrophoresis in Tris-Acetate-EDTA (TAE) 1X.*cfp-R286W ftsA* (pUC57) is properly amplified by Hot Start DNA *Taq* Polymerase (NEB) and *Taq* DNA Polymerase (RBC). The length of the gene is 2070 bp. The ladder used is a 1kb ladder (NEB).

The expression of CFP-FtsA and CFP-R286W-FtsA, as will be discussed later, was challenging both in *vivo* and in *vitro*. For this reason, we engineered an alternative construct for FtsA, sfGFP-FtsA[51]. The sequence of FtsA in this construct is the wild-type sequence of FtsA from *E. coli* inserted in a pET15b vector. Super folder GFP is a protein with excellent properties of folding[52], an important requirement to consider for the optimal expression of fusion proteins with fluorescent proteins. The peculiarity of this construct is the presence of a linker made of 6 amino acids (GSGSGS) between the sGFP and FtsA. In fusion proteins, the presence of a flexible linker made of amino acids, such as glycine and serine, can help the folding of both the proteins. We followed two different approaches to realize sfGFP-FtsA. We tried in a first moment to obtain *sfgfp* fused with *ftsA* by overlapping PCR but we failed, so we subcloned separately *sfgfp* and *ftsA* in pET28b. The overlapping PCR is an ideal protocol to attach two separate PCR products together. The primers are designed in order to have a short overlap of complementary sequence (typically 30 – 60 bp). The overlap can be produced by the addition of bases to the ends of the internal primers for the respective PCR products. The combination of the two PCRs products produces

the fusion between the two genes. The fusion between the two genes of interest can be subcloned in the vector of interest.

We amplified successfully *ftsA*, present in pET15b vector and *sgfp* (Fig.3.6) present in pSB1A2 vector by Phusion High-Fidelity DNA polymerase. The Phusion High-Fidelity DNA polymerase is a polymerase with 5'→3' DNA polymerase activity and 3'→5' exonuclease activity. Two buffers are provided with Phusion High-Fidelity DNA Polymerase: 5x Phusion HF Buffer and 5x Phusion GC Buffer. The error rate of Phusion DNA Polymerase in HF Buffer (4.4 x 10^{-7}) is lower than that in GC Buffer (9.5 x 10^{-7}). Therefore, the HF Buffer should be used as buffer for high fidelity amplification. However, GC Buffer can improve the performance of Phusion DNA Polymerase with GC-rich templates or those with complex secondary structures. For the amplification of *ftsA* we screened just the HF buffer (Fig. 3.5), instead for the amplification of *sfgfp* both HF and GC provided a good amplification (Fig 3.6). Due to these results, we choose the Phusion polymerase as the ideal enzyme for the overlapping PCR. We obtained the fusion of interest *sgfp-gsgsgs*-ftsA (Fig. 3.7) but we failed in subcloning the gene in pET28b. In the appendix are reported someefforts for the optimization of the overlap between the *sgfp* and *ftsA* by PCR (Fig. A1 and A2).

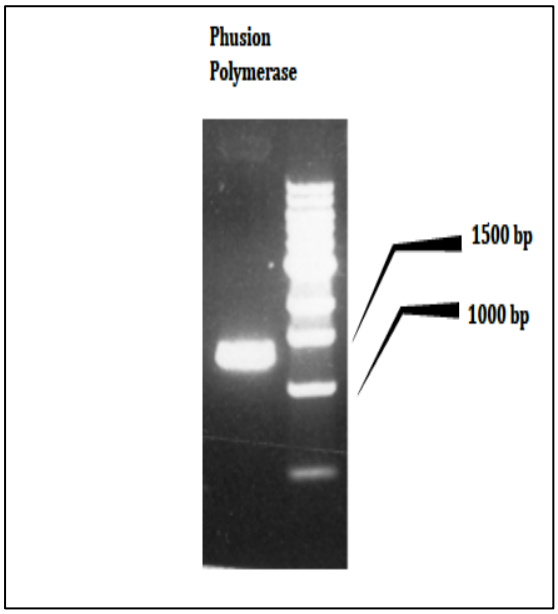

Fig.3.5: 1% agarose gel electrophoresis TAE 1X. *ftsA* (pET15b) is properly amplified by Phusion-High Fidelity DNA Polymerase (Thermo scientific) in HF buffer. The length of the gene is 1263 bp. The ladder used is a 1kb ladder (NEB).

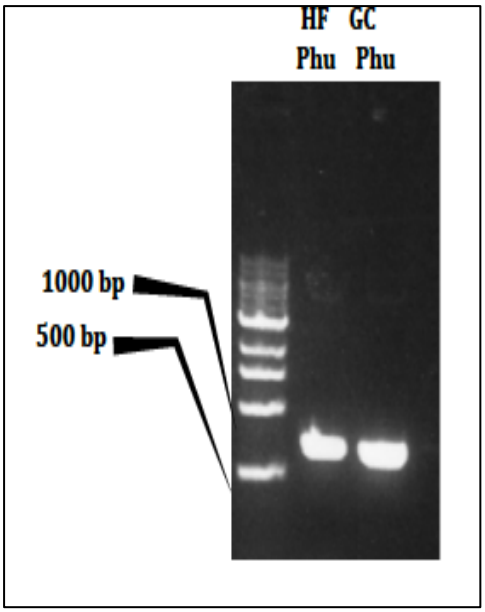

Fig.3.6: 1% agarose gel electrophoresis in TAE 1X. *sgfp* (pSB1A2) is properly amplified by Phusion-High Fidelity DNA polymerase (Thermo scientific) in both HF and GC buffer. The length of the gene is 720bp. The ladder used is a 1kb ladder (NEB).

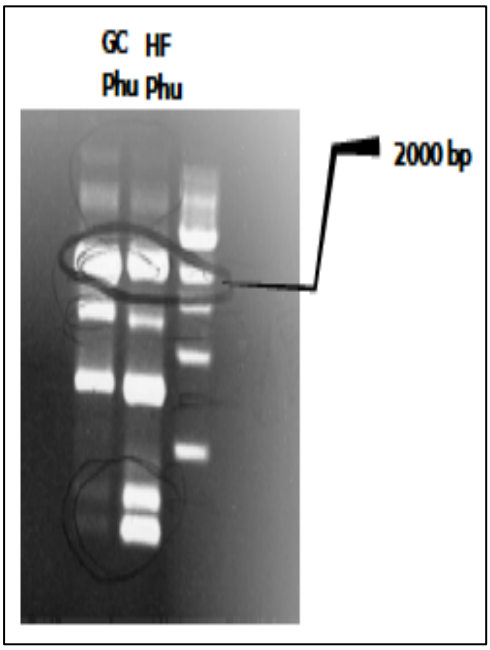

Fig3.7: 1% agarose gel electrophoresis in TAE 1X. The overlap between *sgfp and* ftsA is observed. The overlap is of 1983bp, as shown by the bands highlighted with a circle. The reaction of overlapping extension was performed with Phusion-High Fidelity DNA Polymerase (Thermoscientific) in both HF and GC buffer. The ladder used is a 1kb ladder (NEB).

In contrast we successfully realized a genetic construct encoding sfGFP-FtsA by first sub cloning *sgfp* by NcoI and BamHI in pET28b and then *ftsA* via BamHI and XhoI in the same plasmid. The nucleotide sequence of the linker is GGC TCT GGT AGC GGA TCC. As we can notice in this sequence there is a site for BamHI that we exploited for sub cloning in two steps of the two genes encoding sfGFP and FtsA.

We were able to produce a sufficient pool of fluorescent constructs for FtsZ and FtsA to test in *vitro* and in compartments. In particular, the expression in *vitro* lead us to consider the possibility of expressing a fluorescent version of FtsZ and a non-fluorescent version of FtsA.

In a first moment we were able to co-express fluorescent FtsZ and non-fluorescent FtsA inside compartments, but the co-expression of FtsZ and FtsA did not provide a fine control for our genetically encoded system. With the co-expression in fact, we can control the production of the proteins by just modulating the quantity of DNA to be used. Thus far this approach does not mimic the regulation of protein expression occurring in *vivo* and required for cell division. The *E. coli* genome offers suggestions for the fine control of our genetically encoded system. In fact, in *E*. *coli* the ratio of FtsZ versus FtsA is of 4:1. The higher amount of FtsZ is explained by the fact that ftsZ in the *E. coli* genome overlaps with *ftsQ*. In the final part of the sequence of *ftsQ* is a strong ribosome- binding site (RBS). The strong RBS corresponds to the Shine-Dalgarno consensus sequence and controls the production of FtsZ [53].

These considerations lead us to engineer constructs where initially the expression of FtsZ and FtsA is controlled by a strong ribosome-binding site. We realized three double constructs FtsZ-YFP-MinD-FtsA, FtsZ-YFP-MinD-R286W FtsA and YFP-FtsZ-FtsA . The engineering of the double constructs forecasts that the labeled FtsZ is under the control of the RBS of pET21b and the non-fluorescent FtsA is under the control of a synthetic strong RBS inserted in the forward primer. More in detail, the strong RBS sequence corresponds to the Shine-Dalgarno consensus sequence derived statistically from lining up many well-characterized strong ribosome -binding sites and has the sequence AGGAGG. The complementary sequence (CCUCCU) occurring at the 3'-end of the structural RNA ("16S") of the small ribosomal subunit base-pairs with the Shine-Dalgarno sequence in the mRNA in order to facilitate proper initiation of protein synthesis. The RBS of pET21b is placed 7 nucleotides upstream from the ATG and is exploited for control the expression of FtsZ. The expression of

FtsA instead is controlled by a synthetic RBS placed 7 nucleotides before the ATG of FtsA.

The gene encoding FtsZ-YFP-MinD in pET21b vector was amplified by Deep Vent$_R$ polymerase (NEB) and Phusion DNA Polymerase. The Deep Vent Polymerase is a high fidelity polymerase. The fidelity of Deep Vent$_R$ DNA Polymerase is derived in part from an integral 3′→ 5′ proofreading exonuclease activity. The amplification by Phusion High Fidelity DNA Polymerase was more specific than the amplification by Deep Vent$_R$ polymerase (Fig 3.8).

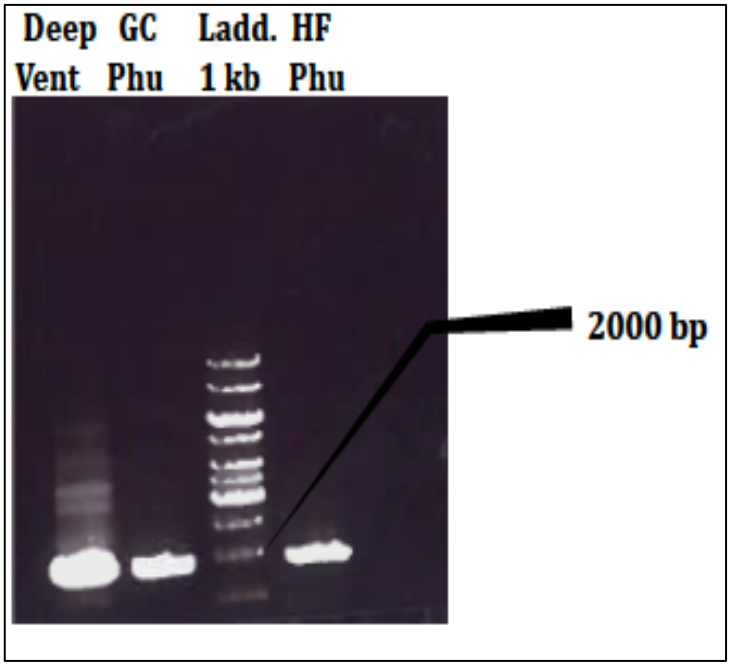

Fig 3.8: 0.8% agarose gel electrophoresis in TAE 1X. *ftsZ-yfp-min*D (1884 bp) is amplified by Phusion High Fidelity DNA polymerase in both the buffers (HF and GC). ftsZ-yfp-minD is amplified also by Deep Vent$_R$, but the amplification is less specific, as we can see from the extra bands in the sample. The ladder used is a 1kb ladder (Fermentas).

FtsA and FtsA R286W from pET21b, were amplified successfully by the same polymerases as shown in figure 3.9.

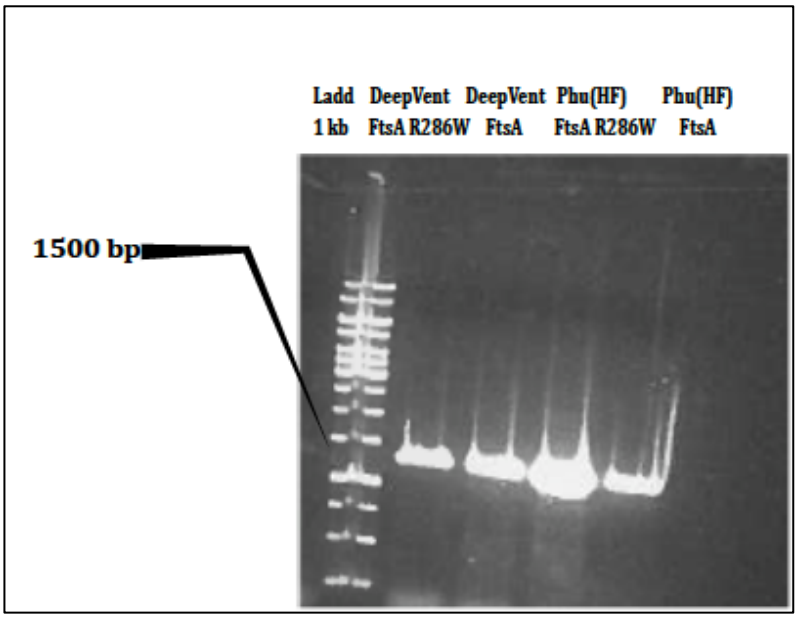

Fig 3.9: 0.8% agarose gel electrophoresis in TAE 1X. ftsA and ftsA R286W (1263 bp) are amplified by Phusion High Fidelity DNA Polimerase in HF buffer and also by Deep $Vent_R$. The ladder used is a 1 kb ladder (Fermentas).

After amplification by PCR, the gene encoding FtsZ-YFP-MinD was successfully sub cloned in pET21b by NdeI and SacI. In the resulting vector containing the gene encoding FtsZ-YFP-MinD, we sub cloned separately the genes coding for FtsA and FtsA R286W by SacI and XhoI. Similarly the gene coding for YFP-FtsZ was amplified using the same polymerases and sub cloned in pET21b and then the gene coding for FtsA was sub cloned in the same vector. In the table 3.1 are reported in detail the structure of the double constructs.

Table 3.1: A detailed description of the double constructs used. In red are indicated the parts derived from the pET21b sequence.

T7-XbaI-RBS- NdeI site - FtsZ (1-368) - EcoRI site - YFP-Venus - MinD peptide - STOP - SacI site-HindIII-RBS-A-NheI-T-FtsA-XhoI-T7 term
T7-XbaI-RBS- NdeI site - FtsZ (1-368) - EcoRI site - YFP-Venus - MinD peptide - STOP - SacI site-HindIII-RBS-A-NheI-T-FtsA R286W-XhoI-T7 term
T7-XbaI-RBS- NdeI site-YFP –FtsZ-SacI-SalI-RBS-A-NheI-T-FtsA-XhoI- T7 term

Finally the pool of synthetic constructs was enriched with the sub cloning of FtsZ and FtsA without 6xHis tag in pET21b. In the figure 3.10 and 3.11 are shown images of the two genes amplified before subcloning. We owned in our hands a sufficient pool of proteins to combine together. All the constructs obtained were confirmed by sequencing.

In the Table A1 of the appendix is reported a complete description of all the primers used for produce all the constructs described in this section.

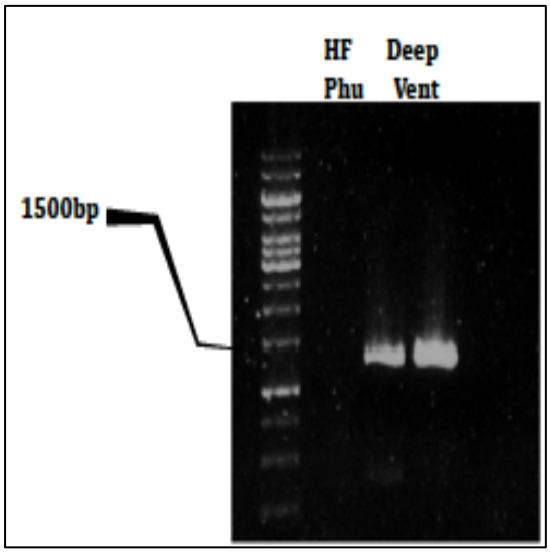

Fig 3.9: 0.8% agarose gel electrophoresis in TAE 1X. *ftsA* (1263 bp) is amplified by Phusion High Fidelity DNA polymerase in HF buffer and also by Deep Vent$_R$. The ladder used is a 1kb ladder (Fermentas).

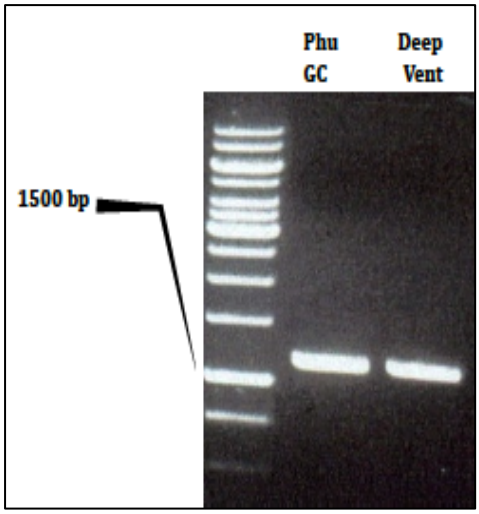

Fig. 3.10: *ftsZ* (1205 bp) is amplified by Phusion High Fidelity DNA Polymerase in HF buffer and also by Deep Vent$_R$. The ladder used is a 1kb ladder (Fermentas).

3.2.2 In *vitro* expression of FtsZ and FtsA

The expression in *vitro* of a genetically encoded system is a preliminary step to follow before the encapsulation in compartments such as phospholipids vesicles and w/o emulsions. The evaluation of the data in *vitro* gave us the opportunity to establish conditions for the expression in compartments, in terms of the type of T/T system to use and the parameters to set up, as for example time and temperature. The expression in *vitro* was evaluated by fluorescence spectroscopy exploiting the fluorescent properties of our constructs.

FtsZ-YFP-MinD was expressed in *vitro* by *E. coli* extract (PROMEGA S30) and by the PURESYSTEM for 6 h at 37°C in a cuvette (Fig.3-1). The evaluation of the expression by fluorescence was possible, exploiting the excitation and emission wavelengths of the fluorescent tag, YFP-Venus (Ex=515nm,Em=528 nm), present in the construct. The protein was successfully produced by both the T/T systems, but the production was higher with the PURESYSTEM. The result is expected, because the PURESYSTEM is free of inhibitory substances such as nucleases, proteases, and enzymes that hydrolyze nucleotide triphosphate, so permits to use a low amount of DNA and obtain a high level of protein expression. After 3h, from the start of the reaction, we noticed a significant

increase of expression of FtsZ-YFP-MinD with the PURESYSTEM.

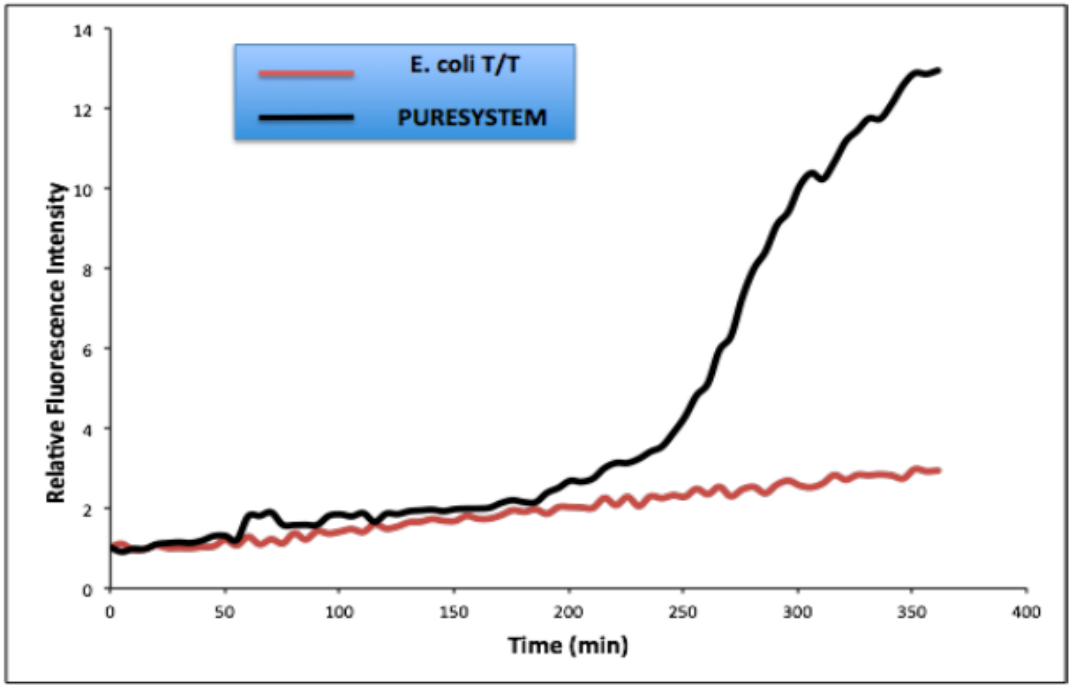

Fig 3.1: In *vitro* expression of FtsZ-YFP-MinD. FtsZ-YFP-MinD is expressed by *E. coli* extract (red line) and by PURESYSTEM (black line). The expression by PURESYSTEM increased after 3h.

The possibility of expressing FtsZ-YFP-MinD in *vitro* encouraged us to express also YFP-FtsZ. The yellow fluorescent protein in this construct is the monomeric YPet (A206K YPet, Ex=517, Em=530). YFP-FtsZ was expressed for 6 h in cuvette at 37 °C. In contrast with FtsZ-YFP-MinD, YFP-FtsZ was produced more by *E. coli* extract than by PURE system, but both the systems expressed the proteins in a fast way. Furthermore, after approximately one hour, was possible to see an increase of production of the protein expressed by the PURESYSTEM. We demonstrated that transcription and translation in *vitro* of fluorescent labeled constructs is possible and gives rise to a good yield of protein.

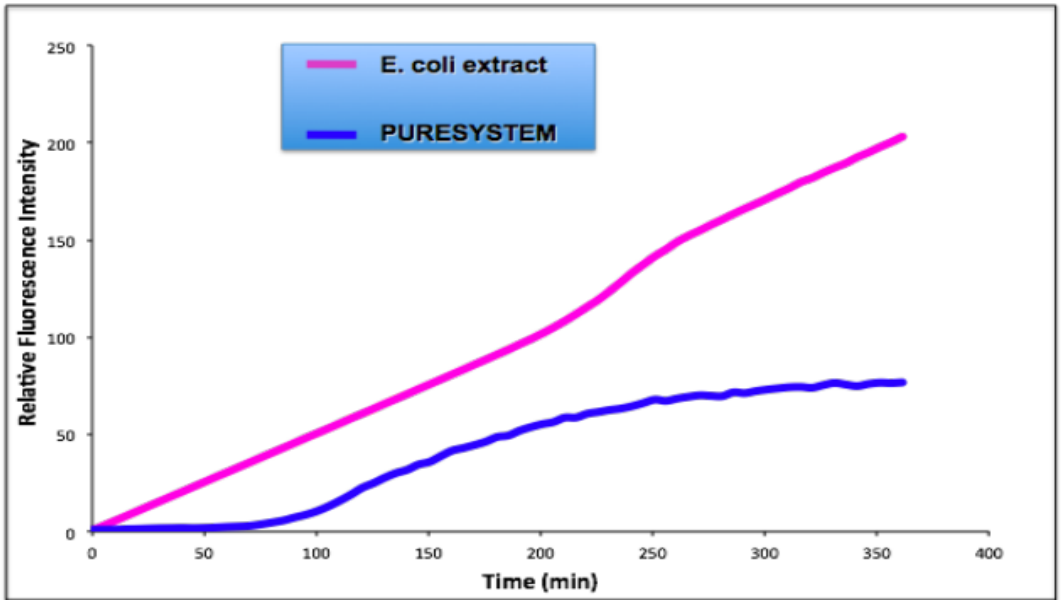

Fig.3.12: In *vitro* expression of YFP-FtsZ. YFP-FtsZ by E. coli extract (pink line) and by PURESYSTEM (blue line). The expression is higher by E. coli extract than by PURESYSTEM.

Definitively we were able to express fluorescent version for FtsZ and then we expressed fluorescent constructs for FtsA. We expressed CFP-FtsA and sfGFP-FtsA. The CFP present at the N-terminus of FtsA is a monomeric CyPet (A206K CyPet) that has an Ex=435 nm and an Em=477 nm. The in *vitro* expression of CFP-FtsA and of CFP R286W FtsA by *E. coli* extract, at 37°C for 6 h, failed (Fig.3.3). In reality *E. coli* extract expresses the protein but the proteins while are expressed precipitate in the cuvette. For these reasons and for the problems encountered with the purification of CFP-FtsA and the mutant version, we designed new constructs for FtsA.

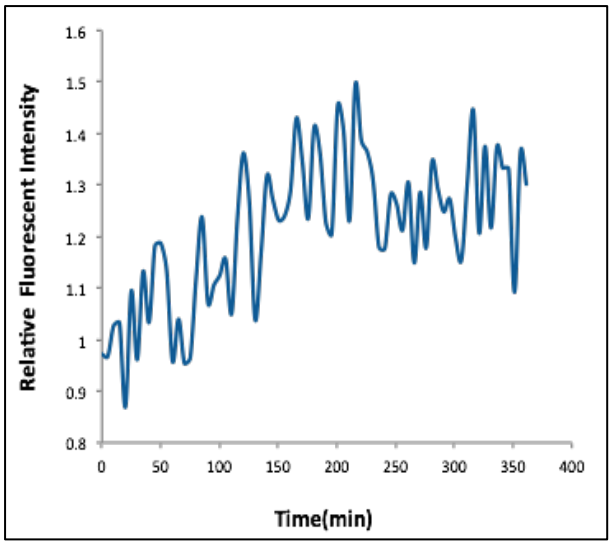

Fig. 3.13: *E. coli* extract does not express properly CFP-FtsA. The protein is expressed but during the expression precipitates and does not fold properly.

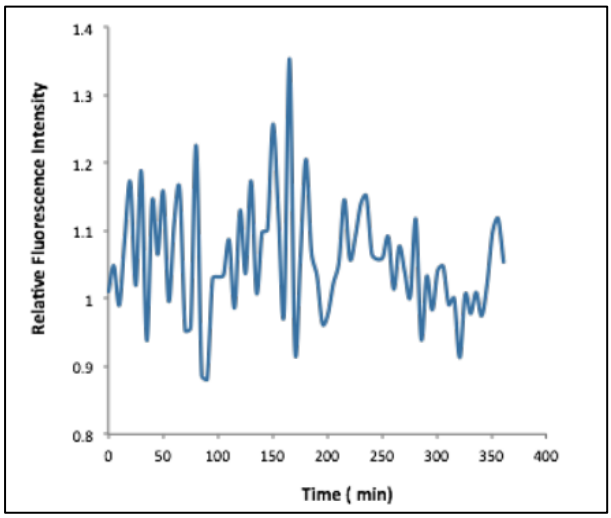

Fig. 3.14: *E. coli* extract does not express properly CFP-FtsA R286W. The protein is expressed but during the expression precipitates and does not fold properly.

At this point an evaluation of the biochemical nature of FtsA was necessary for the understanding of the proper conditions to set up for the expression of a fluorescent constructs of FtsA. FtsA is not a membrane protein but interacts with the membrane and the overexpression in *vivo* gives rise to inclusion bodies. In other words, the expression of membrane proteins or protein that are interacting with the membrane is challenging because their hydrophobic nature and require the evaluation of different strategies finalized to improve the process of folding[54].

The expression of a non-soluble protein could be improved by co-expression with an interaction partner protein or a molecular chaperone or by offering to the T/T system an artificial hydrophobic environment such as a detergent or a compartment[55]. An interaction partner protein is a protein that naturally interacts with the non-soluble, i.e FtsA interacts with FtsZ in the divisome. A molecular chaperone is a protein that help the folding of another, i.e DnaK, is a protein that in *E. coli* is involved in the process of folding. The reconstruction of a hydrophobic environment for the in *vitro* T/T system forecasts the use of mild detergents otherwise detergents that keep the native structure of the protein, or the direct expression inside w/ o emulsions and vesicles.

In our case we evaluated that *E. coli* extract is the ideal T/T system for the expression of FtsA, because the extract contains chaperones that help the folding of the protein. The sequence of FtsA, in sfGFP-FtsA, is the wild-type sequence from *E. coli* and the N-terminus is connected with the sfGFP through a linker GSGSGS. The choice to place a flexible linker between FtsA and sfGFP, was strategic in order to obtain a desired improvement of the folding of the fluorescent tag and FtsA.

E. coli extract (PROMEGA S30) was not able to express sfGFP-FtsA at 37 °C (Fig.3.15, panel A) in a time course reaction of 6 h. sfGFP (Ex=485, Em=510) as mentioned before, has excellent properties of folding[54] but although this natural features and the presence in *E. coli* extract of factors involved in the process of folding, the expression of sfGFP-FtsA was challenging. For this reason we evaluated to follow some of the strategies described before. We tried to express sfGFP-FtsA with FtsZ (Fig.3.15, panel C) in the presence of a mild detergent, such as Triton X -100 at 0.1% vol/vol (Fig.3.15, panel B) and in w/o emulsions (Fig.3.15, panel C). We did not have success, but in comparison the expression in w/o emulsion (3.19) gave some slight improvements. All the negative attempts of expression of fluorescently labeled versions of FtsA lead us to consider non-fluorescently labeled versions of FtsA for our system.

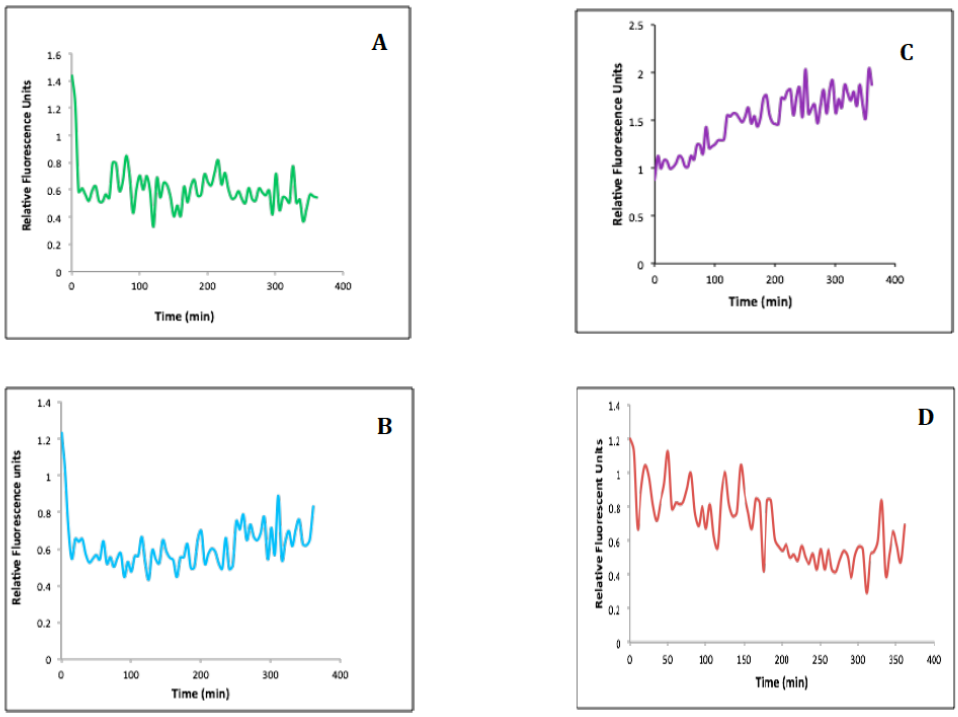

Fig 3.15: sfGFP-FtsA is not expressed properly by E, coli extract (panel A) in the presence of 0.1 % vol/vol Triton X-100 (B) and of the interaction partner protein, FtsZ (C). The expression is slightly improved when performed in w/o emulsion.

We decided to express in our system a non-fluorescently labeled version of FtsA, so we needed to demonstrate that FtsA was effectively produced by in *vitro* T/T. We radiolabeled FtsA, performing reactions of T/T in *vitro* in the presence of S^{35}, which is incorporated in the protein during its production, then just 5 µL of the reaction product were loaded on a SDS gel at 10%. The radioactivity confirmed that FtsA is expressed by in *vitro* T/T PURESYSTEM and also that YFP-FtsZ and FtsZ-YFP-MinD were successfully expressed. We did not have in our hands a radioactively labeled ladder, so we labeled the bands correspondent to the molecular weight of our interest with few µL of S^{35}, in order to verify the MW of our proteins. FtsA has a MW of 42 kDa, FtsZ-YFP-MinD of 70.2 kDa and YFP-FtsZ of 70.4 kDa. Further we tested also the expression of CFP-FtsA and CFP R286W (MW= 75.7 kDa) and of sfGFP-FtsA. sfGFP-FtsA is not expressed by PURESYSTEM .

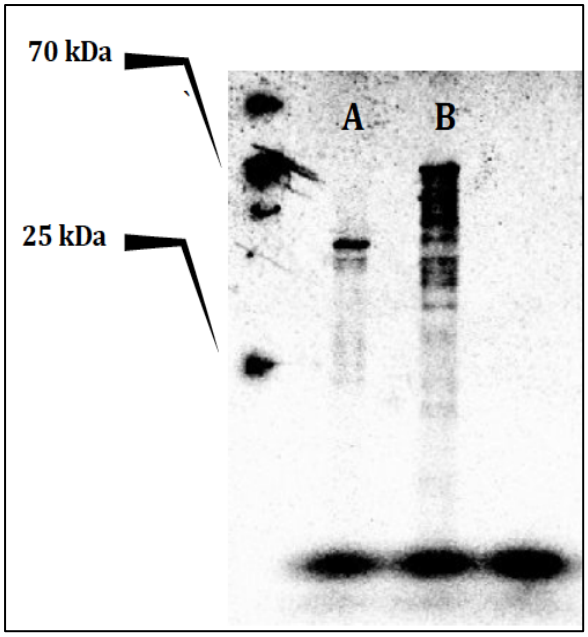

Fig 3.16: PURESYSTEM expresses FtsA and FtsZ-YFP-MinD. Lane A: FtsA (40 kDa) and lane B FtsZ-YFP-MinD (70 kDa). Protein ladder 10-250 kDa with MW=70 kDa and MW=25kDa labeled with 2μL of S35.

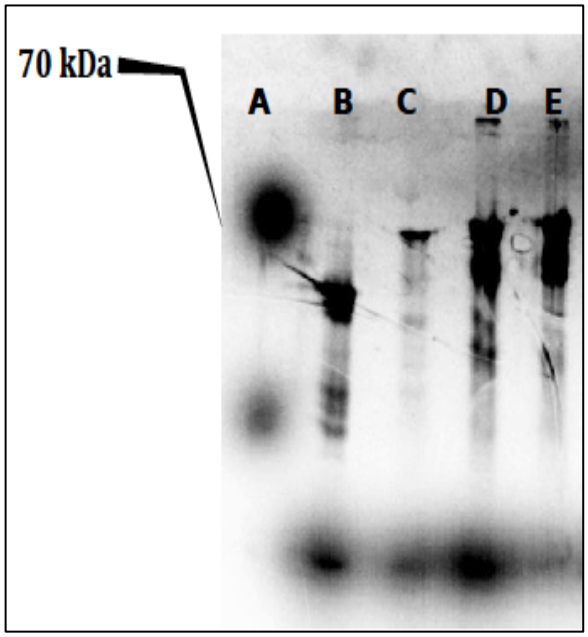

Fig 3.17: PURESYSTEM expresses FtsA, YFP-FTsZ, CFP-FtsA and CFP-R286W FtsA. From the left, lane B is expression of FtsA (42KDa,number of Methionines=9), lane C of YFP-FtsZ (70,2KDa, Met=21) lane D of CFP-FtsA (75.7KDa,Met=20) and lane E of CFP-FtsA R286W (75.7KDa,Met=20). sfGFP-gsgsgs-FtsA(72KDa**)**is not expressed by PURESYSTEM. LaneA is the protein ladder 10-250 kDa with MW=70 kDa labeled with 2μL of S35.

Instead, for CFP-FtsA and CFP R286W FtsA, that were not properly expressed by *E. coli* extract *in vitro*, we had the opportunity to confirm by radioactivity that these proteins are expressed, simply by performing the reaction with the PURESYSTEM (Fig. 3.17). Furthermore, as shown in figure 3.18, we were able to express CFP-FtsA inside phospholipid vesicles (DOPG: PC, 20:80). The vesicles were prepared following the Yomo method[56], hydratated

with 25 μL of a PURESYSTEM reaction expressing CFP-FtsA and incubated for 2 h at 37 °C. After incubation the vesicles were observed at fluorescent microscope. Thus far this result demonstrate the importance of a compartment for the expression of insoluble proteins.

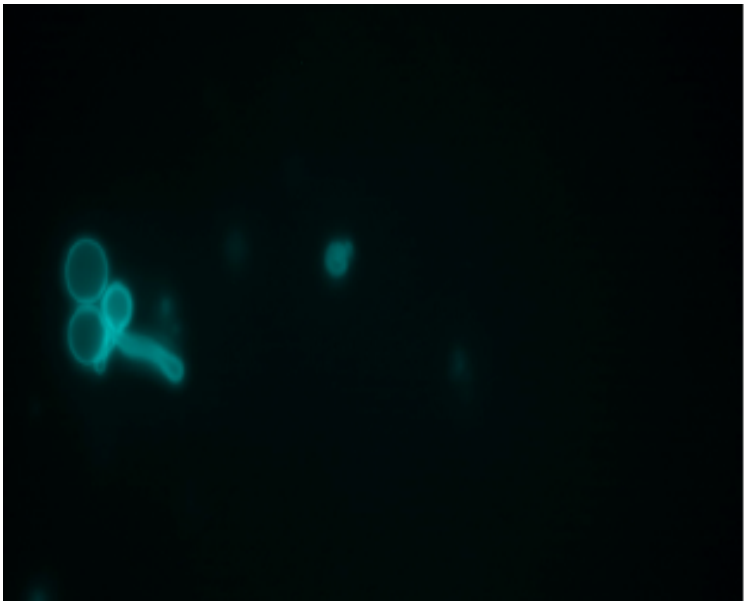

Fig 3.18: CFP-FtsA is expressed by PURESYSTEM in phospholipids vescicles, DOPG: PC, 20:80. The expression was evaluated by fluorescence microscopy and CFP (CyPet) fluorescence is false colored in cyan. Is possible to see fluorescence after 2 h of incubation of the vescicles at 37 °C.

3. 2.3 Expression in vesicles and in w/o emulsions.

Once we confirmed the possibility of expression in *vitro* of these constructs by T/T, we proceeded with the expression in w/ o emulsions. At the beginning we co-expressed two proteins at same time and then we moved to the expression of constructs containing both the proteins of interest (Fig. 3.8).

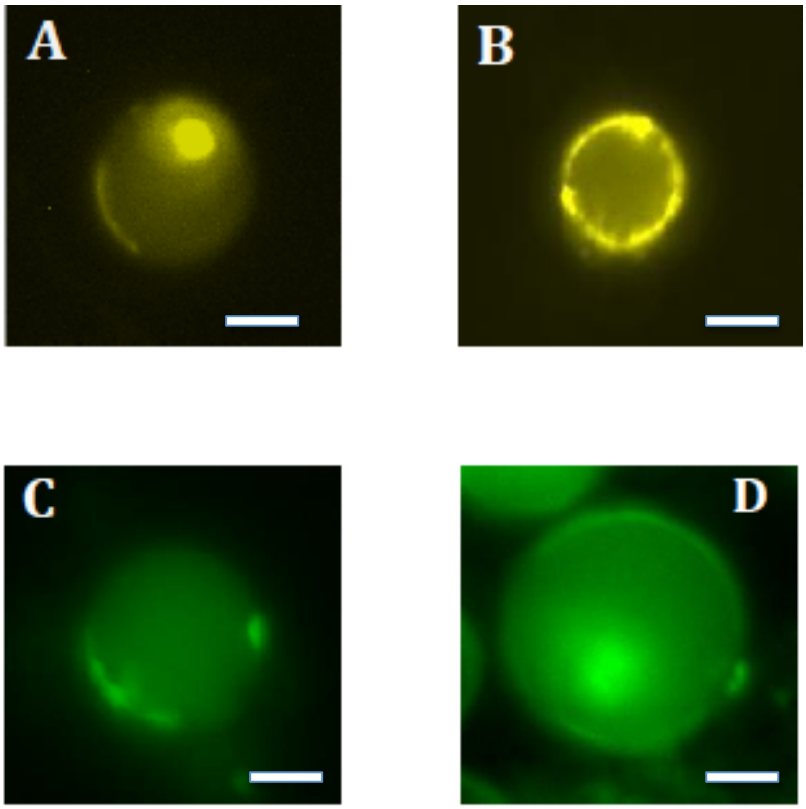

Fig. 3.18 FtsZ-YFP-MinD is expressed by *E. coli* extract and encapsulated in w/o emulsions (panel A). Scale bar is 8 μm. FtsZ-YFP-MinD and FtsA (panel B) are co-expressed by *E. coli* extract and assemble in ring-like structures. Scale bar is 5 μm. Fluorescent YFP Venus is false colored in yellow. YFP-FtsZ (panel C) is expressed by *E. coli* extract. Scale bar is 10 μm. YFP-FtsZ and FtsA are coexpressed (panel D) by the same T/T system, forming ring-like structure. Fluorescent YFP, YPet, is false colored in green. Scale bar is 12 μm.

The co-expression of FtsZ and FtsA, as already mentioned before, does not provide a fine control for our genetically encoded system. We need a fine control for the expression of the proteins of our system, taking in account that in *E. coli* the ratio of FtsZ versus FtsA is of 4:1. The modulation of the strength of the RBS sites could regulate the ratio of the two proteins in our system. In a first attempt we engineered constructs for FtsZ and FtsA under the control of a strong RBS. The constructs realized are FtsZ-YFP-MinD-FtsA and YFP-FtsZ-FtsA. We expressed all these constructs in w/o emulsions and in phospholipids vesicles using *E. coli* extract (PROMEGA S30) and PURESYSTEM as systems of expression (Fig. 3.20). Both the two system in *vitro* T/T gave good level of expression of

proteins (Fig 3.19 and Fig. 3.20). The constructs used were not designed with His tags, so non-specific binding of the proteins to the compartments is not expected.

The expression of YFP-FtsZ-FtsA R286W in w/o emulsions did not provide significant results. The co-expression of FtsZ and FtsA, as already mentioned before, does not provide a fine control for our genetically encoded system. We need a fine control for the expression of the proteins of our system, taking in account that in *E. coli* the ratio of FtsZ versus FtsA is of 4:1. The modulation of the strength of the RBS sites could regulate the ratio of the two proteins in our system. In a first attempt we engineered constructs for FtsZ and FtsA under the control of a strong RBS. The constructs realized are FtsZ-YFP-MinD-FtsA and YFP-FtsZ-FtsA. We expressed all these constructs in w/o emulsions and in phospholipids vesicles using *E. coli* extract (PROMEGA S30) and PURESYSTEM as systems of expression (Fig. 3.20). Both the two system in *vitro* T/T gave good level of expression of proteins (Fig 3.19 and Fig. 3.20). The constructs used were not designed with Histidine tags, so non-specific binding of the proteins to the compartments is not expected. The expression of YFP-FtsZ-FtsA R286W in w/o emulsions did not provide significant results.

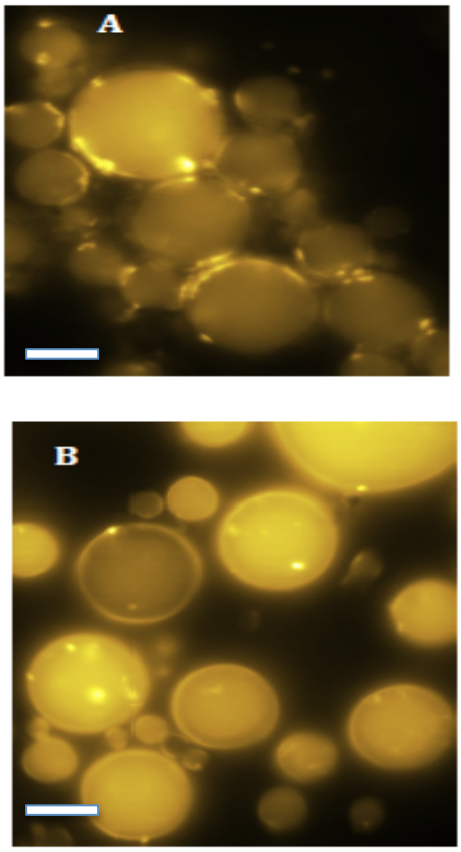

Fig. 3.19: FtsZ-YFP-MinD (panel A) is expressed by *E. coli* extract and does not form ring like structure. FtsZ-YFP-MinD-FtsA, in panel B is expressed by *E. coli* extract and forms ring like structure. The fluorescence was evaluated by fluorescence microscopy. The YFP (Venus) has an Ex=515 nm and an Em=528 nm and was visualized using a GFP filter and false colored in yellow. The production of FtsZ-YFP-MinD in the w/o emulsion show that the protein forms aggregates spread in the compartments. Scale bar is 22 mm.

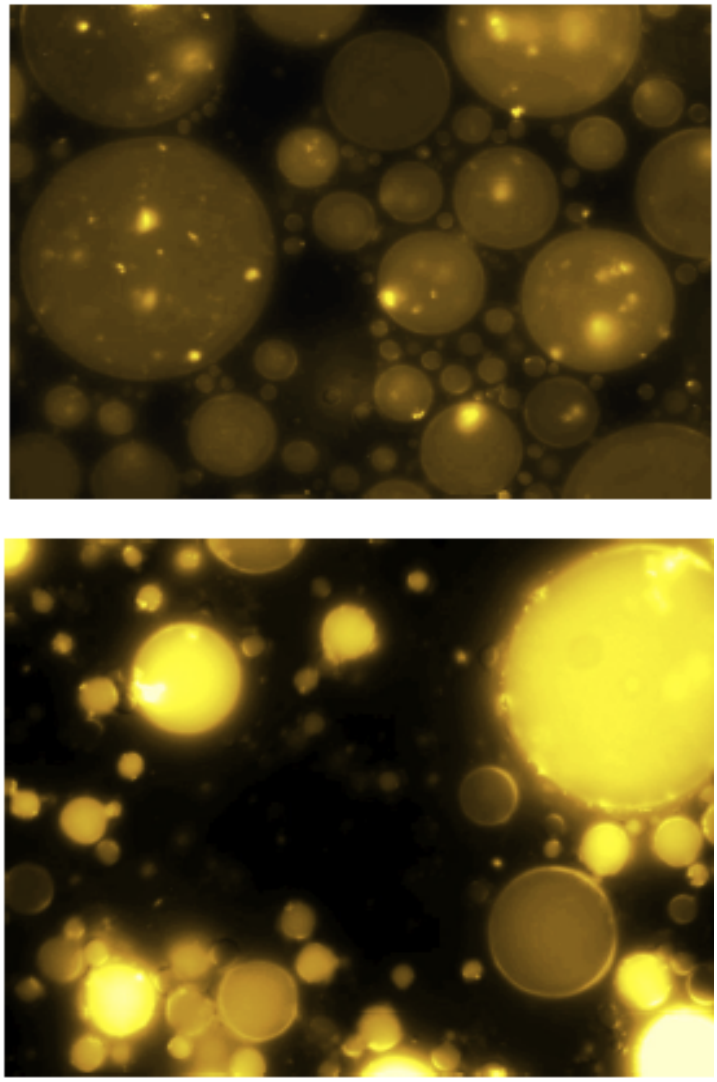

Fig.3.20: From the top FtsZ-YFP-MinD is expressed by PURESYSTEM in w/o emulsions. The protein is expressed and forms aggregates in the emulsions. The expression of the YFP (Venus) is false colored in yellow. FtsZ-YFP-MinD-FtsA is expressed by PURESYSTEM in w/o emulsions and forms ring-like structure. The fluorescence was evaluated by fluorescence microscopy The YFP(Venus) has an Ex=515 nm and an Em=528 nm and was visualized using a GFP filter. Scale bar is 22 μm.

In general, the expression of these constructs was evaluated by fluorescence microscopy. When YFP-FtsZ and FtsZ-YFP-MinD are expressed alone, they do not assemble together forming ring-like structure. In the presence of FtsA we noticed formation of ring-like structure that do not have the ability of constrict the droplets. A possible way for explain the lack of constriction force is the fact that the droplets have round shape, while *E.* coli has instead is tubular.

Ericksson and colleagues exploited multi lamellar and tubular liposomes and were able to observe constriction mediated by FtsZ-YFP-MinD.

We developed a self-sustainable compartment able to produce fluorescently tagged proteins that polymerize and form rings in w/o emulsions. The experiments were repeated several times and every time, in the presence of FtsA, it was possible to observe the formation of rings. In order to get a more robust system we co-expressed YFP-FtsZ-FtsA and a non-fluorescent FtsZ. The co expression of YFP-FtsZ-FtsA with FtsZ lead to bigger rings (Fig. 3.20).
The fact that bigger rings were formed confirmed that the rings are real, even though constriction was never observed. An enrichment of the system was possible and a minimal synthetic division machinery system was realized assembling biological parts from the scratch.

Furthermore we synthesized our minimal division machinery system in phospholipids vesicles. The vesicles, made of PC: DOPG 80:20 were prepared following the Yomo method[56], mentioned before and described in the Materials and Methods section. The formation of the rings in the presence of FtsA was more difficult to be evaluated in vesicles. Herein we report just the images that show a more relevant expression of the protein of interest. The figure 3.21 showed that the proteins YFP-FtsZ-FtsA and FtsZ are expressed by the PURESYSTEM inside of vesicles and form ring-like structure. In order to exclude the possibility that lipid artifacts could form the rings, we will need to test, in the future, different lipids compositions and express different combinations of proteins.

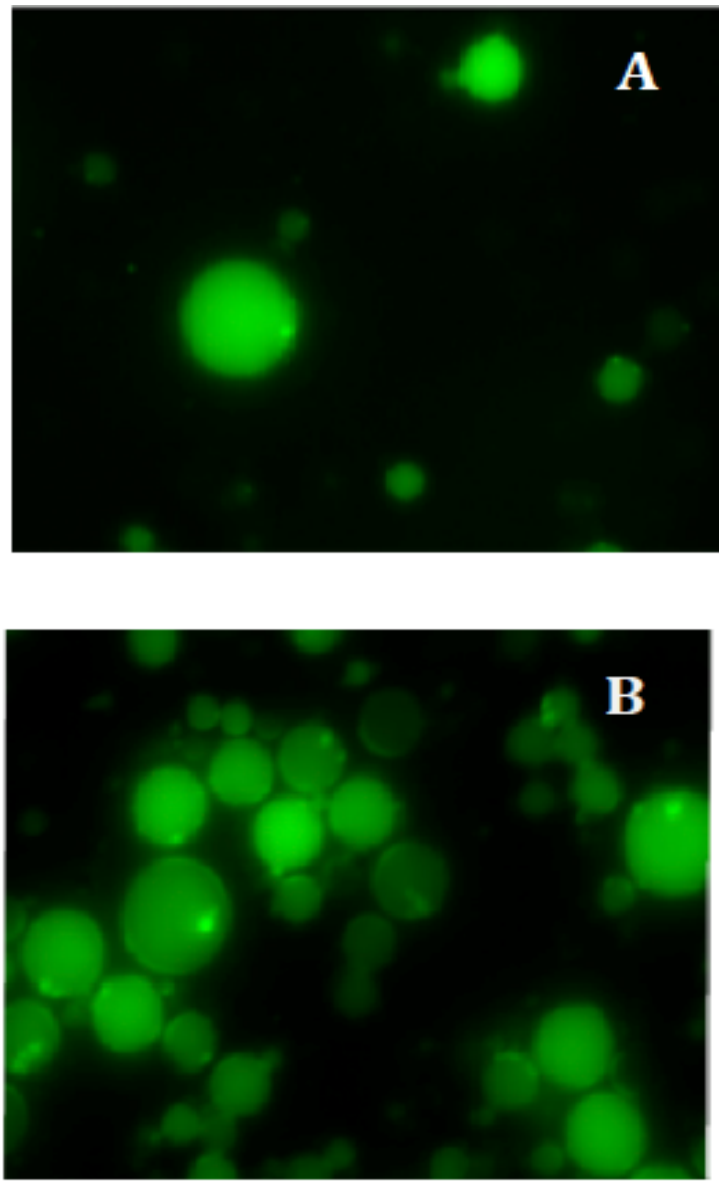

Fig. 3.21: YFP-FtsZ (A) is expressed by *E. coli* extract and does not form ring-like structure (A) In panel A YFP-FtsZ-FtsA is expressed by *E. coli* extract and form ring-like structure. The expression was evaluated by fluorescence microscopy. The YFP (YPet) has an Ex= 517 and an Em= 330 is false colored in green and visualized by using a GFP filter. Scale bar is 10 μm. Magnification is 63 X.

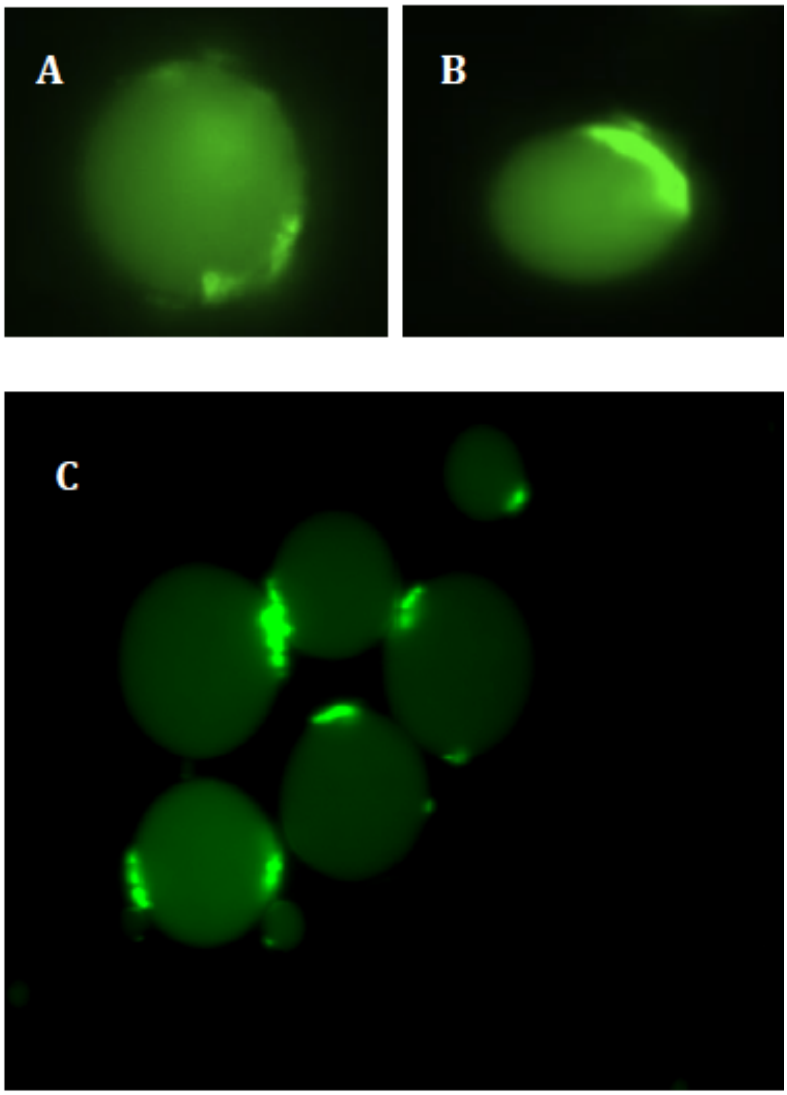

Fig. 3.22: YFP-FtsZ co-expressed with FtsZ give rise to big rings in w/o emulsions. YFP-FtsZ-FtsA (A) is expressed by *E. coli* extract and form ring-like structures. YFP-FtsZ -FtsA, co expressed in w/o emulsion by *E. coli* extract give rise to bigger rings (panel B) is expressed by *E. coli* extract and forms bigger ring-like structure. This phenomena was present in the major part of the w/o emulsions observed (panel C). The fluorescence was evaluated by fluorescence microscopy The YFP(Venus) has an Ex=515 nm and an Em=528 nm and was visualized using a GFP filter.

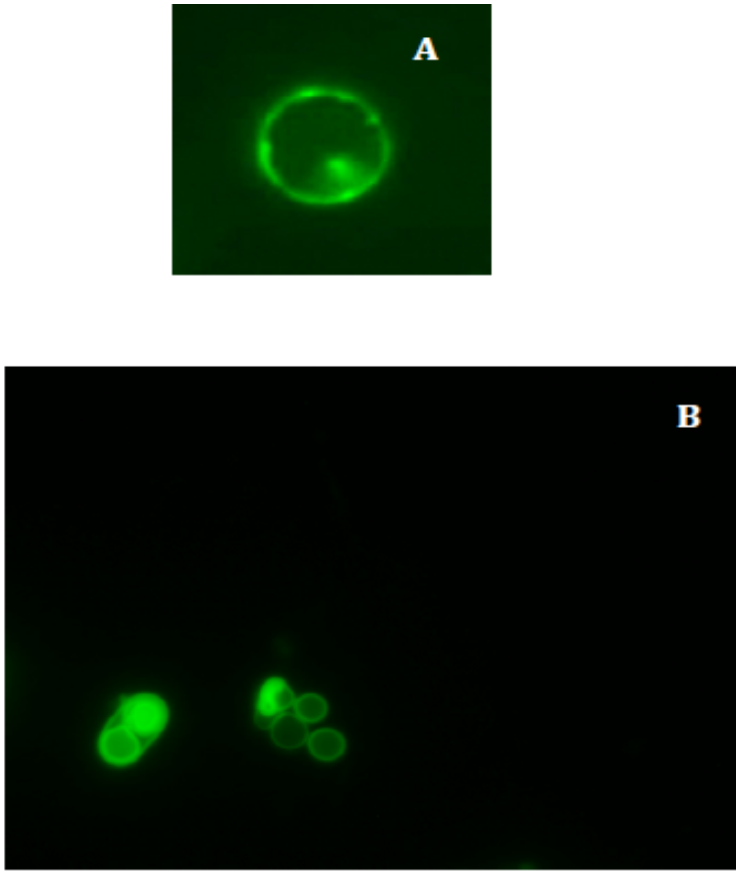

Fig. 3.21: Coexpression by PURESYSTEM of YFP-FtsZ-FtsA and FtsZ in DOPG: PC, 80:20 (panel A). The proteins once expressed, seems to form ring-like structure. The YFP(YPet) in the construct is false colored in green. YFP-FtsZ-FtsA coexpressed with FtsZ by PURESYSTEM (panel B).The proteins are expressed and form ring like structure.

3.3 Materials and Methods

3.3.1 Bacterial strains and plasmids.

The bacterial strains used for the amplification of the plasmids of interest were *E. coli* Novablue or DH5alpha. A description of the strains is reported in table 3.1. The genes coding for FtsZ-YFP-MinD, YFP-FtsZ, CFP-FtsA, CFP-R286W FtsA were synthesized by Genscript in pUC57. The gene coding for sGFP (BBa_I746916) was taken from the registry of standard biological parts (http://partsregistry.org) and was contained in pSB1A2 vector. The sequence of FtsA in sGFP-FtsA is the wild-type sequence from *E. coli* in pET15b. The sequences of FtsZ and FtsA in the double constructs, FtsZ-YFP-MinD-FtsA, YFP-FtsZ-FtsA and YFP-FtsZ-R286W FtsA, are synthetic like the sequence of FtsZ and FtsA without the 6Hisx-tag subcloned in pET21b.

Table 3.1: *E. coli* strains description.

DH5-alpha	F- endA1 glnV44 thi-1 recA1 relA1 gyrA96 deoR nupG Φ80dlacZΔM15 Δ(lacZYA-argF)U169, hsdR17(rK- mK+), λ-nalidixic acid resistant
NovaBlue	endA1 hsdR17(rK12- mK12+) supE44 thi-1 recA1 gyrA96 relA1 lac F'[proA+B+ lacIqΔM15 ::Tn10(TetR)])Tethracycline resistant.

3.3.2 PCR amplification and subcloning of FtsZ and FtsA constructs.

All the genes coding for fluorescent and non-fluorescent version of FtsZ and FtsA were amplified by PCR and subcloned in pET21b or in pET28b, in the case of the gene encoding for sfGFP-FtsA. The program used for the amplification of the genes amplified by *Taq* DNA Polymerase (RBC), Hot Start DNA Polymerase (NEB) and Deep Vent Polymerase is reported in table 3.2. In table 3.3 is reported instead the program used for the amplification by Phusion High Fidelity DNA polymerase. The polymerases used within the annealing temperature and the

extension time exploited, for the amplification of each construct are reported in table 3.3.

Table 3.2:PCR program used with Taq DNA polymerase, Hot Start Taq DNA polymerase and Deep Vent DNA Polymerase.

Initial Denaturation	95	1-3	1
Denaturation	95	0.5	25-40
Annealing	T_m-5	0.5	25-40
Extension	72	1 min/kb	25-40
Final Extension	72	5-15	1

Table 3.3: PCR program for the amplification of plasmidic DNA by Phusion High Fidelity DNA polymerase.

Cycle step	**2-step protocol**		**3-step protocol**		**cycles**
	temp (°C)	**time (s)**	**temp (°C)**	**time (s)**	
Initial denaturation	98	30	98	30	1
Denaturation	98	5-10	98	5-10	25-35
Annealing	-	-	X	10-30	25-35
Extension	72	15-30 s/1 kb	72	15-30 s/1 kb	25-35
Final extension	72	10 min	72	10 min	1
End	4	hold	4	hold	1

After amplification the DNA was digested by restriction digestions (Table.3.3) and ligated in the vector of interest using T4 DNA Ligase (NEB or Fermentas).

Table 3.4: DNA Polymerases, restriction enzymes employed and details about annealing temperature and extension time for each construct.

Construct	**Polymerases**	**Annealing and Extension**	**Restriction Enzymes**
FtsZ-YFP-MinD	Taq, Hot Start Taq	Ann=61.2°C Ext=2:30 min	NdeI, XhoI
YFP-FtsZ	Taq, Hot Start Taq	Ann=61.1°C Ext=2:01	NdeI, BamHI
CFP-FtsA	Taq, Hot Start Taq	Ann=58.4°C Ext=2:07 min	NdeI, BamHI
CFP R286W-FtsA	Taq, Hot Start Taq	Ann=58.4°C Ext=2:07 min	NdeI, BamHI
sGFP	Phusion	Ann= Up to 72°C (Two step protocol) Ext=11 s	NcoI, BamHI
FtsA	Phusion	Ann=70.3 Ext=19s	BamHI, XhoI
RBS-FtsZ-YFP-MinD	Phusion, DeepVent$_R$	Ann=65°C Ext=28 s Ann=60°C Ext=113s	NdeI, SacI
RBS-FtsA	Phusion, DeepVent$_R$	Ann=69 °C Ext=19s Ann=64 °C Ext=1.2 min	SacI, XhoI
RBS-	Phusion, DeepVent$_R$	Ann= 68 °C Ext=28.3 s Ann=63 °C Ext=1.9 min	NdeI, SacI
RBS-FtsA	Phusion	Ann=68 °C Ext=19 s	SacI, XhoI
FtsZ	Phusion, DeepVent$_R$	Ann=66.8°C Ext=18 s Ann=61.°C Ext=1.2 min	NdeI, BamHI
FtsA	Phusion, DeepVent$_R$	Ann=68 °C Ext=19 s sAnn=63 °C Ext=1.9 min	NdeI, BamHI

3.3.3 Transcription-translation reactions in *vitro*.

Plasmids were amplified by *E. coli* DH5alpha or NovaBlue and purified with Wizard Plus SV Minipreps DNA Purification System (Promega) or QIAprep Spin Miniprep Kit (Qiagen). Subsequently, the DNA was phenol-chloroform extracted, ethanol precipitated, and resuspended in deionized and diethylpyrocarbonate (DEPC) treated water. 1μg of DNA was used in the case of transcription-translation reaction with *E. coli* extract (PROMEGA S30) both in case of expression of a single gene that in case of co-expression. The reactions were supplied with 40 units of RNAse inhibitor from human placenta (NEB). 250 ng DNA were used for each transcription-translation reaction with the PUREXPRESS *in vitro* protein synthesis kit (NEB) supplemented with 20 units of human placenta RNase inhibitor (NEB) The reaction components were assembled on ice and then incubated at 37 °C in the spectrophotometer in case of in *vitro* expression for 6 h, directly inside w/o emulsion and vesicle in case of expression in compartments for approximately 2 h.

3.3.4 Radioactive labeling of proteins expressed in *vitro*

The proteins YFP-FtsZ, FtsZ-YFP-MinD, FtsA, CFP-FtsA and CFP-R286W FtsA were labeled by adding 20 μCi of S-35 (purchased from Perkin Elmer) to the reaction of T/T of PURESYSTEM. The reactions were assembled as described before. After the addition of the plasmidic DNA, the reaction was incubated for 2 h at 37 °. Just 5 μL of reaction were loaded on a SDS gel at 10%. The protein ladder used is a Page Ruler Plus Prestained Ladder (10-250 kDa) purchased from Fermentas in which some of the bands were labeled with 2 μL S^{35} (by painting).

3.3.5 W /o emulsions

The oil phase was freshly prepared by mixing 4.5% (vol/vol) Span 80 and 0.5 % (vol/vol) Tween 80 in 0.95 mL of mineral oil. This mixture was vortexed until the Span 80 was completely dissolved in the mineral oil. 0.05 mL of reaction in case of *E. coli* extract and 0.025 mL for PURESYSTEM were added to the oil phase and vortexed vigourosly until the solution became turbid.

3.3.6 Vesicles preparation

Vesicles were made with 1,2-dioleoyl-sn-glycero-3-phospho-(1'-rac-glycerol) (sodium salt) (DOPG) purchased from Sigma, L-α-phosphatidylcholine from egg yolk (egg lecithin) (Sigma), using a method similar to that described by Yomo and colleagues[56]. Lipid stocks were made by dissolving 1 g DOPG in 25 mL chloroform to obtain a 40mg/mL solution. Similarly, a 20 mg/mL lecithin stock was prepared by dissolving 400 mg lecithin in 20 mL chloroform. With a glass pipette, lipids were transferred to a round bottom flask. The organic solvent was then evaporated with a Buchi Rotovapor R-210 for 30 min. This procedure resulted in a thin lipid film inside of the round bottom flask. Next, 1 mL deionized water was added to hydrate the lipid, giving a concentration of 12 mM lipid. The liposome dispersion was homogenized with IKA T10 basic homogenizer at power setting 4 for 1 min and extruded eleven times through a polycarbonate filter (Whatman, Brentford, UK) with a pore size of 400 nm. 40 µL aliquots were flash frozen in liquid nitrogen or dry ice and lyophilized in a SpeedVac (Centritrap DNA concentrator, Labconco) at 40°C. The lyophilized empty liposomes were stored at −20 °C.

3.3.7 Instrumentation

Reactions were monitored by fluorescence spectroscopy with a Photon Technology International (PTI) QuantaMaster 40 UV VIS spectrofluorometer equipped with two detectors (T-format). Excitation and emission wavelengths were specific for each fluorescent protein. When encapsulated in compartments were monitored through fluorescent microscopy using a Zeiss Observer Z1 microscope with an AxioCam MRm camera. All the images showed in this chapter were acquired with a 63X objective and with a filter 38 HE (GFP). The images were analyzed using the Axio Vision 4.8.The lipid fillm for the vesicles was obtained by evaporating the organic solvent using a Buchi Rotovapor R-210.

Chapter 4

Reconstitution of a minimal divisome with purified proteins in compartments.

4.1 Introduction

We aimed to synthesize directly inside compartments a minimal division machinery system made of FtsZ and FtsA. To our knowledge we are the first to attempt to build division machinery in situ. A more traditional approach, forecasts the direct encapsulation of purified components of the divisome inside compartments. In fact there are many advances, as discussed before, demonstrating that the reconstruction of a minimal divisome with purified proteins is possible. It was shown that FtsZ-YFP-MinD purified and encapsulated in tubular liposomes is able to reproduce the typical phenomena of cell division, that the purified Min system is able to oscillate and generate waves in lipid supported bilayers and that the reconstruction of proto-ring elements of the divisome in liposomes is possible. At the beginning of this work we tried to reconstitute our minimal division machinery system made of FtsZ and FtsA by purifying some fluorescent versions for FtsZ, such as FtsZ-YFP-MinD and YFP-FtsZ, and fluorescently labeled FtsA such as CFP-FtsA and CFP R286W FtsA. Moreover FtsZ-YFP-MinD and YFP-FtsZ were encapsulated in w/o emulsions and visualized inside the compartments by fluorescence microscopy. In the presence of guanosine thriphosphate (GTP) FtsZ formed aggregates similar to the polymers, observed inside w/o emulsions.

In general, fluorescent versions of FtsZ were purified easily and were able to make polymer-like structure inside w/ o emulsions. In contrast to the purification of fluorescent constructs of FtsA, similarly to the expression in *vitro*, was challenging. The experimental approach followed for the reconstruction of a minimal division machinery system in cell-like compartments with purified proteins will be described in the following paragraphs. Additionally the bottleneck of this approach will be explained.

4.2 Results and Discussion

4.2.1: In *vivo* expression and purification of FtsZ constructs.

FtsZ and FtsA, as mentioned many times, are key proteins for our minimal division machinery system. A summary of the strategy followed for the expression and purification of FtsZ and FtsA constructs is reported in figure 4.1. Constructs coding for FtsZ and FtsA with 6xHis tag were expressed in E. coli BL21 (DE3) Rosetta. The 6Hisx tag , both for FtsZ constructs and FtsA constructs, was placed at the N-terminus. Then the proteins were over-expressed by induction with IPTG. The cells were lysed and loaded on a Ni/NTA^{2+}(nitrilotriacetic acid) column. The ability of the nickel to chelate the His residues was exploited. The fractions obtained from the column were loaded on a SDS PAGE.

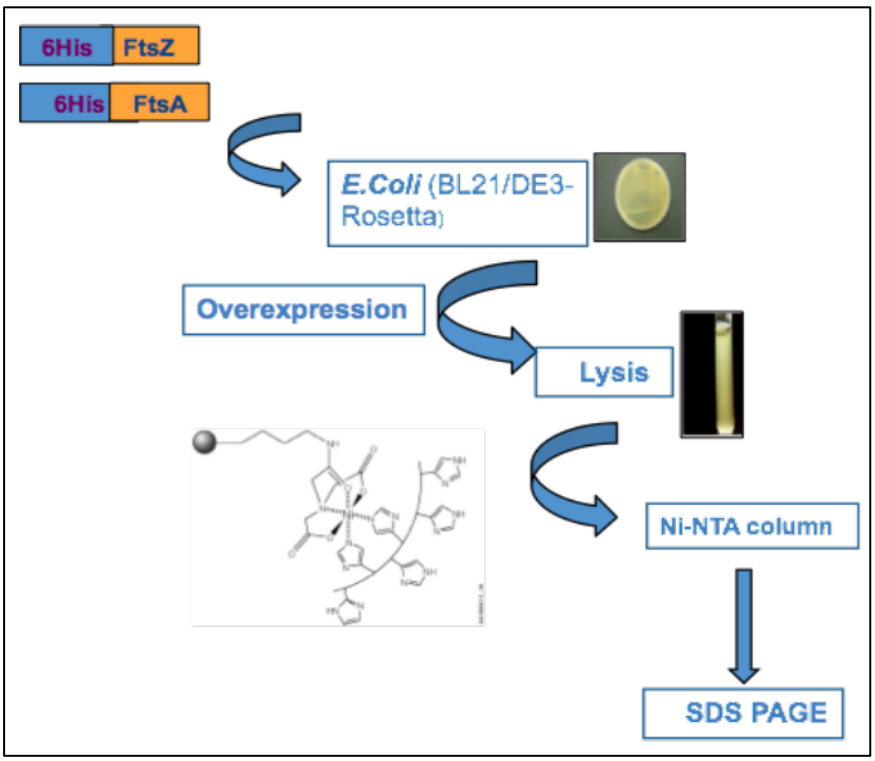

Fig 4.1: Our protein purification strategy. Constructs coding for FtsZ/FtsA with tags of 6 Hisx, were expressed in *E. coli* BL21 DE3/Rosetta and overexpressed by induction with IPTG. Then the cells were lysed and loaded on a Ni/NTA $^{2+}$column. The resulting fractions were analyzed by SDS PAGE.

FtsZ in *E. coli* is present in the cytoplasm or in the Z –ring. When FtsZ is part of the Z ring, the protein localizes in proximity of the inner cytoplasmic side of the membrane. FtsA, instead, is tethered to the membrane through an amphiphatic helix. Considering this topography of FtsZ and FtsA in *vivo*, we expect that FtsZ behaves as a soluble protein and FtsA as a no soluble protein. At the beginning before to set up a strategy of purification, we tested the solubility of the proteins after over-expression. The over-expression of the proteins occur after induction by Isopropyl-Beta D-Thiogalactopyranoside (IPTG).

The IPTG binds to the *lac* repressor and releases the tetrameric repressor from the *lac* operator in an allosteric manner, thereby allowing the transcription of genes in the *lac* operon, such as the gene encoding for beta-galactosidase, a hydrolase enzyme that catalyzes the hydrolysis of β-galactoside into monosaccharides[57]. The induction of expression by IPTG could imply variations of the solubility of the proteins in the supernatant or in the pellet. For this reason we performed tests of solubility in order to understand the localization of the proteins and in order to set up a proper protocol for the purification of the same.

FtsZ has a MW of 40.2 kDa. In absence of induction by IPTG, the amount of protein expressed in the supernatant is less than in the pellet. In contrast FtsZ is overexpressed both in the supernatant and in the pellet by induction with 0.4 mM of IPTG. (Fig. 4.2).

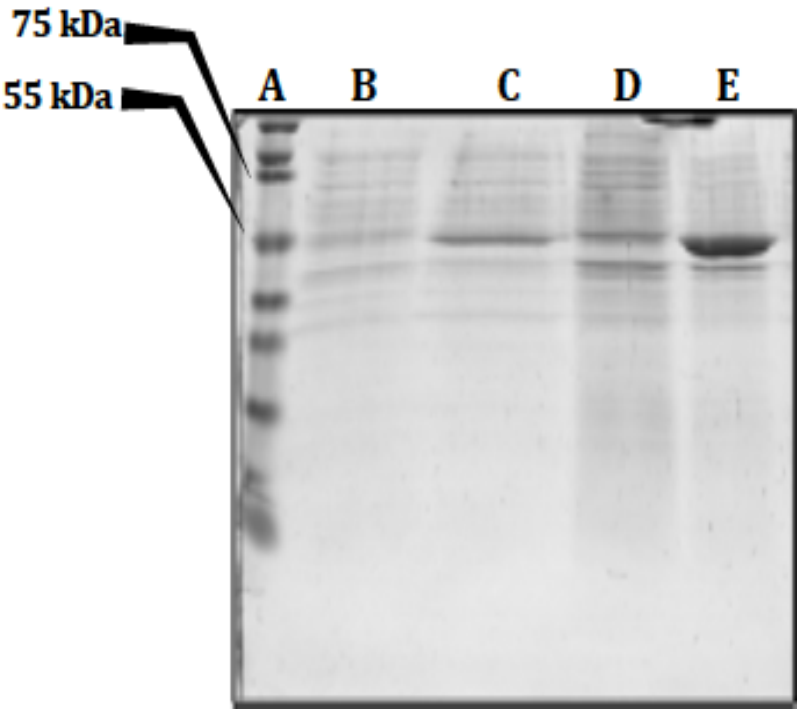

Fig 4.2: Test of solubility for FtsZ. The MW is of 40.2 kDa. The protein is expressed both in the supernatant (B) and in the pellet(C). After induction with 0.4 mM of IPTG, the expression of the protein in the supernatant is increased (lane D) and even more in the pellet (E). Lane A is the protein ladder from 10-250kDa (NEB).

The screening of the solubility of FtsZ without fluorescent tag, was useful to understand if the tag influenced the behavior of FtsZ. Then the solubility of YFP-FtsZ and FtsZ-YFP-MinD was tested. Both the proteins were over-expressed in BL21 (DE3) Rosetta and a test of solubility in small scale was performed. The behavior of FtsZ in these constructs is not so much different from FtsZ without fluorescent tags. Details about the engineering of YFP-FtsZ and FtsZ-YFP-MinD were described in the third chapter.

We expressed FtsZ-YFP-MinD in *E. coli* BL21 (DE3) Rosetta cells. The amount of protein in the supernatant after induction, compared with the amount of the protein before the induction (Fig.4.3, lane A), was increased after induction with just 0.1 mM of IPTG (Fig 4.3, lane C). In the presence of 0.4 mM IPTG, the amount of protein was significantly increased both in the supernatant and in the pellet (Fig.4.3, lane E and lane F).

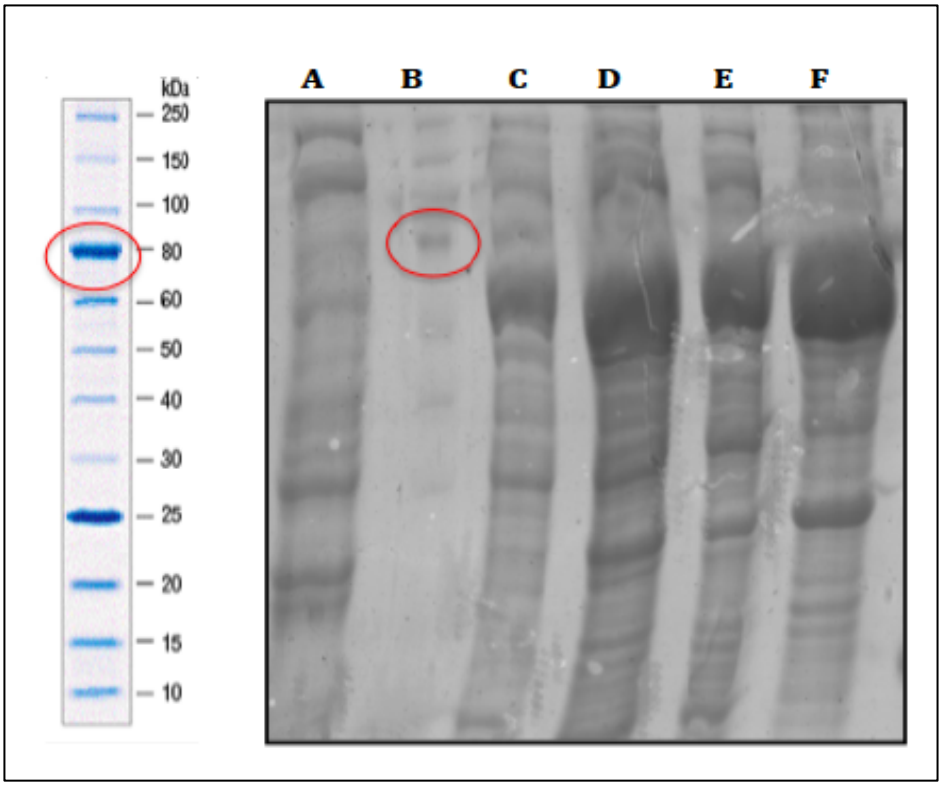

Fig.4.3: Solubility of FtsZ-YFP-MinD after overexpression by IPTG. FtsZ-YFP-MInD has a MW of 70.3 kDa. Lane B is the protein ladder from 10-250 kDa (NEB). Lane A corresponds to *E. coli* cells before the induction, there is non a significative expression of the protein. Lane C corresponds to the supernatant fraction after induction with 0.1 mM IPTG and lane E corresponds to the supernatant fraction after the induction with 0.4 mM IPTG. The amount of the protein in the supernatant is increased by induction with 0.4mM IPTG. Lane D corresponds to the expression of FtsZ-YFP-MinD in the pellet fraction after induction with 0.1 mM IPTG and lane F after the induction with 0.4mM IPTG.

The advantage of having more protein in the supernatant facilitated also the process of FtsZ-YFP-MinD purification. We evaluated that 0.1 mM IPTG was a sufficient concentration for the overexpression of FtsZ-YFP-MinD. 4 L of expression were performed. Then the cells were lysed by sonication and FtsZ-YFP-MinD was purified by nickel affinity chromatography. This chromatography exploits the ability of the NTA resin functionalized with the nickel to chelate the histidines that tag the proteins. The buffer used for the equilibration of the column and the removal of the aspecific bindings is composed by 50 mM NaH_2PO_4, 300 mM NaCl, 5 mM imidazole, pH 7.4 (binding buffer). The column was washed with the same buffer plus 20 mM and 60 mM imidazole and the

protein was eluted with 250mM imidazole in binding buffer. Aliquots from the 1st to 6th of the elution, plus wash and flow-through fractions were loaded on a SDS PAGE (Appendix, Fig A3.). The eluted fractions were collected and dialyzed in 2 L of 50 mM TrisHCl, 50 mM NaCl and 1 mM beta-mercaptoethanol (BME). The MW of FtsZ-YFP-MinD is of 70.2 kDa and the MW of the imidazole is of 0.068 kDa, so the imidazole was easily removed using a Snake Skin Dialysis membrane (Thermoscientific) with 7 K molecular weight cut off (MWCO). After dialysis the protein was concentrated using a stirred cell concentrator supplied with an Amicon membrane of 10 KDa MW cut off. At the end of the chromatography we collected a volume of 40 mL of protein, correspondent to the fractions eluted from the column with a high concentration of imidazole (255 mM), then the protein was concentrated to a volume of approximately 4 mL and stored in 5% vol/vol glycerol. After purification the absorbance at 280 nm was measured by UV spectroscopy. The absorbance at 280 nm is correspondent to the absorption peak of the tyrosine and tryptophan residues present in the protein. We calculated the concentration of FtsZ-YFP-MinD using the extinction coefficient (ε) of YFP (Venus) at 515 nm, that is of 92.2 $M^{-1}cm^{-1,}$ and the absorbance detected at 515 nm from the UV spectrum. We exploited the Beer-Lambert law ($A= \varepsilon cl$) for calculating the concentration. The resulting concentration was 10.8 μM. Finally, we confirmed the quality of purification acquiring excitation and emission scan of the protein purified. Venus YFP, as mentioned previously, has an excitation peak of 515 nm and an emission peak of 528 nm .The peaks were confirmed by fluorescence spectroscopy in our purified FtsZ-YFP-MinD.

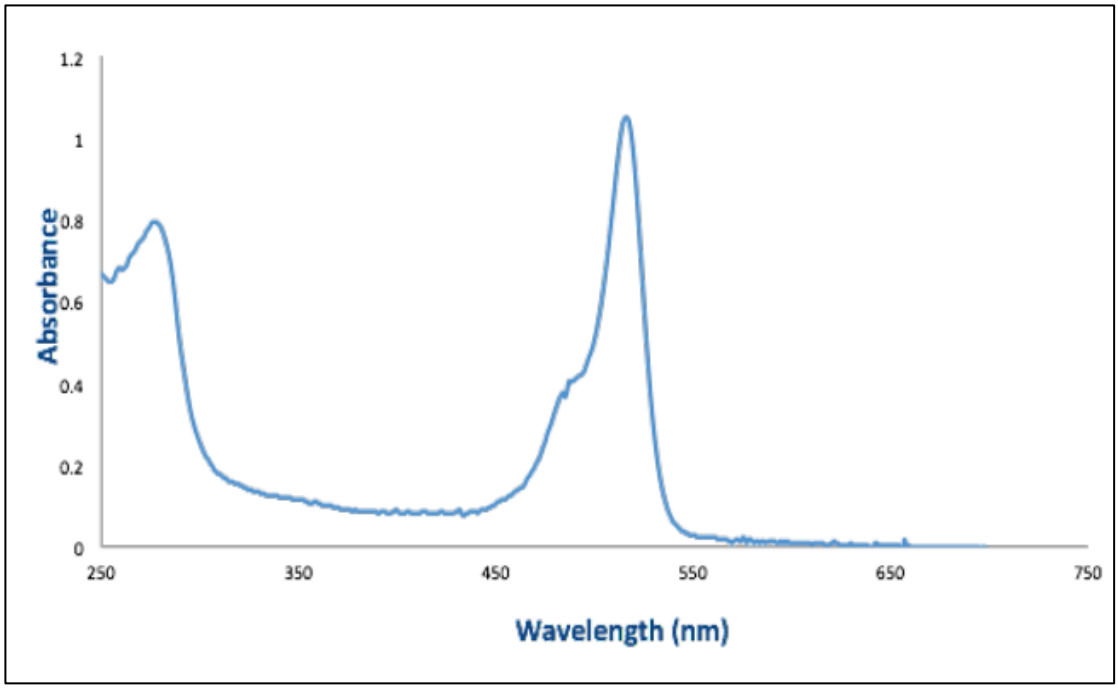

Fig.4.4: FtsZ-YFP-MinD UV spectrum. Two peaks are detected. The first peak is detected at 280 nm and is correspondent to the absorbance of the protein and is determined by the presence of aromatic amino acids in the protein. The second peak at 515 nm, instead, corresponds to the chromophore and is equivalent to the excitation wavelength of the YFP/Venus present in the protein. The amount of the protein was calculated by exploiting the extinction coefficient at 515 nm of the YFP, Venus.

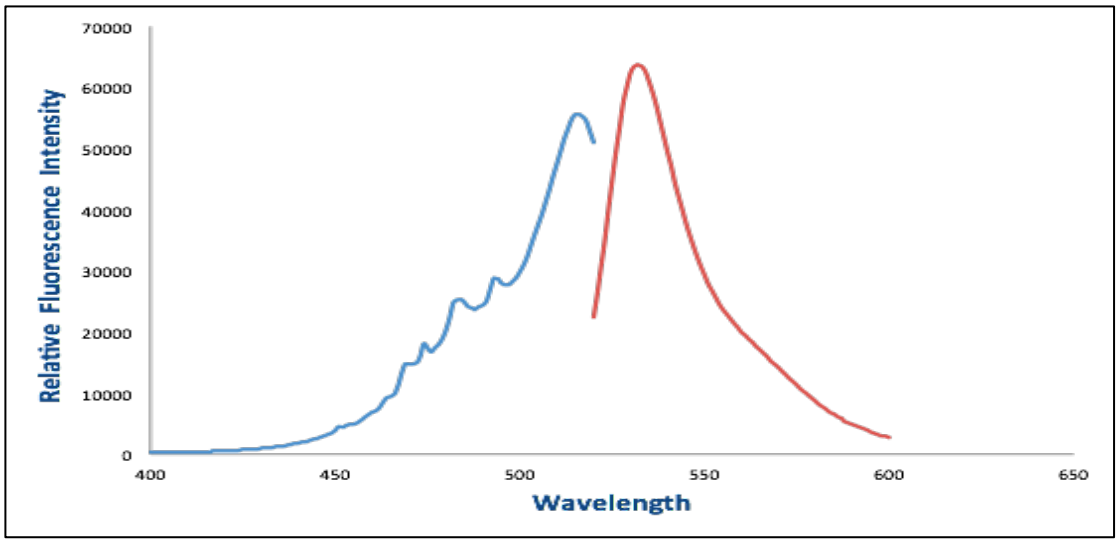

Fig. 4.5: Excitation and emission scan of FtsZ-YFP-MinD plotted in the same graph. FtsZ-YFP-MinD has an excitation peak at 515 nm and an emission peak at 528 nm. The purification lead to the right protein.

After the purification of FtsZ-YFP-MinD we proceeded with the purification of YFP-FtsZ. YFP-FtsZ was expressed in *E.coli* BL21(DE3) Rosetta and a test of solubility, after the induction by IPTG, was performed. We over expressed YFP-FtsZ with just 0.4 mM IPTG. The induction increased the level of expression in the supernatant (Fig.4.6). The protein was soluble. Then we proceeded with the same purification strategy adopted before, expressing 4 L of protein, lysing the cells by sonication and loading the lysed cells on a nickel column. After chromatography the fractions of washing and of elution steps obtained from the column were loaded on a SDS gel at 12% (Appendix, Fig A.4). We collected and dialyzed not only the fractions coming from the elution with 255 mM imidazole but also the fraction coming from the washing step with 65m M imidazole. The fluorescence in the fractions collected was remarkable. After dialysis and concentration, the protein was stored in 15 % glycerol at -80° C. At the end of the purification the absorbance of the protein at 280 nm was measured(Fig.4.7). The concentration of the protein was calculated, exploiting the absorbance at 517 nm that corresponded to the excitation wavelength of YPet. The extinction coefficient, used for calculating the concentration, was relative to the excitation wavelength of YPet (517nm) and is of 104,000 $M^{-1}cm^{-1}$. Also in this case we exploited the Beer's law, and the concentration calculated was 10.4 μM. The quality of the purification was confirmed by fluorescence spectroscopy, acquiring excitation and emission scan of YFP-FtsZ. The YFP/YPet has an excitation peak at 517 nm and an emission peak at 530 nm. These peaks were confirmed by the fluorescence spectra (Fig. 4.8). As mentioned before we dialyzed the imidazole and stored the protein collected from the washing step with 65 mM imidazole. The UV and the fluorescence spectrum are reported respectively in Fig. 4.9 and 4.10. The final concentration calculated for the protein was of 36.3 μM.

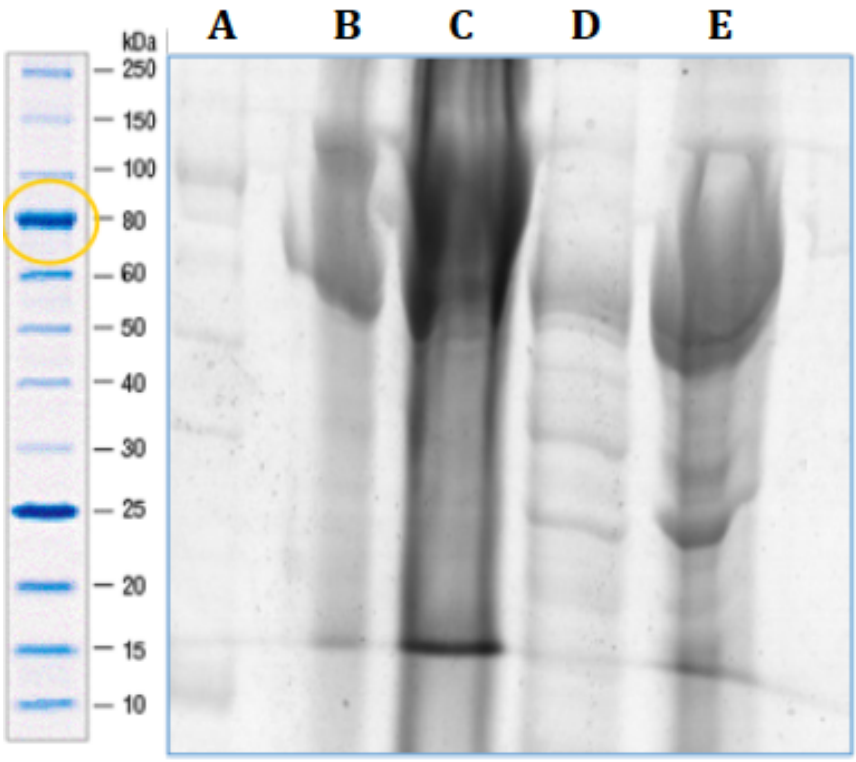

Fig 4.6: Test of solubility for YFP-FtsZ, the protein is soluble. Lane A is the protein ladder from 10-250 kDa (NEB). YFP-FtsZ is over-expressed in the supernatant by induction with 0.4 mM IPTG (lane D) and in the pellet (lane E). In absence of IPTG the protein is more expressed in the pellet (lane C) than in the supernatant (lane B).

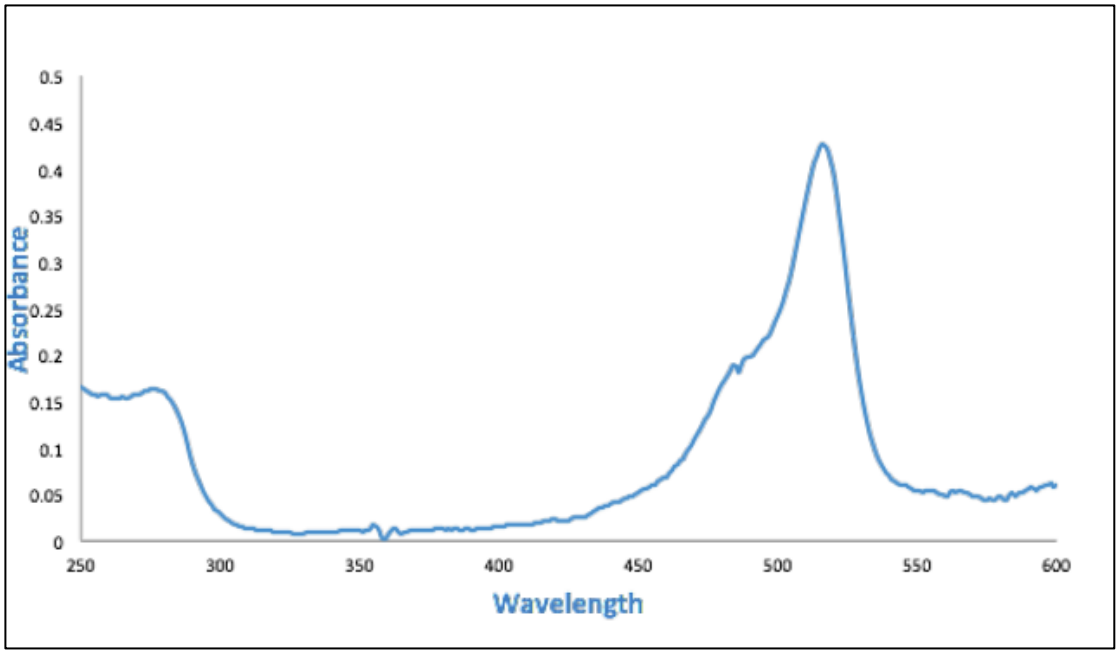

Fig.4.7 : UV spectrum of YFP-FtsZ eluted from the column with 255 mM of imidazole. Two peaks were detected. The first peak is at 280 nm and corresponds to the absorbance of the aromatic residues of the protein. The second peak at 517 nm, corresponds to the chromophore excitation wavelength of the YFP (YPet) present in the protein. The amount of the protein was calculated exploiting the extinction coefficient and the absorbance at 515 nm of the YFP/YPet.

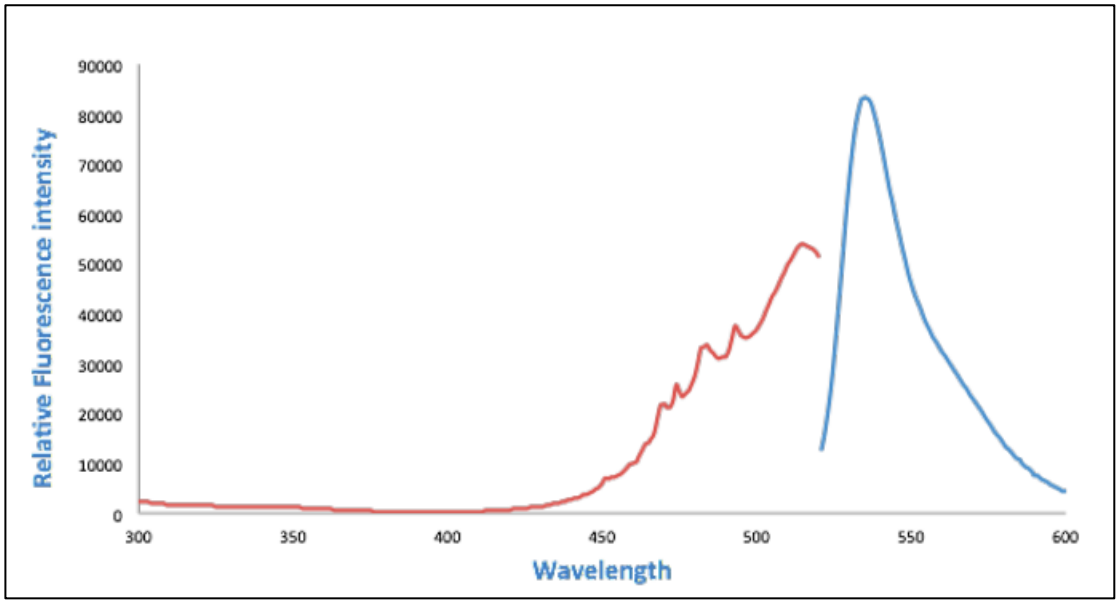

Fig 4.8: Excitation and emission scan of YFP-FtsZ, eluted from the column with 255mM imidazole. YFP-FtsZ has an excitation peak at 515 (red line) nm and an emission peak at 530 nm (blue line). The purification leaded to the right protein.

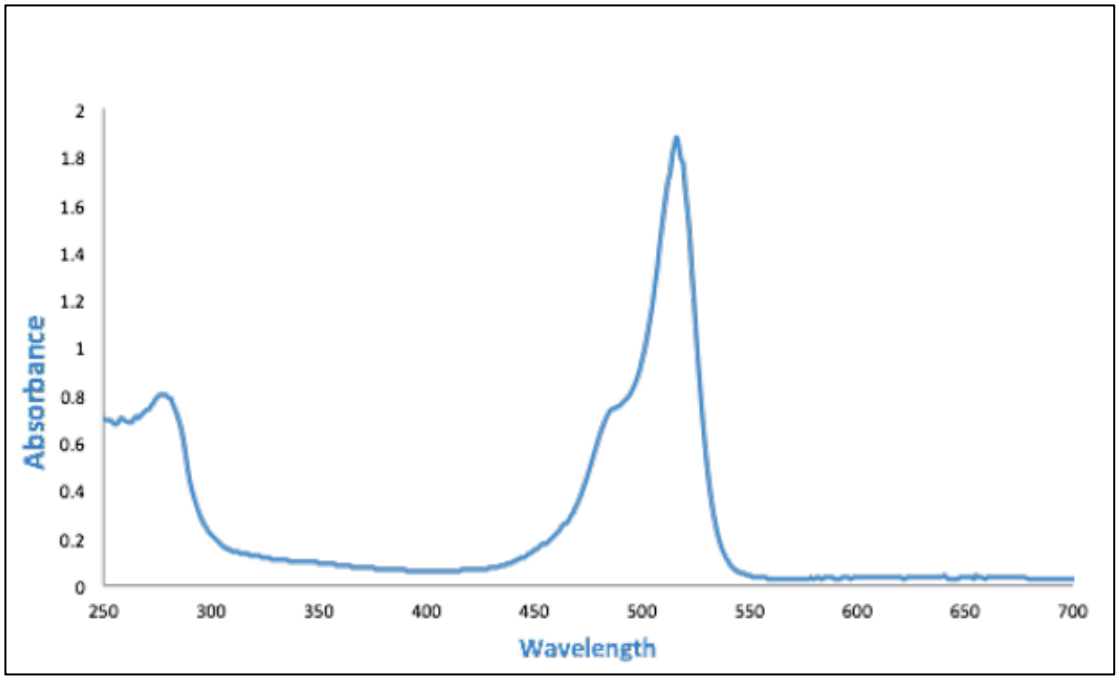

Fig 4.9: UV spectrum of YFP-FtsZ after the washing step with 65 mM of imidazole. Two peaks were detected. The first peak is detected at 280 nm and corresponds to the absorbance of the aromatic residues of the protein. The second peak at 517 nm, corresponds to the chromophore. The amount of the protein was calculated exploiting the extinction coefficient and the absorbance at 515 nm of the YFP/YPet.

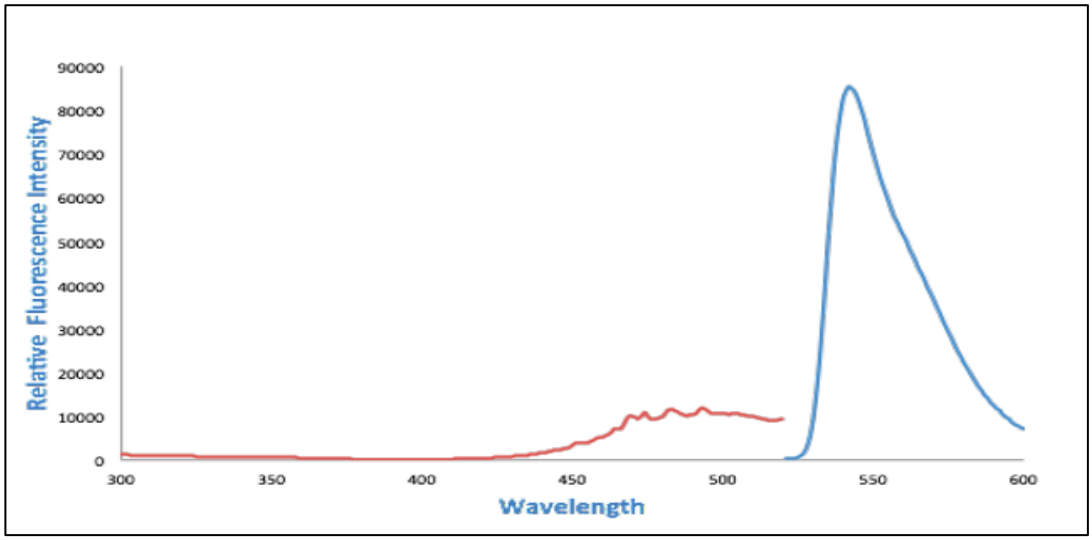

Fig. 4.10: Excitation and emission scan of YFP-FtsZ, after washing with 65 mM imidazole. YFP-FtsZ has an excitation peak at 517 (red line) nm and an emission peak at 530 nm (blue line) The purification leaded to the right protein.

FtsZ-YFP-MinD and YFP-FtsZ behave as soluble proteins and so can be purified under native conditions. The amount of proteins obtained was sufficient for the development of later experiments of encapsulation in w/o emulsions. Two possible fluorescent version of FtsZ for the construction of our minimal division machinery system were purified but were not sufficient to reach the goal of building a minimal system made of FtsZ and FtsA. So we proceeded with the expression in *vivo* and the purification of FtsA constructs.

4.2.2 In *vivo* expression and purification of FtsA constructs.

Prior to the design of the fluorescent constructs for FtsA and test of the solubilities, we investigated the behavior of FtsA in the absence of fluorescent tags. We tested the solubility of FtsA subcloned in a pET-TEV (Fig 4.11) vector. Different concentrations of IPTG were tested. In general, FtsA was more expressed in the pellet than in the supernatant. This result was expected because of the hydrophobic nature of FtsA.

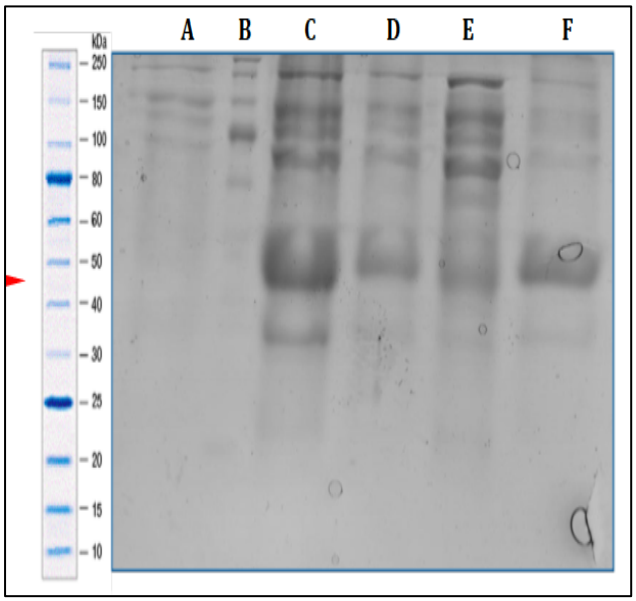

Fig 4.11: FtsA is not a soluble protein. FtsA has a MW of 40.2 kDa. Lane B is the protein ladder from 10-250 kDa (NEB). In lane A, correspondent to the expression of the protein before the induction, is not possible to detect the protein of interest. FtsA, instead, is over-expressed in the pellet (lane C) both with 0.1 mM IPTG and both with 0.4 mM IPTG (lane F). In the supernatant is low expressed both with 0.1 mM and 0.4 mM IPTG (lane C and lane E)

FtsA without a fluorescent tag is mostly present in the pellet. Therefore we designed, sucbcloned and expressed in *E. coli* BL21 (DE3) Rosetta, CFP-FtsA and CFP-R286W FtsA. We tested the solubility of CFP-FtsA in order to understand the purification strategy to set up for later purification (Fig.4.12). Unfortunately there is no sample of control in the gel shown in figure 4.13, but clearly the protein is mostly expressed in the pellet, after induction with 0.1 mM IPTG (lane C) and after induction with 0.4 mM IPTG (lane E). The production in the supernatant was increased by induction with 0.1 and 0.4 mM IPTG (lane B and D). In conclusion, CFP-FtsA is not a soluble protein, for this reason we set-up a purification platform under native conditions, adding a mild detergent in the buffer and we performed a purification under denaturating conditions exploiting as denaturating agent urea.

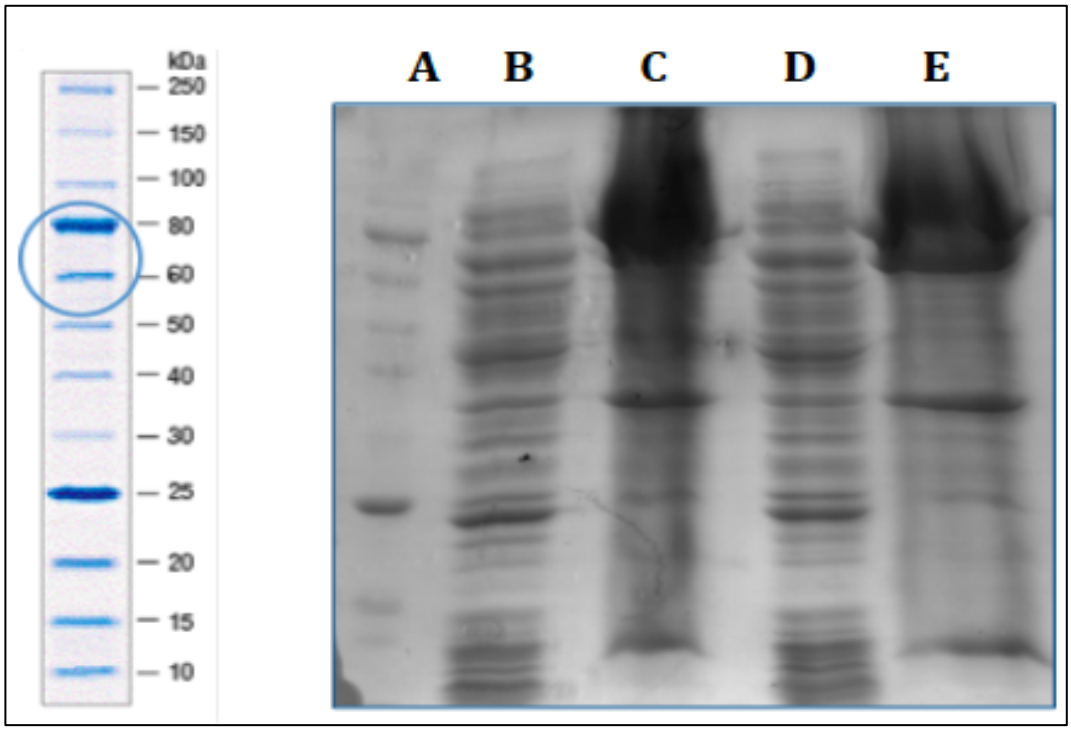

Fig 4.12: CFP-FtsA is not a soluble protein. CFP-FtsA has a MW=75.7kDa. The protein is mostly expressed in the pellet after induction with 0.1mM IPTG (lane C) and after induction with 0.4 mM IPTG (lane E). The protein is low expressed in the supernatant both with 0.1 mM IPTG (lane B) and both with 0.4 mM IPTG (lane D). Lane B is the protein ladder from 10-250 kDa (NEB).

Because of this behavior we evaluated two possible strategies for the expression and purification of CFP-FtsA. The first strategy forecasts the possibility of purifying CFP-FtsA under native conditions exploiting a mild detergent during the process of lysis. The second strategy instead forecasts the possibility of purify CFP- FtsA under denaturating conditions. 4 L of expression were performed. The cultures were induced with 0.1 mM IPTG after the OD_{600} reached the value of 0.6. The over expression was performed at 30°C for 4 h. Then the cells were lysed in 50 mL of 50 mM TrisHCl, 300 mM NaCl, 10 mM $MgCl_2$,pH 8.0 and 1% of IGEPAL (Octylphenyl-polyethylene glycol; CA-630, Sigma-Aldrich). The IGEPAL is classified as a non-ionic, non denaturing detergent otherwise known also as a mild detergent. This kind of detergents disrupt lipid-lipid interaction and lipid –protein interactions rather than protein-protein interactions [58]. These features allows to the non soluble protein to be solubilized in the non ionic detergent without affecting the protein's structural features, such that can be isolated in its biologically active form [59]. The cells lysed in the buffer mentioned before, were sonicated and then loaded on a Ni/Nta^{2+} column. The fractions eluted from the column were loaded on a 12% SDS gel (Fig.4.13). It is possible to see the band corrispondent to CFP-FtsA (MW=75.7 kDa). The protein is present in the fractions from lane E to lane O in figure 4.13, deriving from the elution with 255mM imidazole.

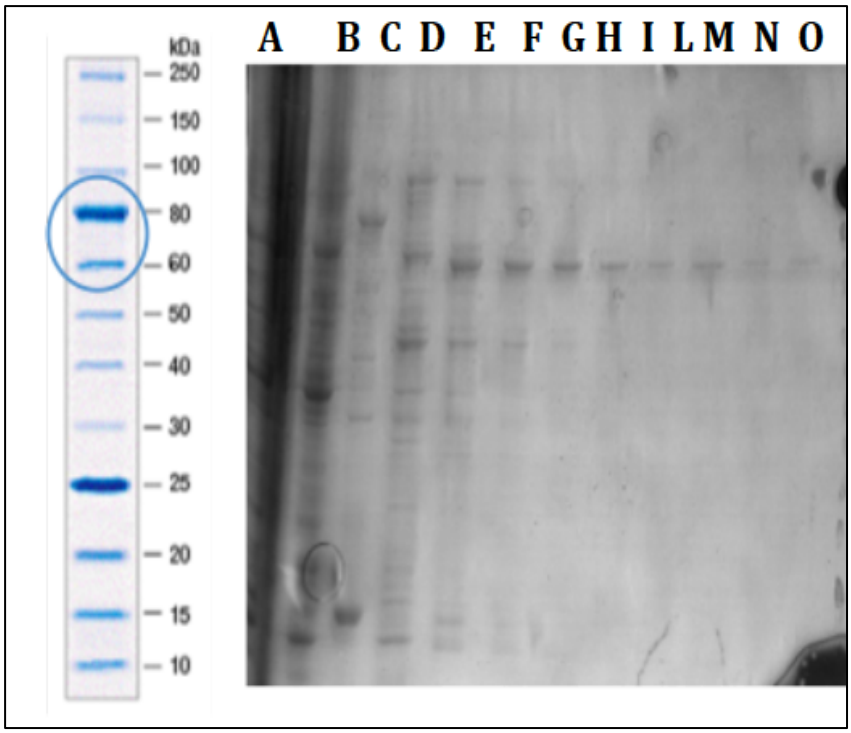

Fig 4.13: Purification of CFP-FtsA (MW=75.7 kDa) under native conditions exploiting 1% of IGEPAL. Lane A is the flow through, lane C is the protein ladder from 10-250 kDa (NEB), lane B is the first washing of the column with binding buffer, containing 5 mM imidazole; lane D is the washing step with 20 mM of imidazole and lane E is the washing step with 65 mM imidazole. Lane from F to O are the lanes correspondent to the protein eluted with 255 mM imidazole.

Although the gel shows that the protein eluted correspond to the MW of CFP-FtsA (75.7 kDa), the detection by UV spectroscopy and fluorescence spectroscopy of the protein dyalized and concentrated, did not show peaks characteristic of CFP. For this reason we decided to purify CFP-FtsA under denaturing conditions (Fig.4.13). The urea was added just in the lysis buffer, the buffer instead used for the affinity chromatography were not provided with urea.

The urea denaturates the protein, so the protein loose the secondary and tertiary structure and consequentially also the functionality. The choice of using the urea, as denaturant agent, was dictated by the fact that the urea does not interfere with SDS, so the fractions collected from the column could be directly loaded on the gel without any further step of clean-up, ie. the guanidine

hydrochloride (GuHCl) interfere with SDS, so eventually the sample need to be precipitated with Trichloroacetic acid (TCA precipitation).The protein denatured does not have functionality so is necessary after the purification to re-fold the protein and the urea needs to be diluted. The 8 M urea present in the fractions collected from the column from the elution step, approximately 40 mL, was diluted with 50 mL of a buffer 10mM BME, 0.1 mM CHAPS ([(3cholamidopropyl)dimethylammonio]-1 –propanesulfonate]), 50 mM TrisHCl, 50 mM NaCl pH 7.4. The buffer was added dropwise, o/n from a column in a beaker containing the protein. After dialysis and concentration, an UV spectrum and emission and excitation scans were acquired. In the UV spectrum was not possible to see the excitation peak correspondent to the CyPet present in the protein (CyPet has an Ex=435 nm and an Em=477 nm). The excitation and emission scan, instead, were not correspondent to the expected peaks of the protein.

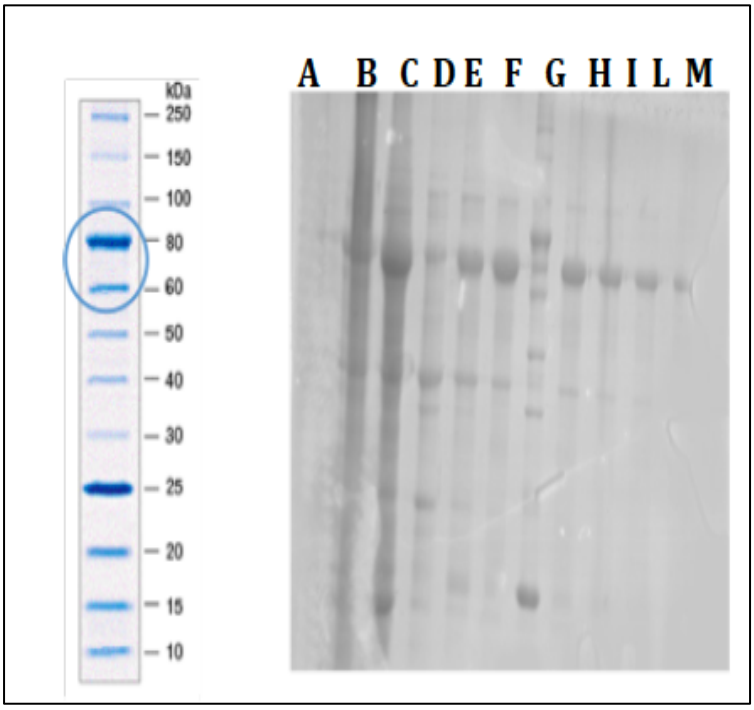

Fig. 4.13: CFP-FtsA is purified under denaturing conditions, using 8 M urea.Lane G is the protein ladder from 10-250 kDa (NEB). The fractions from lane H to lane M are the fraction eluted with 255 mM imidazole. The fraction in the lane E and lane F are the fractions from the washing step respectively with 20 mM imidazole and 65 mM imidazole, respectively Lane C and lane D are correspondent to the fraction after the washing with just 5 mM imidazole. Lane B is the flow through.

We tried to follow the same protocol also for the purification of CFP-FtsA R286W but the difficulties encountered were the same. Probably the fact that we were never be able to see the proper peaks of excitation and emission of CyPet, is a because the protein does not refold in the proper way. The difficult, to obtain a functional fluorescent version for FtsA pushed us to synthesize a minimal division machinery system directly inside w/o emulsion and phospholipids vescicles. Howewer we tried to encapsulate in w/o emulsions the protein that we were able to purify and observed some interesting phenomena.

4.2.3 Encapsulation of FtsZ and FtsA constructs in w/o emulsions.

After the purification of FtsZ-YFP-MinD, YFP-FtsZ and FtsA were encapsulated in w/ o emulsions and visualized by fluorescence microscopy. The purpose of the encapsulation was to investigate the phenomenon of polymerization of FtsZ in the presence of guanosine triphosphate (GTP)[60,61].The formation of bundles of polymers in presence of $CaCl_2$[62,63], and the possible interactions between FtsZ and FtsA. FtsZ in presence of GTP is able to polymerize and in certain buffer compositions, the effect of polymerization was also increased[60]. The buffers used in our experiments were HEK 100, composed by 50 mM HEPES, 100mM potassium acetate (KAc) pH 7.7, 2.5 mM EDTA and HMK composed by 50 mM HEPES, pH 7.7, 100 mM KAc and 5 mM $MgCl_2$. In each buffer there is always the presence of KAc. The potassium plays an important role in the assembly of FtsZ subunits during polymerization. In fact in *E. coli* cells the physiological concentration of KAc is of 350mM.

In figure 4.14 are reported images of w/o emulsions encapsulating FtsZ-YFP-MinD and YFP-FtsZ. The emulsions were produced in the way described in the previous sections. The protein represent the aqueous phase of the w/o emulsions. In general the concentration of the protein, of the GTP and $CaCl_2$ adopted in our experiments were alike to in a total volume of 50 μL. The emulsions once produced, were visualized by fluorescence microscopy.

5 μM FtsZ-YFP-MinD was encapsulated in w/o emulsions and forms aggregates (panel A). The aggregates were more spread in the emulsions in the presence of 2 mM GTP (panel B). The buffer used was the HEK buffer. 5 μM YFP-FtsZ (Fig 4.15, panel C and panel D) was encapsulated in emulsion, in HEK buffer. In absence of GTP was rare to observe aggregates (Fig 4.15, panel C) in presence, instead, of 2 mM GTP (Fig 4.15, panel D), the effect of aggregation is spread in the volume of emulsion. Similarly 5 μM YFP-FtsZ alone in HMK buffer formed rare polymers in absence of GTP (Fig 4.15, panel E). 5 μM YFP-FtsZ plus 2 mM GTP in HMK buffer formed evident aggregates. The term aggregation is used here instead of polymerization, because just the electron microscopy is needed in order to understand if proto filaments are formed or not[64-66].

Finally in figure 4.15 is reported an image obtained encapsulating YFP-FtsZ in w/o emulsions with the addition of 100 mM $CaCl_2$. It is possible to observe a strong effect of aggregation, perhaphs due to the bundling of the polymers of FtsZ. Finally we tried also to encapsulate FtsA with YFP-FtsZ inside w/o emulsions with a concentration of 1 μM but there were not significative differences between samples.

Although we were able to see changing in the morphology of FtsZ with the addition of 2 mM GTP and 10 mM $CaCl_2$, this artificial model is not satisfying because it does not permit us to see interactions between FtsZ and FtsA, and does not mediate division.

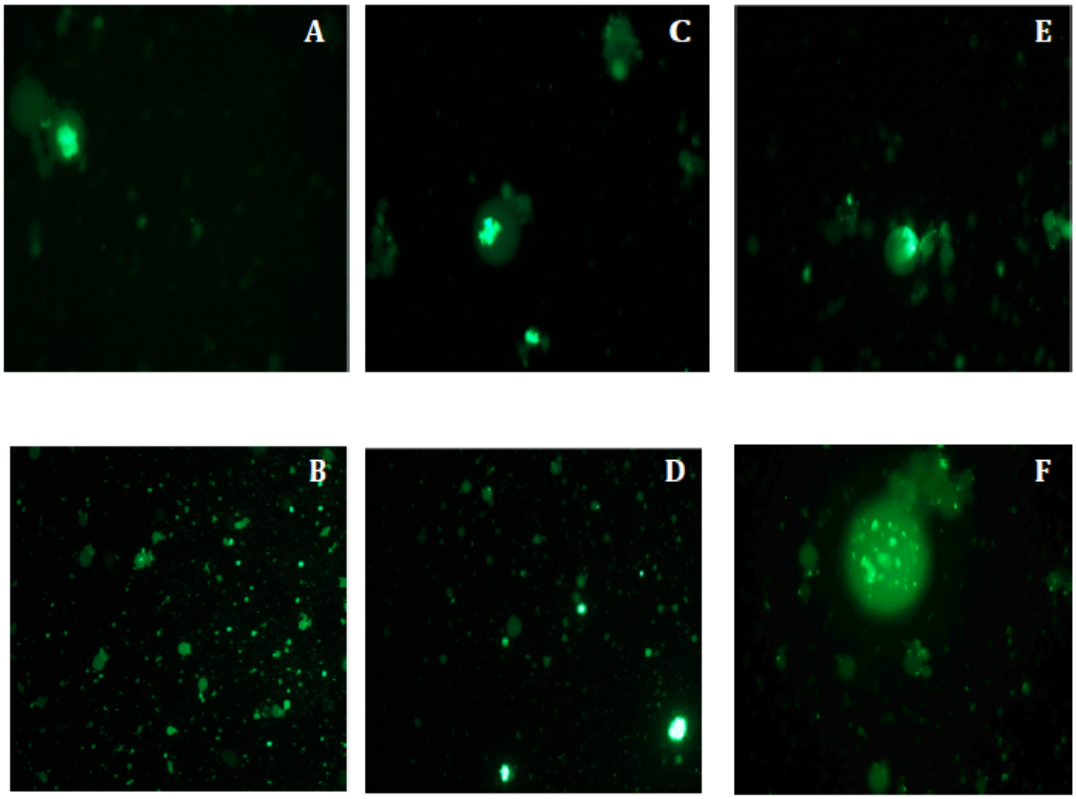

Fig 4.14: Fluorescence microscopy images of the encapsulation of FtsZ-YFP-Mind and YFP-FtsZ inside w/ o emulsions. FtsZ-YFP-MinD in HEK buffer is encapsulated in the emulsions and form rare aggregates (panel A). With the addition of 2 mM GTP we can notice a more spread effect of polymerization (panel B). YFP-FtsZ in buffer HEK forms rare polymers (panel C). In presence of 2 mM GTP YFP-FtsZ aggregates more (panel D). In buffer HMK the formation of polymers in presence of 2 mM GTP is increased (panel F) compared with the sample without GTP (panel E) and compared with the other conditions described before. YPet fluorescence is detected with a FITC filter and is false colored in green.

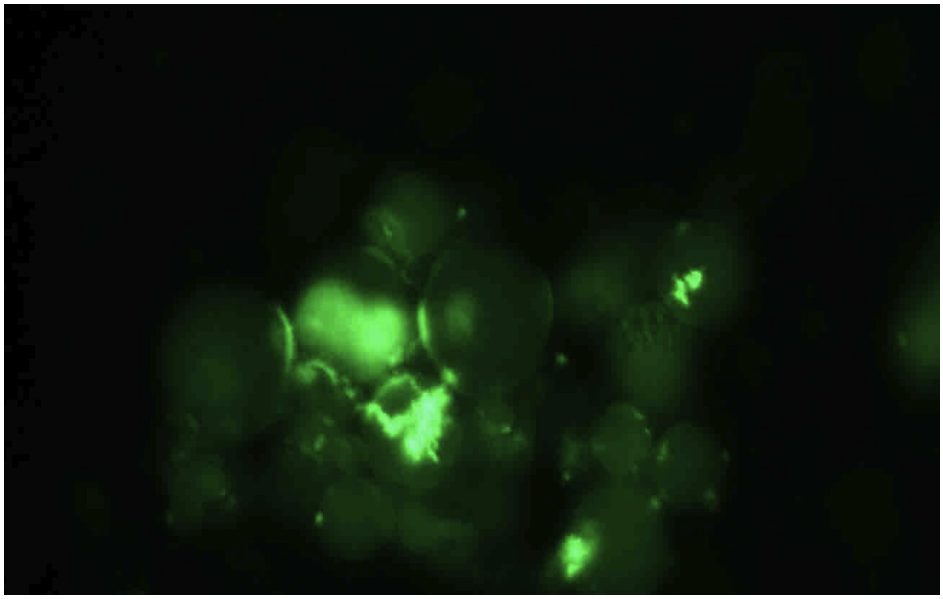

Fig 4. 15: Bundling of YFP-FtsZ effect generated by the addition of 10 mM $CaCl_2$ in aqueous phase of the emulsion The protein encapsulated appears more aggregated than in the presence of just GTP. The YPet fluorescence is visualized by fluorescence microscopy detected with a FITC filter and false colored in green.

4.3 Materials and Methods

4.3.1Bacterial strains and plasmids.

FtsZ (pET-TEV), FtsA (pET-TEV), FtsZ-YFP-MinD (pET21b), YFP-FtsZ (pET21b) CFP-FtsA and CFP- R286W FtsA (pET21b) were expressed in E . coli BL21 (DE3) Rosetta (F^- ompT hsdSB(R_B^- m_B^-) gal dcm λ(DE3 [lacI lacUV5-T7 gene 1 ind1 sam7nin5])pLysSRARE(Cam^R). This strain contains the pLysSRARE plasmid, which is similar to pLysS but also contains tRNA genes for codons that are rarely used in *E. coli*, ie. tRNA genes as argU (AGA, AGG), ileX (AUA), glyT (GGA), leu W(CUA). Rosetta cells are chloramphenicol resistant and have DE3 λ prophage carrying the T7 RNA polymerase gene and $lacI_q$.

4.3.2 Test of protein solubility.

E. coli BL21(DE3)cells were transformed as described above with plasmids coding for FtsZ, FtsA, FtsZ-YFP-MinD, YFP-FtsZ and CFP-FtsA. 10 mL of LB supplemented with 100 μg/ml ampicillin, were inoculated with 100 μL of E. coli BL21(DE3) Rosetta from an overnight culture and grown at 37°C, 220 rpm. Once the culture reached an OD_{600} of 0.6, a pre-induction sample of 500 μL was collected (in the major part of the cases) centrifuged at 13000 rpm for 10 min, and stored at -20 °C. Then the cultures were induced with 0.1 mM or 0.4 mM IPTG. The post induction incubation of the cells was for 4 h and in the case of the overexpression of CFP-FtsA at 30°C. In order to separate the soluble and insoluble protein fractions to load on the SDS-PAGE gel, the cellwere lysed. Cells were harvested by centrifugation at 5000 rpm at 4°C for 10 min and resuspended in 500 μL of 50 mM Tris-HCl, pH 7.4. Cells were sonicated 1 min with a cycle time of 15 s on and 30 s off to avoid excessive heating and formation of foam. After centrifugation at 13000 rpm at 4°C for 20 min the supernatant was collected in new eppendorf tubes and stored at -20 °C (soluble fraction). The pellet was stored at -20 °C (insoluble fraction).

4. 3.3 SDS-PAGE

As soon as 5 mL volume resolving gel was moved into the gel chamber, it was covered with2 mM of n-butanol to exclude O_2 and ensure a gel flat interface. After 15 min polymerization, n-butanol was removed and the stacking gel was poured with a comb inserted to form the wells and define the lanes and allowed to polymerize for 10 min. The samples that were loaded onto the SDS-PAGE gel were prepared as follows: the pellet (insoluble fraction) was resuspended in 200 µL of Tris-HCl, pH 7.0 and 200 µL of SDS loading buffer (1 M Tris-Cl pH 6.8 2.4 mL, 20% SDS, Glycerol (100%) 3 mL, B-mercaptoethanol 1.6 mL Bromophenol blue 0.006g 10 mL (store -20 deg C) 10 µL aliquot from the supernatant (soluble fraction) was mixed with 10 µL of SDS loading buffer; the pre-induction pellet was resuspended in 50 µL of SDS loading buffer. All three samples were heated for 5 min at 94 °C. While the soluble fraction was ready to be loaded, the insoluble fraction and the pre induction sample were centrifuged. 20 µL from each sample were loaded on SDS-PAGE gel lanes. The ladder a Protein Ladder (P7703S, NEB) and the volume used was of 5µL.The gel was run at 140 V, 400 mA, for 2 h. Staining was performed with Coomassie Staining solution(50% MeOH ,10% Acetic Acid ,0.05% Brilliant Blue R-25) and was allowed to continue overnight with mild shaking. Destaining was performed for 3 h with de-staining solution(50% MeOH ,40% milli-Q water ,10% Acetic Acid) with mild shaking. The samples of the different fraction coming from the column were heated in loading buffer at 94 °C and loaded on a 10% SDS gel.

4.3.4 Affinity chromatography protein purification.

Cells were harvested by centrifugation at 4000 X g for 20 min at 4 °C and the supernatant discarded. Pellets were resuspended in ca. 50 mL of Binding Buffer (50 mM NaH_2PO_4, 300 mM NaCl, 5 mM imidazole, pH 7.4). For the resupension of the pellet of CFP-FtsA we used 50 mM TrisHCl, 300 mM NaCl, 10 mM $MgCl_2$, pH 8.0 and 1% IGEPAL (Octylphenyl-polyethylene glycol; CA-630,

Sigma-Aldrich). The lysis buffer for the purification under denaturant conditions was made of 8 M urea, 300 mM NaCl and 50 mM NaH_2PO_4 pH 8.In general to the pellets resuspended were added 0.4 mg/mL Lysozime, 1mM phenyl methane sulfonyl fluoride(PMSF) and 0.1% BME. The lysis was performed through sonication with a cycle time of 15 s on and 30 second off for 2 min of sonication time keeping falcons in ice. Cell lysate was centrifuged at 9000 X g for 30 min at 4 °C and the crude extract (supernatant) was diluted 5 fold with Binding Buffer. Ni/Nta agarose resin from Qiagen stock solution 2 g/mL was loaded into a 2.5x10 cm gravity-flow chromatography column until a final volume of 5 mL packed in the bottom. The column was washed with 3 column volumes of water. Then the resin was charged with 100 mM $NiSO_4$ and washed for 3 column volumes with Binding Buffer(50 mM NaH_2PO_4, 300 mM NaCl, 5 mM imidazole, pH 7.4).The diluted crude extract was loaded and allowed to go through the resin in order to have 1 mL per min flowed through. A sample of flow through was collected and stored at 4 °C to load later on the SDS PAGE gel. The column was washed with 3 column volumes of Binding Buffer + 20 mM imidazole and 3 column volumes of Binding Buffer plus 60 mM imidazole and the fractions of washing were collected in 50 mL falcon tubes. Elution was made with Elution Buffer made by Binding Buffer plus 250 mM imidazole and 8 fractions of 4-5 mL elution were collected. Regenerating the column required washes with 3 column volumes of water and 1-2 column volume of stripping buffer (100 mM EDTA, pH 8).

4.3.5 Dialysis.

The fractions of FtsZ-YFP-MinD and YFP-FtsZ eluted from the column, were collected in a Snake Skin Dialysis membrane (Thermoscientific) with 7 K molecular weight cut off (MWCO) and dialyzed f in 2 L of 50 mM TrisHCl , 50 mM NaCl, 1 mM BME. For the dialysis of CFP-FtsA the buffer composition was slightly different (50 mM TrisHCl , 50 mM NaCl, 1 mM BME, 0.1 mM CHAPS).

4.3.6 Protein concentration and storage.

The proteins from a volume varying between 40 mL-100 mL were concentrated with a stirred cell concentrator of different sizes, depending from the volume to concentrate. The membrane used was an Amicon membrane of 10K MWCO. The protein were stored at - 80°C in 5 % glycerol.

4.3.7 Instrumentation

The sonicator used is a MISONIX S-4000. The program used for the extraction of the proteins from the *E .coli cells* exploits an amplitude of 70 and is provided with a tip. The UV-Vis used, is an Agilent 8453 spectrophotometer. The absorbance was measured, using 60 μL of sample and setting a range of absorbance from 250 nm to 70 nm. Excitation and emission scan were acquired using a Photon Technology International (PTI) Quanta Master 40 UV VIS spectrofluorometer equipped with two detectors (T-format). The emission scans were acquired starting from the excitation wavelength + 5 nm to the emission wavelength + 50 - 100 nm or larger. The integration was set to 1 s, and for high quality scan the average was set to 2: the system repeat two times the measurement and average the readings. The excitation scans were acquired inserting a range of acquisition for the excitation (ie. for YPet 450-525) and the exact value of emission of the protein for the emission. Finally the fluorescent proteins encapsulated in w/o emulsion were visualized using a Nikon Eclipse 90i microscope with a Nikon DS-5MC camera and a FITC filter FITC with an excitation of 465 - 495 nm and an emission of 515 - 555 nm. The magnification used for collect the images is 40X.

Chapter 5

Conclusions and future directions

5.1 Conclusions.

This dissertation offers new routes towards the design of artificial cells and proposes new possible approaches for the reconstruction of cell body division in cell-like compartments.

Cell-like compartments hosting purified proteins from *E. coli* cell division machinery system, although show typical features of cell division are not able to divide, as demonstrated in chapter 4. A "simple" encapsulation of purified proteins in w/o emulsions does not result in a living system.[67,68] In fact a system like that, is not only incapable of division but is also not self sustainable. Towards the development of a genetically encoded system, synthesizing a minimal division machinery directly inside w/ o emulsions and phospholipid vesicles,we made a step forward through the construction of an artificial minimal cell. Our system, described in chapter 3, is capable of transcription and translation of the DNA in fuctional proteins of the divisome such as FtsZ and FtsA and although is not able to divide, it is such a system come closer to the criterion of autopoiesis[9], an essential feature of cellular life. We provided a possible strategy for the fine control of the protein production, engineering constructs under the control of strong RBS sites and envisioning a possible modulation of the strength for the reproduction of a ratio of 4:1 for FtsZ and FtsA.

Furthermore FtsZ and FtsA, once produced in the compartments, show an unusual behavior, assembling together and forming ring-like structure. This is another cellular imitation that we were able to reproduce in our synthetic minimal cell. As in *vivo* where the Z ring, made of FtsZ subunits interacts with FtsA and localize in proximity of the membrane, in cell like compartments YFP-FtsZ interacts with FtsA and direct itself to the membrane. Definitively the reconstruction of a primitive event of cell division was possible. The round shape, of the liposomes and of w/o emulsions does not help the generation of the constriction force and does not permit a spatial localization of the proteins.

For this reason we developed and characterize w/o emulsion ATPS and w/o emulsions A3PS compartment that present an internal compartmentalization optimal for the spatial localization of the proteins of our system. The reconstruction of a genetically encoded system in these compartments is possible, as demonstrated by the expression of YFP/YPEt and we can spatially localize the protein produced. Furthermore w/o emulsion ATPS have a budding morphology and undergoes to chemical division when fed with micelles of SDS. These features are useful for the reconstruction of cell body division mechanism.

5.2 Future directions.

The next step in this work is to encapsulate the genetically encoded system for the synthesis of FtsZ and FtsA, in w/o emulsions ATPS and w/o emulsions A3PS. This combination will result in an artificial cell provided of an internal compartmentalization and potentially able of division. If the artificial cell will not be able to divide, will be at least capable of spatially localize the proteins and the ring-like structures formed by FtsZ and FtsA. Another possible and challenging future direction, that could represent another step towards the construction of artificial cell, could be the encapsulation of a genetically encoded system for FtsZ and FtsA in GVs/ATPS

Furthermore is possible that ATPS w/o emulsions and A3PS w/o emulsions could be used as novel systems for delivery, not only of chemical drugs but also of proteins, genes and why not of elementary molecules.

Appendix

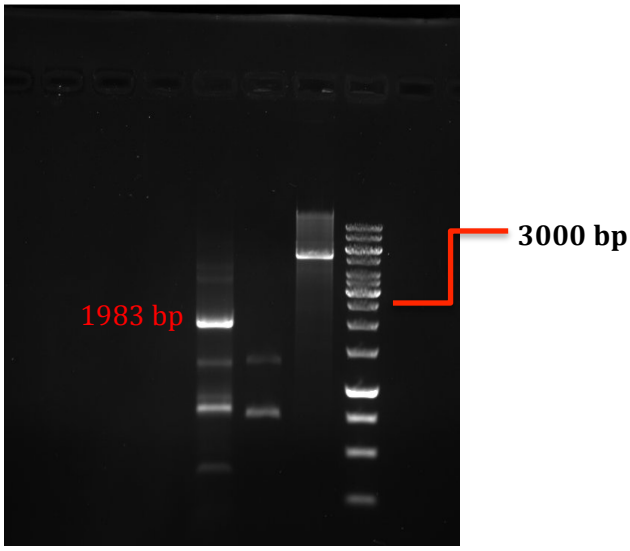

Fig A.1: Optimization of overlapping PCR. Trying to obtain less aspecific bands, using as annealing temperature the melting temperature of the overlapping region in the forward primer +3°C, as the protocol for Phusion High Fidelity DNA Polymerase forecasts. The resulting annealing temperature is 63.8 °C. The reaction of extension and overlap is carried on by Phusion High Fidelity DNA Polymerase in HF buffer. The length of *sfgfp-ftsA* is 1983bp. The ladder used, is a 1 kb ladder (Fermentas).

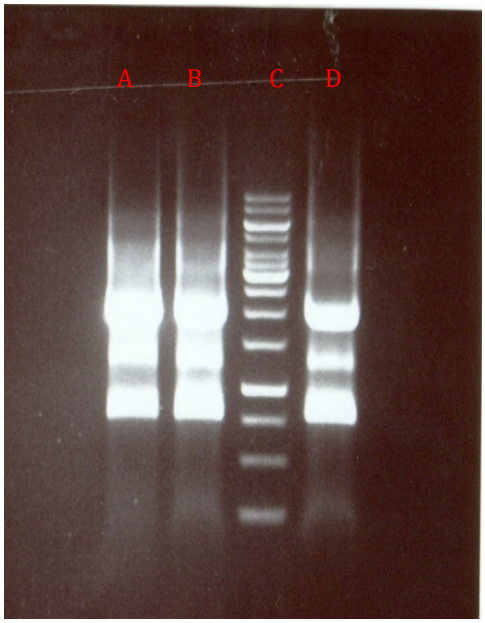

Fig. A2: Overlapping PCR. Trial to obtain an higher amount of the band correspondent to *sgfp-ftsA*.The DNA was overlapped and extendend by a mixture of Taq and Phusion High Fidelity DNA polymerases (1.5 U of Taqand 0.5 U of Phusion).The length of the gene is 1983 bp.The problem of aspecific bands still persist, but the amount of *sgfp-ftsA* produced is higher. The program used for the reaction, forcasts, melting and denaturation temperature at 95° for 2 min, anneling at 60°C for 30 min and extension at 72 °C for 2 min. The program was stopped and the polymerases were added.The program was repeated for 25 times, and a final extension at 72 °C for 10 min was performed. Lane A corresponds to a reaction performed with 100 ng of DNA template, lane B to a reaction with 50 ng and lane D corresponds to a reaction with 25 ng. The ladder used is 1kb (Fermentas).

Table A1: List of the primers used for the genetic constructs.

CONSTRUCT	PRIMER	PRIMER SEQUENCE 5' – 3'	Tm	Length (bp)
FtsZ-YFP-MinD	Primer 1 (fwd)	CCCGGCCCATATGGGC AGCTCT	66.2°C	22
	Primer 2 (rev)	CGCGCGCCTCGAGTTA ACCGCC	67.4°C	22
YFP-FtsZ	Primer 1 (fwd)	CCCGGGCCATATGGGC AGCCACCAT	69.3 °C	25
	Primer 2 (rev)	CCGGCCGGATCCTTAT CAGTCGGC TTG	66.1 °C	27
CFP-FtsA	Primer 1 (fwd)	GGCCGGCCCATATGGG CTCACATCAT	67.5 °C	28
	Primer 2 (rev)	CCCGGGCGGGATCCTT ATCAAAATTCT TTACG	62.3 °C	29
CFP-R286W FtsA	Primer 1 (fwd)	GGCCGGCCCATATGGG CTCACATCAT	67.5 °C	28
	Primer 2 (rev)	CCCGGGCGGGATCCTA TCAAAATTCT TTACG	62.3 °C	29
sGFP-GSGSGS-FtsA	Primer 1 (fwd)	GCAGCAGGCCCATGGA TGCGTAAAGGCGAAGA GCT	70.7 °C	35
	Primer 2 (rev)	CGGGGCGGATCCGT ACCAGAGCCTTTGA CAGTTCATCCATACC	70.5 °C	45
	Primer 3 (fwd)	GCAGCAGGATCC ATGATCAAGGCGACGG ACAG	67.6°C	32
	Primer 4 (rev)	CGGCGGCTCGAGTTAC TCTTTTCGCAGCCAAC TATT	67.3°C	36
FtsZ-YFP-MinD-FtsA	Primer 1 (fwd)	GCAGCACATATGTTC GAACCGATGGAACT	62.3°C	29
	Primer 2 (rev)	TAATATGAGCTCTTA ACCGCCGAACAGACGT	62.1°C	31
	Primer 3 (fwd)	GACGACAAGCTT **AAG GAG**AGCTAGCTATGA TCAAAGCTACGGACCG	67.1°C	46
	Primer 4 (rev)	CGCCGCCTCGAGTTA TCAAAATTCTTTACG CAGCC	65.8°C	35

CONSTRUCT	PRIMER	PRIMER SEQUENCE 5' – 3'	Tm	Length (bp)
FtsZ-YFP-MinD-R286W FtsA	Primer 1 (fwd)	GCAGCA**CATATG**TTC GAACCGATGGAACT	62.3°C	29
	Primer 2 (rev)	TAATAT**GAGCTC**TTA ACCGCCGAACAGACGT	62.1°C	31
	Primer 3 (fwd)	GACGAC**AAGCTT** **AAG GAG**A**GCTAGC**TATGA TCAAAGCTACGGACCG	67.1°C	46
	Primer 4 (rev)	CGCCGC**CTCGAG**TTA TCAAAATTCTTTACG CAGCC	65.8°C	35
YFP-FtsZ-FtsA	Primer 1 (fwd)	GCAGCA**CATATG**GTG TCCAAAGGCGAAGAAC TG	65°C	33
	Primer 2 (rev)	GGC GGC **GAG CTC** TTA TCA GTC GGC TTG TTT AC	66.1°C	32
	Primer 3 (fwd)	GAAGAA**GTCGAC** **AAGGAG**A**GCTAGC**T ATGATCAAAGCTACGG ACCG	67°C	46
	Primer 4 (rev)	CGCCGC**CTCGAG**TTA TCAAAATTCTTTACGC AGCC	65.8°C	35
FtsZ (no His tag)	Primer 1 (fwd)	GCGGAC**CATATG**GAA CTGACCAATGATGC	62.8°C	29
	Primer 2 (rev)	TGCTGC**CTCGAG**TTA TCA GTC GGC TTG TTTAC	64.2	32
FtsA (no His tag)	Primer 1 (fwd)	GCGGAC**CATATG** GAACTGACCAATGATG C	63.7°C	29
	Primer 2 (rev)	CGCCGC**CTCGAG**TTA TCAAAATTCTTTACG CAGCC	64.6°C	35

Table A1: In this table are listed the sequences of the primers designed for our genetic constructs the length and the melting temperature (Tm). In different colours are highlighted part of the sequence correspondent to restriction enzymes sites. In the single construct **CATATG** highlighted in red is the site correspondent to NdEI, **CTCGAG** highlighted in orange is the site correspondent to XhoI and finally **GGATCC** highlighted in blu is the site correspondent to BamHI. In the double construct **CCATGG** highlighted in violet is the site for NcoI, **GAG CTC** highlighted in purple is the site for SacI, **AAGCTT** highlighted in green is the site for HindIII, **GCTAGC** highlighted in cyan is the site for NheI, **GTCGAC** highlighted in grey is the site for SalI. In black is highlighted the consensus sequence of the RBS.

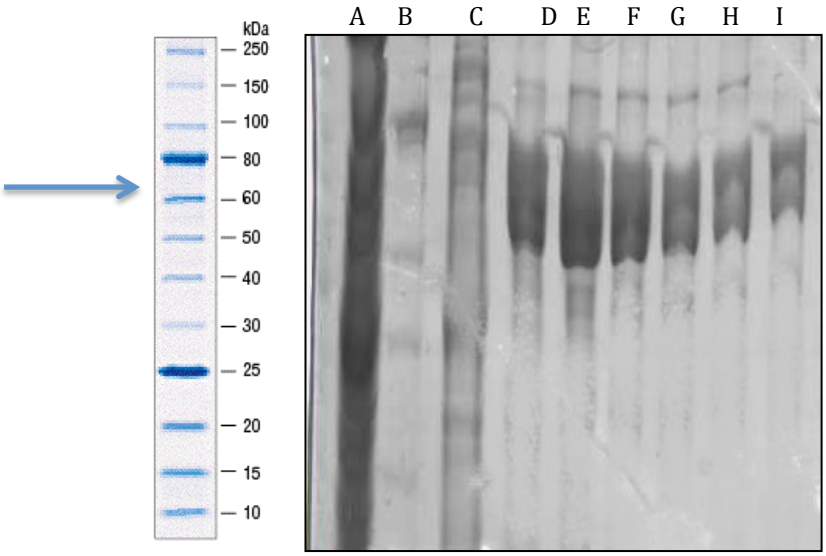

Fig. A3: FtsZ-YFP-MinD (MW=70.2), aliquots eluted from the Ni/NTA^{2+} column, and loaded on 12% SDS-PAGE. Lane A is the flow through. B and C are the washing step with respectively, 5 mM imidazole+ Binding Buffer and 20 mM imidazole + Binding Buffer. Lanes from D to I are the fractions eluted with 255 mM imidazole

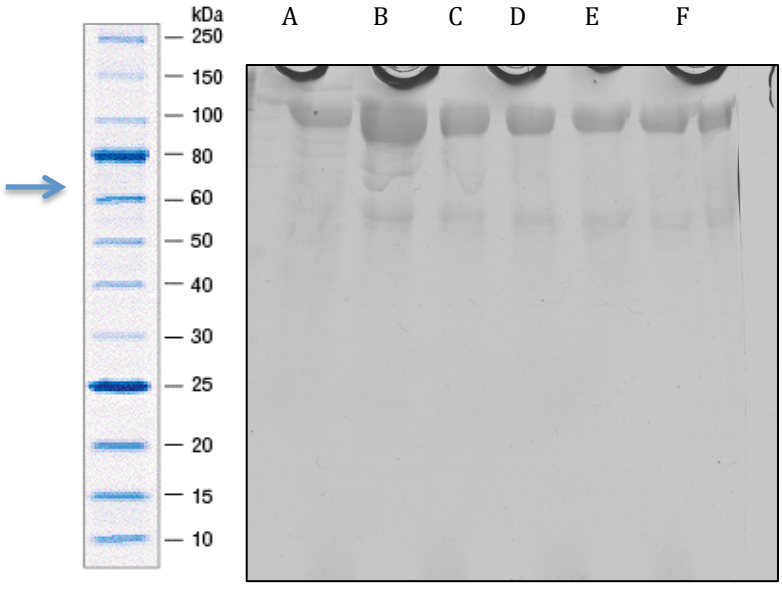

Fig A4: YFP-FtsZ (MW: 70.2kDa). Lane A is the fraction from the washing with just binding buffer. Lane B is the fraction from the washing with 60 mM imidazole.Lane from C –F are the fractions deriving from the elution with 255mM imidazole.

Acknowledgments

First I would like to thank my supervisor Sheref Mansy. Sheref offered me the opportunity to approach to synthetic biology and to the fascinating topic described in this thesis. Sheref always put the bar high, stimulating to improve myself both as scientist that as person.

Second I would like to thank Christine Keating Christine gave to me the opportunity to join her group at the Department of Chemistry of the Penn State University. Christine was simply great all the time that I spent in her lab, encouraging and reinforcing my passion for science.

A big acknowledgement is for the people working in the Mansy lab, in particular I want to thank Cristina Del Bianco and Amy Carr Spencer.

Cristina helped me with my initial training, she was always supportive and collaborative since I joined the Mansy lab, thanks to her I learned basic techniques in molecular biology.

Amy Carr Spencer was more than a lab mate. I thank her for all the beautiful conversations about life and science, for all the awful discussion that we had in the lab and for all the moments spent together.

I am thankful to Laura Martini and Domenica Torino, that started with me this adventure in the Mansy lab, to Roberta Lentini who withI had fun in and out of the lab, Silvia Perez, Fabio Chizzolini , Dario Cecchi e Michele Forlin.

I couldn’t made through the PhD school without the support of my family . My parents and my brother, gave to me all the positive energy to face this PhD, trusting in me and encouraging me every single day.

Finally I want to thank Mirko, to be always present although the difficulties, Sabrina and Francis to be in different moments, at different times and for different reasons, the most beautiful part of my life in these years. Thank you, you were everything for me.

Bibliography

1. Channon K, Bromley EH, WoolfsonDN, Synthetic biology through biomolecular design and engineering. *Curr. Opin. Struct Biol*, 2008, *18*(4) 491-8.
2. Jack W. Szostak, David P. Bartel & P. Luigi Luisi Synthesizing life, *Nature* ,**2001,** 409 (387-390).
3. Forlin, Lentini, Mansy Cell imitations, *Curr.Opin.Chem.Biol* , **2012,***16,*586-592.
4. Pereto J., Catala J., The Renaissance of Synthetic Biology*, Mit Press,* **2008,**2.128-130.
5. Schwille P. Bottom-Up Synthetic Biology:Engineering in a Tinkerer's World,*Science,***2011,** *333*,1252-
6. Rene´e Roodbeen and Jan C. M. van Hest**,** Synthetic cells and organelles: compartmentalization strategies, *Bioessays*, **2009** *31*(12), 1299-308.
7. Cristiano Chiarabelli, Pasquale Stano, Pier Luigi Luisi, Chemical approaches to synthetic biology, *Curr.Opin.Biotech,***2009**,*20*, 492-497
8. 8. Adams, D. W. & Errington, J. Bacterial cell division: assembly, maintenance and disassembly of the Z ring. *Nature reviews. Microbiology* **7**, 642–53 (2009).
9. Erickson, H. P. FtsZ, a tubulin homologue in prokaryote cell division. *Trends in cell biology* **7**, 362–7 (1997).
10. Margolin, W. FtsZ and the division of prokaryotic cells and organelles. *Nature reviews. Molecular cell biology* **6**, 862–71 (2005).1.
11. Wu, L. J. & Errington, J. Nucleoid occlusion and bacterial cell division. *Nature reviews. Microbiology* **10**, 8–12 (2012).
12. Lutkenhaus, J. Assembly dynamics of the bacterial MinCDE system and spatial regulation of the Z ring. *Annual review of biochemistry* **76**, 539–62 (2007).
13. Ma, X. & Margolin, W. Genetic and functional analyses of the conserved C-terminal core domain of Escherichia coli FtsZ. *Journal of bacteriology* **181**, 7531–44 (1999).
14. Geissler, B., Elraheb, D. & Margolin, W. A gain-of-function mutation in ftsA bypasses the requirement for the essential cell division gene zipA in Escherichia coli. *Proceedings of the National Academy of Sciences of the United States of America* **100**, 4197–202 (2003).
15. Löwe, J. & Van den Ent, F. Conserved sequence motif at the C-terminus of the bacterial cell-division protein FtsA. *Biochimie* **83**, 117–20 (2001).
16. Geissler, B., Elraheb, D. & Margolin, W. A gain-of-function mutation in ftsA bypasses the requirement for the essential cell division gene zipA in Escherichia coli. *Proceedings of the National Academy of Sciences of the United States of America* **100**, 4197–202 (2003).
17. Shiomi, D. & Margolin, W. Dimerization or oligomerization of the actin-like FtsA protein enhances the integrity of the cytokinetic Z ring. *Molecular microbiology* **66**, 1396–415 (2007).

18. Pichoff, S. & Lutkenhaus, J. Tethering the Z ring to the membrane through a conserved membrane targeting sequence in FtsA. *Molecular microbiology* **55**, 1722–34 (2005).
19. Erickson, H. P., Anderson, D. E. & Osawa, M. FtsZ in bacterial cytokinesis: cytoskeleton and force generator all in one. *Microbiology and molecular biology reviews : MMBR* **74**, 504–28 (2010).
20. Osawa, M., Anderson, D. E. & Erickson, H. P. Reconstitution of contractile FtsZ rings in liposomes. *Science (New York, N.Y.)* **320**, 792–4 (2008).
21. Osawa, M., Anderson, D. E. & Erickson, H. P. Curved FtsZ protofilaments generate bending forces on liposome membranes. *The EMBO journal* **28**, 3476–84 (2009).
22. Loose, M., Fischer-Friedrich, E., Ries, J., Kruse, K. & Schwille, P. Spatial regulators for bacterial cell division self-organize into surface waves in vitro. *Science (New York, N.Y.)* **320**, 789–92 (2008).
23. Jiménez, M., Martos, A., Vicente, M. & Rivas, G. Reconstitution and organization of Escherichia coli proto-ring elements (FtsZ and FtsA) inside giant unilamellar vesicles obtained from bacterial inner membranes. *The Journal of biological chemistry* **286**, 11236–41 (2011).
24. Feigenson, G. W. Imaging coexisting fluid domains in biomembrane models coupling curvature and line tension. **425**, 23–26 (2003).
25. Long, M. S., Cans, A. & Keating, C. D. Budding and Asymmetric Protein Microcompartmentation in Giant Vesicles Containing Two Aqueous Phases. **6**, 756–762 (2008).
26. Cans, A., Andes-koback, M., Keating, C. D. & Biol, R. N. C. Positioning Lipid Membrane Domains in Giant Vesicles by Micro-organization of Aqueous Cytoplasm Mimic. 7400–7406 (2008).
27. Andes-koback, M. & Keating, C. D. Complete Budding and Asymmetric Division of Primitive Model Cells To Produce Daughter Vesicles with Different Interior and Membrane Compositions. (2011).
28. KuriharaK, TamuraM, ShohdaK, ToyotaT, SuzukiK, SugawaraT:Self-.-repr oduction of supramolecular giant vesicles combined with the amplification of encapsulated DNA. NatChem2011, 3:775-.-781.
29. Harris, D. C. & Jewett, M. C. Cell-free biology: exploiting the interface between synthetic biology and synthetic chemistry. *Current opinion in biotechnology* **23**, 672–8 (2012).
30. Carlson, E. D., Gan, R., Hodgman, C. E. & Jewett, M. C. Cell-free protein synthesis: applications come of age. *Biotechnology advances* **30**, 1185–94 (2011).
31. Maeda, Y. T. *et al.* Assembly of MreB Filaments on Liposome Membranes: A Synthetic Biology Approach. (2011)
32. Shimizu, Y. *et al.* Cell-free translation reconstituted with purified components. *Nature biotechnology* **19**, 751–5 (2001).
33. Hosoda, K. *et al.* Quantitative study of the structure of multilamellar giant liposomes as a container of protein synthesis reaction. *Langmuir : the ACS journal of surfaces and colloids* **24**, 13540–8 (2008).
34. Griffiths, A. D. & Tawfik, D. S. Miniaturising the laboratory in emulsion droplets. (2006).doi:10.1016/j.tibtech.2006.06.009
35. Bernath, K. *et al.* In vitro compartmentalization by double emulsions : sorting and gene enrichment by fluorescence activated cell sorting. **325**,

151–157 (2004).
36. Miller, O. J. *et al.* Directed evolution by in vitro compartmentalization. **3**, 561–570 (2006).
37. Sunami, T., Matsuura, T., Suzuki, H. & Yomo, T. Cell-Free Protein Production. **607**, 243–256 (2010).
38. Noireaux, V.; Libchaber, A. A Vesicle Bioreactor as a Step Toward an Artificial Cell Assembly. Proc. Nat
39. Bolinger, P.-Y.; Stamou, D.; Vogel, H. Integrated Nanoreactor Systems: Triggering the Release and Mixing of Compounds Inside Single Vesicles. J. Am.Chem. Soc. 2004, 126, 8594-8595.
40. Walde, P.; Ichikawa, S. Enzymes inside Lipid Vesicles: Preparation, Reactivity and Applications. Biomol. Eng. 2001, 18, 143-177.
41. Sunami, T., Matsuura, T., Suzuki, H. & Yomo, T. Cell-Free Protein Production. **607**, 243–256 (2010)
42. Matsuura, T. *et al.* Importance of compartment formation for a self-encoding system. *Proceedings of the National Academy of Sciences of the United States of America* **99**, 7514–7 (2002).
43. Alberts, B., Johnson, A., Lewis, J.; Raff, M.; Roberts, K.; Walter, P. Molecular Biology of the Cell. 4th ed. 2002. Garland Science, New York. Ellis, J. R. Macromolecular Crowding: Obvious but Underappreciated. Trends Biochem. Sci. 2001, 26, 597-604. (b) Minton, A. P. Macromolecular
44. Albertsson, P. A. Partition of Cell Particles and Macromolecules, 2nd ed. 1971, Wiley-Interscience, New York.
45. Hatti-Kaul, R. Aqueous Two-Phase Systems- Methods and Protocols. 2000, Humana Press, Totowa New Jersey
46. Keating, C. D. Aqueous Phase Separation as a Possible Route to Compartmentalization of Biological Molecules. **XXX**, (2011).
47. Keighron, J. D. & Keating, C. D. Towards a Minimal Cytoplasm. 3–30 (2011).doi:10.1007/978-90-481-9944-0
48. Fiordemondo, D. & Stano, P. Lecithin-Based Water-In-Oil Compartments asDividingBioreactors.1965–19732007).doi:10.1002/cbic.200700112.49. (2007).
49. Pichoff, S. & Lutkenhaus, J. Unique and overlapping roles for ZipA and FtsA in septal ring assembly in Escherichia coli. *The EMBO journal* **21**, 685–93 (2002).
50. Beuria, T. K. *et al.* Adenine nucleotide-dependent regulation of assembly of bacterial tubulin-like FtsZ by a hypermorph of bacterial actin-like FtsA. *The Journal of biological chemistry* **284**, 14079–86 (2009).
51. Strahl, H. & Hamoen, L. W. Membrane potential is important for bacterial cell division. *Proceedings of the National Academy of Sciences of the United States of America* **107**, 12281–6 (2010).
52. Pédelacq, J.-D., Cabantous, S., Tran, T., Terwilliger, T. C. & Waldo, G. S. Engineering and characterization of a superfolder green fluorescent protein. *Nature biotechnology* **24**, 79–88 (2006).
53. The proper ratioof FtsZ to FtsA is required for Cell Division to occur in Escherichia coli. Lutkenhaus et al. *Journal of Bacteriology* **1992**, *174*, 6145-6151.
54. Schwarz, D., Dötsch, V. & Bernhard, F. Production of membrane proteins using cell-free expression systems. *Proteomics* **8**, 3933–46 (2008).

55. Martos, A. *et al.* Isolation, characterization and lipid-binding properties of the recalcitrant FtsA division protein from Escherichia coli. *PloS one* **7**, e39829 (2012).
56. Sunami T, Matsuura T, Suzuki H, Yomo T. (2009) Synthesis of functional proteins withinliposomes. In:Cell-Free Protein Production: Methods and Protocols (Methods in MolecularBiology Vol. 607) , Endo, Yaeta; Takai, Kazuyuki; Ueda, Takuya (eds.). Humana Press, pp.
57. Hansen LH, Knudsen S, Sørensen SJ.(1998).The effect of the lacY gene on the induction of IPTG inducible promoters, studied in Escherichia coli and Pseudomonas fluorescens Curr Microbiol. 1998 Jun;36(6):341-7.
58. Speers AE, Wu CC, (2007), Proteomics of integral membrane proteins-theory and application, 107(8):3687-714.
59. Seddon AM, Curnow P, Booth PJ,(2004),Membrane proteins ,lipids and detergents: not just a soap-opera, (1666) (1-2):105-17
60. Small, E. Dynamic FtsZ polymerization is sensitive to the GTP to GDP ratio and can be maintained at steady state using a GTP-regeneration system. *Microbiology* **149**, 2235–2242 (2003).
61. Huecas, S. *et al.* The interactions of cell division protein FtsZ with guanine nucleotides. *The Journal of biological chemistry* **282**, 37515–28 (2007).
62. Lan G, Dajkovic A, Wirtz D, Sun SX (2008) Polymerization and bundling kinetics of FtsZ filaments. Biophys J 95:4045–4056
63. Popp, D., Iwasa, M., Narita, A., Erickson, H. P. & Maéda, Y. FtsZ condensates: an in vitro electron microscopy study. *Biopolymers* **91**, 340–50 (2009).
64. Huecas, S. *et al.* Energetics and geometry of FtsZ polymers: nucleated self-assembly of single protofilaments. *Biophysical journal* **94**, 1796–806 (2008).
65. Lafontaine, C. *et al.* Behaviour of bacterial division protein FtsZ under a monolayer with phospholipid domains. *Biochimica et biophysica acta* **1768**, 2812–21 (2007).
66. Margolin, W. Sculpting the bacterial cell. *Current biology : CB* **19**, R812–22 (2009).
67. Schwille, P. Bottom-up synthetic biology: engineering in a tinkerer's world. *Science (New York, N.Y.)* **333**, 1252–4 (2011).
68. Martos, A., Jiménez, M., Rivas, G. & Schwille, P. Towards a bottom-up reconstitution of bacterial cell division. *Trends in cell biology* **22**, 634–43 (2012).
69. Chiarabelli, C., Stano, P., Anella, F., Carrara, P. & Luisi, P. L. Approaches to chemical synthetic biology. *FEBS letters* **586**, 2138–45 (2012).